Mechanisms of Cellular Remodeling during Plasmodium falciparum Sequestration and Transmission

Mechanisms of Cellular Remodeling during *Plasmodium falciparum* Sequestration and Transmission

A dissertation presented

by

Deepali Bharati Ravel

to

The Division of Medical Sciences

in partial fulfillment of the requirements

for the degree of

Doctor of Philosophy

in the subject of

Biological and Biomedical Sciences

Harvard University

Cambridge, Massachusetts

August 2017

Dissertation Advisor: Professor Matthias Marti Deepali Bharati Ravel

Mechanisms of Cellular Remodeling during *Plasmodium falciparum* Sequestration and Transmission

ABSTRACT

Despite significant progress in global malaria control, *Plasmodium falciparum* remains a major cause of morbidity and mortality world-wide. The need for new interventions demands better understanding of the underlying cellular mechanisms that mediate parasite survival and transmission. Asexual growth and the development of sexual stages, termed gametocytes, take place in human red blood cells, and sexual reproduction takes place in the mosquito vector. Blood stage parasites sequester in host tissues to survive, requiring extensive cellular remodeling. Sequestering asexual stage parasites export hundreds of proteins into the host cell to change its deformability and cytoadherence. Developing gametocytes also sequester in deep tissues before reentering circulation to mediate transmission, and they too are characterized by protein export, deformability changes, and likely cytoadherence. Although significant progress has been made in understanding remodeling changes that occur to mediate sequestration and transmission, many open questions remain.

In this work, we identified and characterized proteins involved in cellular remodeling of asexual and sexual stage parasites. We first investigated red blood cell remodeling and sequestration during blood stage development, focusing specifically on the *Plasmodium* helical interspersed sub-telomeric c (PHISTc) protein family. Using a combination of biochemistry, biophysics, flow cytometry, and microscopy, we showed that PHISTc proteins are exported to the

host cell of asexual and sexual stages and are required for the delivery of specific antigens to the surface of asexual stage infected red blood cells. Further, they play this specialized role in antigen delivery without drastically altering cellular architecture.

Next, we investigated the mechanisms that drive the transition of stiff, sequestered gametocytes into deformable, circulating gametocytes. Using biophysical and transcriptional approaches, we identified genes that are enriched or depleted in deformable gametocytes. Some of these candidate genes likely remodel the host red blood cell while others may remodel the parasite itself, with some candidates required for the formation of deformable, infectious gametocytes. We anticipate that these genes either drive or delineate the deformability transition and could represent possible targets of therapeutics or diagnostics used to reduce malaria transmission.

Together, these studies reveal both conserved and stage-specific mechanisms involved in the successful sequestration and transmission of *Plasmodium falciparum.*

TABLE OF CONTENTS

DEDICATION

To Dadima, Dadu, Naniji, and Nanaji, who planted our seeds of learning

ACKNOWLEDGEMENTS

I am grateful to many people who have played a part in my journey to becoming a scientist.

Matt Marti been an inspirational and kind mentor for the past six years. Thank you for your endless optimism, humor, and support! Your scientific creativity and enthusiasm are infectious, and your love of collaboration and bridging fields has been a great example of how to tackle big problems. I always leave our meetings (even the transatlantic ones!) with new insights and ideas. Thank you also for supporting my interests in teaching and global health, both in Boston and Brazil.

I have also had the privilege of being mentored by Manoj Duraisingh, especially in this last year. Thank you for adopting me and my PHISTc's and for setting a tremendous example of how to be a rigorous experimentalist and still have fun and take risks with science. You have created an incredible group, and I am grateful to have been part of it!

To the members of the Marti group – thank you for the many years of fun and support in and out of the lab! Thanks especially to Pierre-Yves Mantel, Karell Pellé, Regina Joice, Ilana Goldowitz, Nicanor Obaldia, Evan Meyer, Sandra Nilsson, Johan Ankarklev, Daisy Hjelmqvist, Marina Ribeiro, Ping Lui, Will Beyer, Elamaran Meibalan (especially for fun holding down the Boston fort!), Priscilla Ngotho, and Mariana De Niz. Finally, Nicolas Brancucci, thank you for being a wonderful friend, mentor, and Stop and Shop buddy, and Kassie Dantzler, thank you for being the best of friends from Stage I-V and beyond – I could not have asked for a better companion for exploring global health, baking, and New England. To the members of the Duraisingh lab – thank you for being such a great first and last home at HSPH. I could not have asked for a warmer welcome or for a more caring, engaged, collaborative lab – ice cream cakes, science(ish) songs, and nerdfests will be missed! Thanks especially to Selasi Dankwa, Caeul Lim, Markus Ganter,

Elizabeth Egan, Gabe Rangel, Christof Gruering, Estela Shabani, Cristina Moreira, Mudit Chaand, Usheer Kanjee, Jon Goldberg, Martha Clark, Adi Paul (for years of advice and dance floor inspiration!), Erik Scully, Kristen Skillman, Natasha Archer, Nicky Peterson, and Brendan Elsworth (who I can always count on for protein export insights, tofu, or great company, as needed!). Thanks also to collaborators who have made grad school such a rich learning experience – Teun Bousema, Sanna Rijpma, Lisette Meerstein-Kessel, Marilou Tetard, Benoit Gamain, Leandro Lemgruber, Dan Neafsey, Tim Straub, Jane Hung, Anne Carpenter, Stefanie Lopes, Fabio Costa, and Marcus Lacerda.

Outside of the lab, I have had wonderful support from the HSPH IID department and parasitology groups, the HMS Division of Medical Sciences, the HMS BBS program, and the HSPH BPH program. Thanks to Joann Garrido, Andi Sabarof, Maura Meager, Carmen Mejia, Kate Hodgins, Danny Gonzalez, Anne O'Shea, Maria Bollinger, and David Cardozo, and especially to Dyann Wirth for creating an incredible environment to learn how to use science to address global health problems. Thanks also to all of my fellow students and postdocs in these communities, particularly Nicole Espy, Jemila Kester, Richa Gawande, Eli Gerrick, Selina Bopp, Allison Demas, Elaine Oberlick, Jamie Lahvic, Evan O'Loughlin, Marc Presler, and Diana Cai. Finally, Sheena Shah-Simpson, thank you for many fun times and always great advice – I am so grateful to have you as part of my home and lab family! And to my students and fellow volunteers in the HMS HPREP program – thank you for being my biggest reminders of how cool, and important, biology really is.

I am grateful to my Dissertation Advisory Committee, Marcia Goldberg, Jacquin Niles, and Manoj Duraisingh, for their constant support, thoughtful questions, and advice, and to my Dissertation Defense Committee, Jeff Dvorin, Dyann Wirth, and Dan Goldberg. From earlier

science years – thanks to Joy Killough, Shuguang Zhang, Hidde Ploegh, and Jose Gomez-Marquez.

Finally, thank you to the incomparable Ravel-Agnihotri clan for artisan-crafted jokes, regular inquiries about the health of my parasites, and never-ending love and encouragement, and to Baba, for guiding all. Mom and Dad, thank you for teaching us that it's always the time to explore and for inspiring me with your unique paths to using education to serve. Annu, thank you for being the best little (and sometimes big) sister and for a lifetime of true friendship, advice, hugs, and nargles. Aseema, thank you for being such a source of strength and joy and for inspiring me with your love for the beauty and limitlessness of science.

LIST OF FIGURES AND TABLES

FIGURES

CHAPTER 1

CHAPTER 2

CHAPTER 3

TABLES

CHAPTER 2

CHAPTER 3

LIST OF ABBREVIATIONS USED

BSD: Blasticidin S deaminase
CAM: Calmodulin
DD: Destabilization domain
DHODH: Dihydroorotate dehydrogenase
ER: Endoplasmic reticulum
GO: Gene ontology
HA: hemagglutinin
IFA: Immunofluorescence assay
MACS: Magnet-activated cell sorting
MC: Maurer's cleft
PEXEL: *Plasmodium* export element
PNEP: PEXEL-negative exported protein
PPM: Parasite plasma membrane
PV: Parasitophorous vacuole
PVM: Parasitophorous vacuole membrane
qRT-PCR: Quantitative reverse transcriptase polymerase chain reaction
RBC: Red blood cell
SEM: Scanning electron microscopy
SMFA: Standard membrane feeding assay
TEM: Transmission electron microscopy
WT: Wild type

CHAPTER 1: INTRODUCTION

Deepali Ravel[1], Kathleen Dantzler[1], Matthias Marti[1, 2]

[1]Department of Immunology and Infectious Disease, Harvard T.H. Chan School of Public Health, Boston, MA, USA
[2]Wellcome Centre for Molecular Parasitology, Institute of Infection, Immunity & Inflammation, University of Glasgow, Glasgow, UK

Author contributions

D. Ravel wrote sections 1.1., 1.3., and 1.5. D. Ravel and K. Dantzler co-wrote portions of section 1.2. and 1.4., with input from M. Marti, as part of a review article published in 2015 in Current Opinions in Microbiology (Dantzler et al., 2015). D. Ravel adapted sections 1.2. and 1.4. for inclusion in this thesis. Figure 1 is from a review article published by our lab (Nilsson et al., 2015).

1.1. Global malaria burden, control, and eradication

The parasite *Plasmodium falciparum* causes the most severe form of malaria, leading to 212 million new cases and 429,000 deaths in 2015. The greatest burden of mortality occurs in vulnerable populations, particularly young children and pregnant women in sub-Saharan Africa (WHO, 2016). Four additional species of *Plasmodium,* most notably *Plasmodium vivax*, also contribute substantially to malaria burden world-wide (Keeling and Rayner, 2015). In recent decades, there has been substantial progress in reducing the global burden of malaria, largely due to the introduction of insecticide-treated bed nets, artemisinin-based antimalarial drugs, and other biological and public health interventions (WHO, 2016). However, progress towards malaria control, elimination, and eventual eradication is threatened by the emergence of drug and insecticide resistance, the absence of a highly effective vaccine, and the presence of a large asymptomatic reservoir (Lindblade et al., 2013). These challenges demand the development of

new treatments and make effective transmission-blocking interventions particularly important to any malaria elimination or eradication program. To develop such tools, a deepened understanding of the biology of disease-causing and transmissible parasite stages is essential (Alonso et al., 2011).

1.2. Life cycle of *Plasmodium falciparum* parasites

P. falciparum has a complex life cycle, in which asexual replication and sexual development take place in red blood cells (RBCs) of the human host and sexual reproduction takes place in the mosquito vector (Figure 1). Although the asexual blood stages are responsible for all morbidity and mortality, successful transmission is dependent on generation of the sexual stages, termed gametocytes. To begin blood stage infection, invasive forms termed merozoites enter red blood cells and mature into the subsequent asexual stages: rings, trophozoites, and schizonts. Rings stage parasites are found in circulation, while the older trophozoite and schizonts stages sequester in host tissues across the body (Aingaran et al., 2012). As blood stage parasites replicate asexually, a small fraction divert away from asexual multiplication and towards sexual development in each replication cycle. This life cycle switch is driven by genetic, epigenetic, and environmental signals (Alano, 2007). Sexual stages mature through five morphologically distinct stages, with stages I-IV found sequestered in tissues and mature male and female stage V parasites found in circulation, where they can be ingested by mosquitos (Joice et al., 2014).

Once in the mosquito, gametocytes are activated to form gametes, which fuse to form the zygote. Zygotes then develop into ookinetes, which are motile and invade the mosquito midgut wall to form oocysts. Within the oocysts, sporozoite forms develop before migrating to the salivary gland and being injected into a new host during a blood meal. In the human, these sporozoites travel first to the liver, where they undergo several rounds of asymptomatic amplification before

bursting from liver cells as merozoites and entering the bloodstream to commence asexual replication (Nilsson et al., 2015).

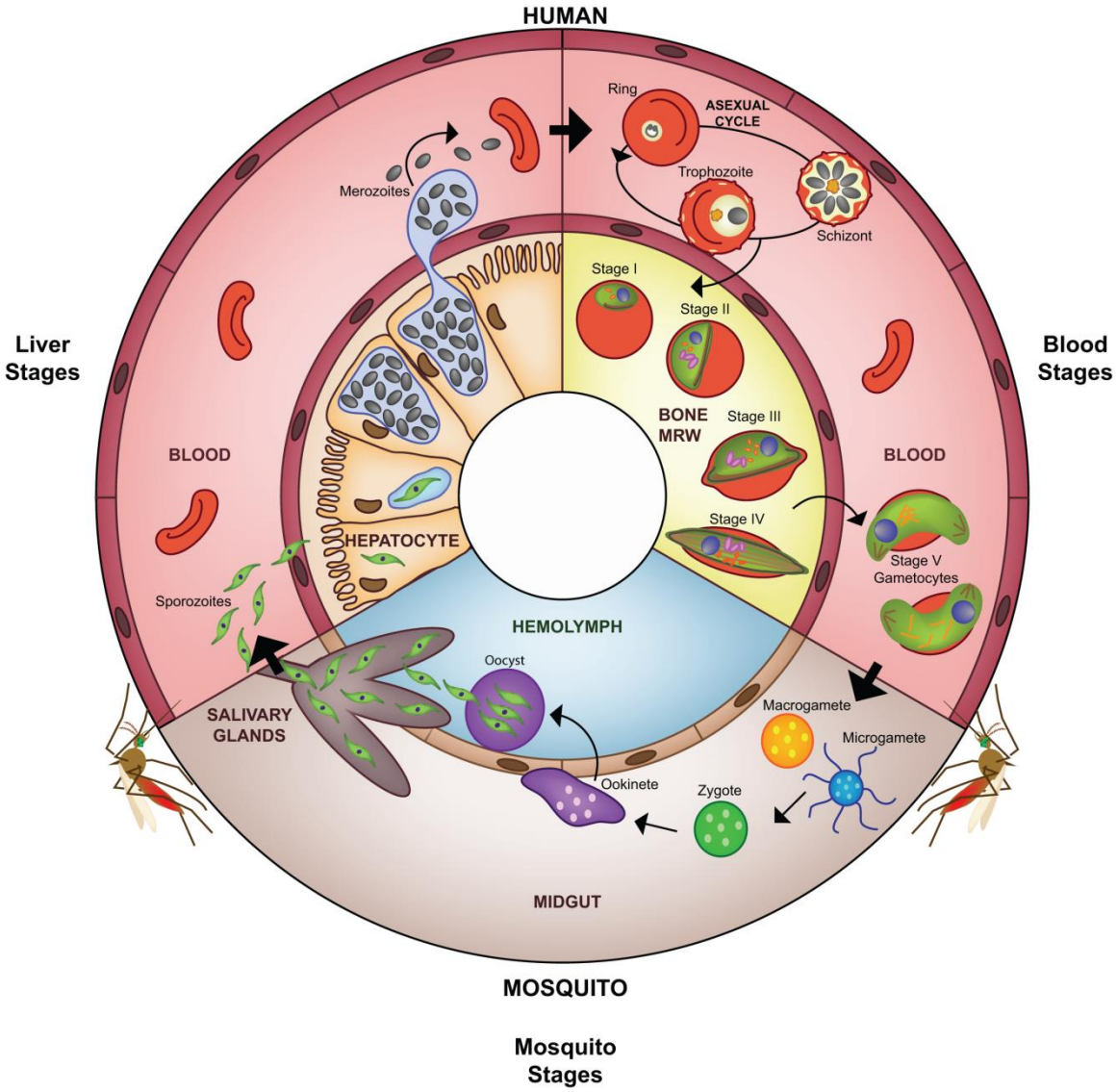

Figure 1. Life cycle of Plasmodium falciparum. Reprinted from [Nilsson, S.K., et al., Targeting Human Transmission Biology for Malaria Elimination. PLoS Pathog, 2015. 11(6): p. e1004871]. The malaria parasite is transmitted to the human host when an infected female Anopheles mosquito takes a blood meal and simultaneously injects a small number of sporozoites into the skin. After reaching the liver, the sporozoites invade hepatocytes in which they develop into a liver schizont and replicate asexually. After about seven days of liver stage development, each infected hepatocyte releases up to 40,000 merozoites that enter the peripheral blood stream. Once in the blood stream, merozoites quickly invade circulating red blood cells (RBCs), thereby initiating the repeated asexual replication cycle. Over the course of 48 hours, the parasite progresses through the ring and the trophozoite stages before finally replicating into 8–32 daughter merozoites at the schizont stage (schizogony). At this point, the parasitized RBC (pRBC) ruptures and releases merozoites into circulation, commencing another round of asexual replication. Mature asexual stages that display increased stiffness, trophozoites and schizonts, adhere to the vasculature in various organs, which allows them to avoid splenic clearance. During each cycle, a small subset

Figure 1 (continued).
of parasites divert from asexual replication and instead produce sexual progeny that differentiate the following cycle into male and female sexual forms, known as gametocytes. A subset of parasites leave the peripheral circulation and enter the extravascular space of the bone marrow, where gametocytes mature and progress through stages I–V over the course of eight to ten days (gametocytogenesis). By stage V, male and female gametocytes re-enter peripheral circulation, in which they become competent for infection to mosquitoes. Once ingested by a mosquito, male and female gametocytes rapidly mature into gametes (gametogenesis). Within the midgut, the male gametocyte divides into up to eight flagellated microgametes (exflagellation), whereas the female gametocyte develops into a single macrogamete. Fertilization of a macrogamete by a microgamete results in the formation of a zygote, which undergoes meiosis and develops into an invasive ookinete that penetrates the mosquito gut wall. The ookinete forms an oocyst within which the parasite asexually replicates, forming several thousand sporozoites (sporogony). Upon oocyst rupture, these sporozoites migrate to the salivary glands, where they can be transmitted back to the human host during a blood meal. Asexual parasites (in RBCs) are represented in pale yellow, sexual parasites in green.

1.3. Remodeling and sequestration during asexual growth

The development of *P. falciparum* asexual stage parasites is marked by extensive remodeling of the host cell, and this remodeling is essential for survival and sequestration of parasites in humans. Cellular remodeling accomplishes several goals, including acquisition of nutrients and avoidance of splenic filtration. In order to mediate nutrient and waste exchange, malaria parasites secrete transporters to the surface of the red blood cell (Desai, 2014; Nguitragool et al., 2011). Because red blood cells lack machinery for protein trafficking, the parasite must first establish a trafficking system *de novo*. This process includes the synthesis of parasite-derived organelle-like structures as well as changes to the erythrocyte membrane and cytoskeleton; these changes, combined with the presence of the large intracellular parasite, then increase the stiffness of the infected red blood cell. To avoid passage through the spleen (where stiff or damaged cells are cleared), parasites also secrete adhesins to the red blood cells surface, which can then bind to receptors on the endothelial cell lining of blood vessels to mediate sequestration. The secretion of these adhesins is a complex process and leads to further stiffening of the red blood cell (Maier et al., 2009). In addition to mediating avoidance of splenic clearance, cytoadherence enables sequestration of parasites in specific tissues as well as binding of infected cells to uninfected cells (termed rosetting), processes that may also promote parasite survival.

Remodeling of the red blood cell during asexual stages begins with the trafficking of proteins from the parasite into the host. Some of these proteins are effectors that will directly mediate changes to the host cell, while many other proteins are components of the complex protein trafficking machinery (Maier et al., 2008). Indeed, it has been predicted that there are about 550 exported proteins, accounting for 10% of the proteome (Spielmann and Gilberger, 2015). To reach the host cell, exported parasite proteins must first pass through the parasite endoplasmic reticulum

(ER), the parasite plasma membrane (PPM), the parasitophorous vacuole (PV), and the parasitophorous vacuole membrane (PVM). An N-terminal signal sequence mediates transport of proteins to the ER (Wickham et al., 2001), and a conserved N-terminal export signal, called the *Plasmodium*-export element (PEXEL) or host-targeting sequence (HT), mediates transfer of proteins through the PVM (Hiller et al., 2004; Marti et al., 2004). At the PVM, the *Plasmodium* translocon of exported proteins (PTEX) transports PEXEL proteins, as well as proteins lacking a PEXEL-motif (termed PEXEL-negative exported proteins, or PNEPs), into the host cell (Beck et al., 2014; de Koning-Ward et al., 2009; Elsworth et al., 2014).

After reaching the host cell, exported proteins destined for the red blood cell membrane or cytoskeleton are thought to diffuse through the host cell as part of chaperone-containing complexes (Knuepfer et al., 2005a, b). Many of these exported proteins will be directed through parasite-derived structures in the host cell called Maurer's clefts (MC). Maurer's clefts are membranous structures that extend from the PVM and eventually anchor to the cytoskeleton under the host membrane (Wickert and Krohne, 2007). These structures are thought to act as a sorting depot for proteins. Vesicles have been observed budding from Maurer's clefts, and the Maurer's clefts are connected to the host cytoskeleton by actin filaments and parasite protein-containing structures called tethers. It is thought that surface proteins are trafficked from Maurer's clefts to the red blood cell membrane and cytoskeleton either through these vesicles or along tethers or filaments (McMillan et al., 2013; Wickert et al., 2003). J-dots are another more recently characterized trafficking structure; these highly mobile compartments in the host cell contain parasite chaperone proteins and are thought to mediate transport of proteins to or from the Maurer's clefts (Kulzer et al., 2012; Kulzer et al., 2010; Zhang et al., 2017).

This extensive trafficking system allows for the secretion of parasite-encoded antigens to the red blood cell surface. These proteins include members of large variable surface antigen families like the *P. falciparum* erythrocyte membrane protein-1 (PfEMP1) proteins, repetitive interspersed family (RIFIN) proteins, sub-telomeric variable open reading frame (STEVOR) proteins, and surface-associated interspersed family (SURFIN) proteins (Wahlgren et al., 2017). Of these, PfEMP1 is the major virulence protein, and it binds endothelial cell receptors such as CD36 and ICAM-1 to mediate cytoadherence (Rowe et al., 2009). To avoid immune recognition of the surface-exposed PfEMP1 proteins, parasites encode for about 60 PfEMP1 variants, which they express by mutual exclusion. To promote binding, PfEMP1 is displayed on the red blood cell surface by structures called knobs, which are electron-dense protrusions of the erythrocyte membrane that also contribute to increased stiffness of the red blood cell (Crabb et al., 1997; Pologe et al., 1987). Several other parasite proteins also associate with the red blood cell cytoskeleton and membrane to decrease deformability (Glenister, 2002; Maier et al., 2008; Mills et al., 2007).

Importantly, remodeling changes during asexual development are also major contributors to malaria pathogenesis. Cytoadherence of parasites in microcapillaries can lead to occlusion of blood flow and induce inflammation and endothelial activation (MacPherson et al., 1985; Turner et al., 1998; Turner et al., 1994). When this cytoadherence occurs in the brain, these changes can lead to cerebral malaria and have lethal consequences. Recently, it has been shown that parasite cytoadherence during cerebral malaria is specifically mediated by binding of PfEMP1 molecules to endothelial protein C receptor (EPCR) (Turner et al., 2013). During placental malaria, a PfEMP1 variant called VAR2CSA instead binds to a receptor on the placenta called chondroitin sulfate A, leading to increased risk of death for both the mother and fetus (Desai et al., 2007; Duffy et al.,

2006; Fried and Duffy, 1996). Because sequestration is so closely linked to pathogenesis, interventions that target asexual remodeling changes, such as vaccines directed toward antigens like PfEMP1 or drugs that disrupt protein trafficking, would therefore have the potential to significantly reduce morbidity and mortality due to malaria infection.

1.4. Remodeling and sequestration during sexual development

During gametocyte development, the host erythrocyte also undergoes remodeling and sequestration, although the parasite-derived structures and processes that drive these changes are poorly understood.

Previous qualitative analyses established the presence of immature *P. falciparum* gametocytes in the bone marrow and spleen of infected individuals (Smalley et al., 1981; Thomson and Robertson, 1935), but quantitative information about gametocyte sequestration and remodeling has only been obtained recently. The recent studies, including a case study of a patient with subacute malaria (Farfour et al., 2012), an autopsy study looking at different sequestration sites in children who died from cerebral malaria (Aguilar et al., 2014; Joice et al., 2014), and a study of bone marrow aspirates of children with nonfatal malarial anemia (Aguilar et al., 2014), together demonstrate by histology and transcript abundance that gametocytes are enriched in the bone marrow parenchyma. In the cerebral malaria study, the majority of bone marrow gametocytes in most patients localized at erythroblastic islands, specialized sites of erythropoiesis, and a minority of gametocytes appeared to be developing inside erythroid precursor cells (Joice et al., 2014). These data suggest that gametocytes can develop in the bone marrow parenchyma before returning to circulation as Stage V gametocytes, but they leave open which parasites (asexually or sexually committed) migrate to the bone marrow. Transcriptional profiling from malaria-infected patient blood demonstrates quantitative presence of a young gametocyte population in circulation,

intimating that at least a subset of these stages are homing to the bone marrow (Pelle et al., 2015). However, presence of asexual stage parasites in the bone marrow parenchyma and formation of gametocytes in erythroid precursor cells *in vitro* (Joice et al., 2014; Peatey et al., 2013) suggests that the bone marrow may also represent a reservoir for asexual replication and gametocyte formation.

In addition to changing location, gametocytes undergo a marked change in morphology and deformability during maturation. Beginning as a round form indistinguishable from asexual stages (termed Stage I), they then develop through several transition stages (Stages II/III) to an elongated spindle form (Stage IV) and finally, the curved sausage-like mature form seen in circulation (Stage V) (Hawking et al., 1971; Sinden et al., 1978). Three groups have recently characterized the mechanical properties of these distinct morphological stages, using filtration through a bead matrix, micropipette aspiration and ektacytometry to show decreased gametocyte-infected red blood cell deformability during Stage I-IV and restored deformability during or prior to Stage V (Aingaran et al., 2012; Dearnley et al., 2012; Tiburcio et al., 2012a). Association and dissociation of polymorphic STEVOR proteins from the infected red blood cell membrane along with changes to the parasite actin and microtubule cytoskeletons correlate with the rigidity switch from Stage IV to V, suggesting a possible role for these proteins in gametocyte deformability. Computational modeling based on infected red blood cell deformability predicts that immature gametocytes cannot pass through sinusoidal slits during splenic filtration (Aingaran et al., 2012), corresponding to the stages observed to sequester in patient studies.

The mechanisms by which gametocytes enter and leave the bone marrow are poorly understood. While we expect that the youngest gametocytes must cytoadhere to the bone marrow endothelial lining in order to leave circulation, only limited binding of early gametocytes to human

endothelial cell lines or to CD36 and ICAM-1 has so far been demonstrated (Silvestrini et al., 2012; Tiburcio et al., 2012b). Further evidence for a gametocyte-specific sequestration mechanism includes minimal levels of PfEMP1 on the surface of early gametocyte-infected red blood cells and downregulation of *var* genes (responsible for PfEMP1 expression) (Tiburcio et al., 2012b). However, as in asexual stages, gametocytes are marked by massive export of proteins into the host cell. Both forward and reverse genetic studies support a role for gametocyte-specific proteins, including the PfGEXPs, which are expressed during early sexual differentiation (Silvestrini et al., 2010), in gametocyte host cell remodeling (Ikadai et al., 2013; Morahan et al., 2011). Our group has recently provided evidence for the existence of immunogenic proteins on the surface of immature gametocytes (Dantzler, 2017), further supporting the possibility that cytoadherence is important for gametocyte sequestration. Interestingly, several of these putative gametocyte surface antigens are shared between asexual and asexual stages, while others are gametocyte-specific.

The mechanisms by which protein export and remodeling occur in asexual and sexual stages are also at least somewhat conserved. As in asexual stages, PEXEL motifs guide the export of proteins into the host cytoplasm of gametocytes. There is evidence for the presence of Maurer's clefts in the gametocyte cytoplasm as well, although some markers of asexual stage Maurer's clefts are not found on clefts in gametocytes (McRobert et al., 2004). The ultrastructure of Maurer's clefts has also been suggested to differ between asexual and gametocyte stages, further pointing towards some differences in protein trafficking (Alano, 2007; Bannister et al., 2005; McRobert et al., 2004). Similarly, the presence of knobs on early gametocytes has been disputed, although their absence on mid- and late-stage gametocytes is generally accepted (Sinden, 1982). As the molecular underpinnings of gametocyte sequestration and circulation are unraveled, these processes may be targeted as part of novel transmission-blocking strategies.

1.5. Summary and aims of the thesis

Cellular remodeling is an essential process to mediate *P. falciparum* survival and sequestration in the human host as well as transmission to the mosquito vector. Remodeling enables the sequestration of mature asexual stages as well as immature sexual stages, with protein trafficking, cytoadherence, and deformability changes accompanying sequestration. Further remodeling then accompanies the release of mature gametocytes from sequestration into circulation to complete transmission. In this dissertation, we identify genes involved in both conserved and stage-specific mechanisms of cellular remodeling.

In the first study, we investigated red blood cell remodeling and sequestration during blood stage development, focusing specifically on the *Plasmodium* helical interspersed sub-telomeric c (PHISTc) protein family. We aimed to answer the question: What is the contribution of PHISTc proteins to *P. falciparum* cytoadherence and deformability? We used biophysical, cell biological, and biochemical approaches to show that PHISTc proteins are exported to the host cell of asexual and sexual stages and required for the delivery of specific antigens, including PfEMP1, to the surface of asexual stage infected red blood cells. Further, they play this specialized role in antigen delivery without altering deformability and cellular architecture. These results thus suggest that PHISTc proteins are indeed required for cytoadherence and sequestration of blood stage parasites.

In the next study, we investigated the mechanisms that drive the transition of stiff, sequestered gametocytes into deformable, circulating gametocytes. We aimed to answer two major questions: (1) What factors mediate the deformability changes separating sequestering and circulating gametocytes? and (2) Are there specific markers for deformable, circulating gametocytes that are capable of infecting mosquitos? Here, we optimized an assay to measure gametocyte deformability and then combined biophysical and transcriptional approaches to define

the transition from immature non-infectious to mature infectious gametocyte. We have identified several putative markers of deformable, infectious gametocytes and have introduced several genes that could drive immature gametocyte stiffness or mature gametocyte deformability. The transcriptomic data sets generated in this study also provide many opportunities to answer new questions relating to genetic correlations between deformability and infectiousness of mature gametocytes. We anticipate that genes identified in this study could serve as targets of novel transmission-blocking interventions and diagnostics.

Through these studies, we aim to gain insights into both conserved and stage-specific cellular remodeling mechanisms involved in the successful sequestration and transmission of *Plasmodium falciparum.*

CHAPTER 2: PHISTC PROTEINS ARE REQUIRED FOR DELIVERY OF ANTIGENS TO THE SURFACE OF *PLASMODIUM FALCIPARUM*-INFECTED RED BLOOD CELLS

Deepali Ravel[1], Pierre-Yves Mantel[2], Leandro Lemgruber[3], Marilou Tetard[4], Kathleen Dantzler[1], Brendan Elsworth[1], William Beyer[3], Marie-Claude Laffitte[3], Nicolas Brancucci[3], Benoit Gamain[4], Manoj Duraisingh[1], Matthias Marti[1, 3]

[1]Department of Immunology and Infectious Disease, Harvard T.H. Chan School of Public Health, Boston, MA, USA
[2] Unit of Anatomy, Université de Fribourg, Fribourg, Switzerland
[3]Wellcome Centre for Molecular Parasitology, Institute of Infection, Immunity & Inflammation, University of Glasgow, Glasgow, United Kingdom
[4]Université Sorbonne Paris Cité, Université Paris Diderot, Inserm, INTS, Unité Biologie Intégrée du Globule Rouge, Laboratoire d'Excellence GR-Ex, Paris, France.

Author attributions

D. Ravel designed all assays included in this chapter under the mentorship of M. Marti and M. Duraisingh.

D. Ravel performed and analyzed all assays included in Figure 3, Figure 4, Figure 5, Figure 6B, Figure 8, Figure 9, Figure 13. P. Mantel generated the transgenic lines presented in Figure 2 and Figure 11A-B, and D. Ravel generated clones of these lines and performed all assays shown in Figure 2 and Figure 11; N. Brancucci assisted D. Ravel with Southern blotting included in Figure 2C. L. Lemgruber performed electron microscopy (with samples prepared by D. Ravel) included in Figure 7 and Figure 12. M. Tetard (under the mentorship of B. Gamain) performed qRT-PCR assays (with samples prepared by D. Ravel) included in Figure 6A. K. Dantzler collected the patient serum samples used in Figure 5A. D. Ravel generated the plasmids and transgenic parasites included in Figure 10 with assistance from W. Beyer, M. Laffitte, and B. Elsworth. D. Ravel wrote the text and generated all figures and tables included in this chapter.

2.1. Abstract

Plasmodium falciparum extensively remodels its host cell to mediate nutrient exchange and avoid immune and splenic pressure during blood stage infection. This remodeling includes changes to the adhesive and biophysical characteristics of infected cells and is mediated by exported parasite proteins. Here, we investigate the role of *Plasmodium* PHISTc proteins in erythrocyte remodeling. PHISTc proteins are exported and contain a helical core domain shared by all PHIST paralogs. They are conserved across primate malarias, and several are expressed in both asexual and sexual blood stages, suggesting conserved function in host pathogen interactions. While several proteins from the PHISTb sub-class have a role in cellular rigidity or cytoskeletal architecture, little is known about the function of PHISTc proteins. To investigate the role of PHISTc proteins in asexual and sexual stage remodeling, we knocked out 9 of the 16 *P. falciparum* paralogs in the reference line 3D7 and knocked out a subset of these in a second line, CS2. Flow cytometry showed that 6 of the 9 PHISTc knock outs have decreased asexual surface reactivity to serum from malaria patients, suggesting that they are required for efficient surface antigen trafficking. Of these 6 PHISTc knockouts with decreased surface antigen display, 2 showed a complete absence of the VAR2CSA PfEMP1 variant at the erythrocyte surface by flow cytometry and immunofluorescence microscopy while 2 others showed normal VAR2CSA display. These data suggest differential specificity for surface antigen delivery between PHISTc proteins. Finally, microsphere filtration showed that none of the 9 PHISTc genes studied affects cellular rigidity of asexual stages, and immunofluorescence microscopy showed that PHISTc disruption also does not affect trafficking of knob or Maurer's clefts markers. Further, immunofluorescence microscopy of epitope-tagged PHISTc proteins shows that they are exported to punctate structures in the host cells during asexual and sexual stages; in asexual sexual stages PHISTc proteins localize first to

the Maurer's clefts and then to distinct structures. Altogether our observations suggest that PHISTc proteins play a specialized role in antigen delivery to the host cell surface without drastically altering cellular architecture and that this role may be conserved across asexual and sexual stage development.

2.2. Introduction

The PHIST, or *Plasmodium* helical interspersed subtelomeric, family is one of the largest families of exported proteins in the *Plasmodium* genus. PHIST proteins were originally identified based on the presence of a conserved helical domain of about 150 amino acids (refered to as the PHIST domain) (Sargeant et al., 2006). Structural predictions suggest that the PHIST domain forms a four helix bundle, which has been experimentally confirmed by structural studies of one PHIST protein, PFI1780w (Oberli et al., 2014). Outside of this conserved domain, PHIST proteins vary widely with respect to sequence, presence of additional domains, expression, subcellular localization, and function. They have been implicated in cytoadherence, rigidity, resistance to heat shock, formation of gametocytes, and other diverse functions. In *P. falciparum,* there have been at least 89 PHIST proteins identified to date (Warncke et al., 2016), representing roughly 2% of its proteome. Despite this large representation in the proteome, most members of the PHIST family remain unstudied. An excellent review of known biology and phylogeny of the PHIST family was presented recently by Warncke et al. (2016).

PHIST proteins are further divided into three main subfamilies – PHISTa, b, and c – based on the presence and position of several conserved tryptophan residues within the PHIST domain. Proteins from the PHISTa subfamily have only been identified in *P. falciparum*. PHISTa proteins are fairly small, containing only a signal sequence and/or PEXEL motif in addition to a PHIST domain. While a few PHISTb proteins have been identified in *P. vivax* and *P.knowlesi,* the

subfamily is significantly expanded in the *P. falciparum* lineage (Sargeant et al., 2006). PHISTb proteins are also longer than PHISTa proteins, containing in several cases an additional MESA erythrocyte cytoskeleton-binding (MEC) domain, implicated in binding of several *Plasmodium* proteins to the red blood cell cytoskeleton (Kilili and LaCount, 2011; Warncke et al., 2016), or a DnaJ domain, implicated in chaperone-like activity (Botha et al., 2007). Several PHISTb proteins, most notably the DnaJ domain-containing protein RESA, have been shown to interact with the red blood cell cytoskeleton to alter cellular deformability (Diez-Silva et al., 2012; Maier et al., 2008; Mills et al., 2007; Parish et al., 2013). Finally, in contrast to the PHISTa and b subfamilies, the PHISTc subfamily appears to be ancestral, with several orthologs shared between primate malarias and with at least one ortholog each in the avian malaria parasite, *P.gallinaceum,* as well as the rodent malaria parasites, *P. berghei, P. yoelli,* and *P. chaubadi* (Frech and Chen, 2013; Sargeant et al., 2006). Proteins from the PHISTc family vary widely in size and contain no other identifiable domains outside of the PHIST domain.

Because PHISTc proteins represent ancestral members of the PHIST family and include members expressed in both asexual and sexual blood stage parasites, we have hypothesized that they play conserved roles in remodeling of red blood cells. A few members of the PHISTc subfamily have been previously investigated. One PHISTc protein, MAL7P1.172 (also refered to as PTP2), has been shown to localize to Maurer's clefts as well as vesicles budding from Maurer's clefts. Its disruption led to an absence of cytoadherence and an accumulation of PfEMP1, the major asexual surface antigen, at Maurer's clefts rather than at the red blood cell surface (Maier et al., 2008; Regev-Rudzki et al., 2013). Disruption of MAL7P1.172 was also shown to disrupt exosome-mediated communication (Regev-Rudzki et al., 2013). The PHISTc protein PF08_0137 was recently shown to be exported to the host cell and interact with resident proteins from J-dot

structures, which have been suggested to be involved in PfEMP1 trafficking (Zhang et al., 2017). Another PHISTc protein, PFI1780w, was shown to localize to foci within the host cell and to weakly interact with the conserved ATS domain of PfEMP1 (Mayer et al., 2012; Oberli et al., 2014; Oberli et al., 2016).

Hypothesizing that PHISTc proteins play a conserved role in red blood cell remodeling, we characterized the role of several members of the PHISTc protein family in surface antigen trafficking and deformability in blood stages. Using a reverse genetic approach, we knocked out 9 PHISTc proteins in 3D7, the gametocyte producing reference line, and knocked out a subset of these genes in CS2, a line amenable to PfEMP1 studies. We assayed cellular deformability as well as presence of the export structures Maurer's clefts and knobs, and we showed that they were unchanged by PHISTc disruption. Flow cytometry showed that 6 of the 9 PHISTc 3D7 knock outs have decreased asexual surface reactivity to serum from malaria patients, suggesting that they are required for efficient surface antigen trafficking. In the CS2 background, 2 PHISTc knock outs showed a complete absence of the VAR2CSA PfEMP1 variant at the erythrocyte surface by flow cytometry and immunofluorescence microscopy, while 2 others showed normal VAR2CSA display. To investigate subcellular localization of PHISTc proteins, we epitope-tagged three of the proteins that we showed have a role in antigen trafficking in asexual stages. We show that they are exported to the host cell in both asexual and sexual stages.

2.3. Results

Genetic disruption of 9 PHISTc genes in P. falciparum

In order to determine the functional role of proteins from the PHISTc family, we first took a reverse genetic approach. We attempted to knock out 11 PHISTc genes expressed in *Plasmodium falciparum* blood stage parasites by double cross-over recombination. 9 of these 11 genes were

successfully knocked out in a clone of 3D7, the gametocyte-producing *Plasmodium falciparum* reference strain, which we refer to as P2G12. The genes are: *MAL7P1.172*, *PF08_0137*, *PF10_0021*, *PF10_0022*, *PF10_0161*, *PF10_0162*, *PF10_0163*, *PF11_0503*, and *PFB0105c*. (Note: *PF10_0021 – 22* are adjacent on Chromosome 10 and were disrupted together in one line, and *PF10_0161 – 0163* are also adjacent on the chromosome and were disrupted in one line). mRNA expression across the *P. falciparum* life cycle is shown for each of these genes in Figure 2A, and the strategy for genetic disruption of each gene is shown in Figure 2B. Each line was cloned out by limiting dilution, and integration was confirmed by Southern blot (Figure 2C).

Disruption of 7 of these PHISTc genes was also attempted in the CS2 strain of *Plasmodium falciparum.* CS2 is a clone of the IT/FCR3 *P. falciparum* line, and it stably expresses the "VAR2CSA" variant of PfEMP1, for which there are defined binding phenotypes and antibodies available (Cooke et al., 1996). CS2 is therefore particularly well suited to PfEMP1 and asexual cytoadherence studies. Disruption of *MAL7P1.172, PF08_0137, PF11_0503, and PFB0105c* was successful, and each line has been cloned out and integration verified by Southern blot (Figure 2C). CS2ΔPF11_0503 and CS2ΔPFB0105c clones showed an unexpected band pattern by Southern blot, so PCR was used to confirm that the loci are disrupted (Figure 2D).

Table 1 lists the genes disrupted in this study and provides additional background information for each.

Table 1. PHISTc genes included in this study.

Gene ID	Transgenic line(s) generated	Size	Previously known function/characteristics
MAL7P1.172 (PF3D7_0731100, PTP2, GEXP11)	Knock out (3D7, CS2) Epitope-tagged (3D7)	103 kDa	Disruption leads to PfEMP1 trafficking defect and defect in exosome-mediated communication (Maier et al., 2008; Regev-Rudzki et al., 2013) Localizes to MC and vesicles budding from MC (Maier et al., 2008; Regev-Rudzki et al., 2013)
PF11_0503 (PF3D7_1148700, GEXP12)	Knock out (3D7, CS2) Epitope-tagged (3D7)	43 kDa	
PF08_0137 (PF3D7_0801000)	Knock out (3D7, CS2) Epitope-tagged (3D7)	147 kDa	Interacts with J-dot resident proteins (Zhang et al., 2017)
PFB0105c	Knock out (3D7, CS2)	35 kDa	Localizes to periphery of liver stage cells (Speake and Duffy, 2009)
PF10_0021 (PF3D7_1001700)	Knock out (3D7)	32 kDa	
PF10_0022 (PF3D7_1001800)	Knock out (3D7) Epitope-tagged (3D7)	30 kDa	
PF10_0161 (PF3D7_1016600)	Knock out (3D7)	36 kDa	Overexpressed construct localizes to foci in host cell (Tarr et al., 2014)
PF10_0162 (PF3D7_1016700)	Knock out (3D7)	98 kDa	
PF10_0163 (PF3D7_1016800)	Knock out (3D7)	38 kDa	

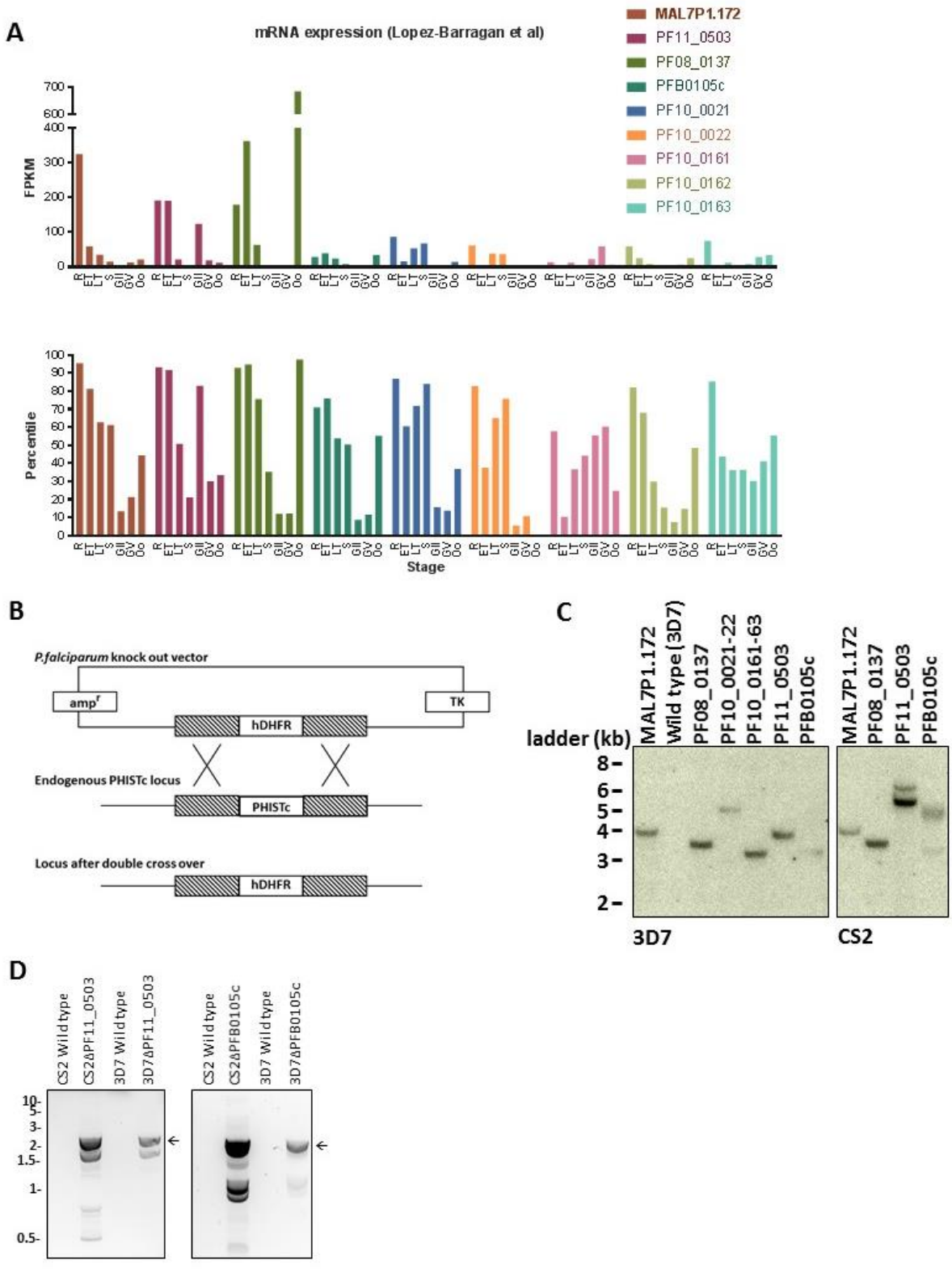

Figure 2. Genetic disruption of 9 PHISTc proteins. (A) mRNA expression across the *P. falciparum* life cycle of PHISTc genes included in this study. *P. falciparum* 3D7 parasites were Illumina-sequenced by López-Barragán et al. (2011), and transcript data was accessed from

Figure 2(continued).
Plasmodb.org on 5/20/2017. (Top) FPKM (Fragments Per Kilobase of transcript per Million mapped reads) for each gene of interest is shown. (Bottom) Percentile indicates ranking of expression for gene of interest compared to all others in sequencing experiment. R = ring, ET = early trophozoite, LT = late trophozoite, S = schizont, GII = stage II gametocyte, GV = stage V gametocyte, Oo = ookinete. (B) Strategy for generating PHISTc knock out lines. The hDHFR resistance marker was inserted into each PHISTc locus using double cross over recombination. (C) Southern blots to confirm knock out construct integration. Genomic DNA from each cloned line was extracted and digested by a unique restriction enzyme combination. Radiolabeled probe against the gene encoding the selectable marker hDHFR was used to visualize the integrated loci. (D) PCRs to confirm integration of CS2ΔPF11_0503 and CS2ΔPFB0105c. Primers were designed against the 3' region of the *PF11_0503* integrated locus and against the 5' region of the *PFB0105c* integrated locus. 3D7ΔPF11_0503 and 3D7ΔPFB0105c, which both showed a normal band pattern by Southern blot (1C), are included as positive controls for the primers. Arrows indicate bands the size of the expected products.

Disruption of PHISTc proteins does not alter deformability of the infected cell

Because several PHISTb proteins have been shown to interact with the red blood cell cytoskeleton or alter cellular deformability, we initially hypothesized that PHISTc proteins could be involved in similar remodeling processes. To measure this, we used a recently developed technique called microsphere filtration to measure deformability of our knock out lines. In these assays, red blood cells are flowed through a bead matrix, and degree of retention in the matrix is used as a measure of deformability, or "filterability" (Deplaine et al., 2011). The pore size of the bead matrix was originally optimized to mimic splenic slits, so the degree of retention in this assay specifically gives a measure of splenic retention.

We expected that contribution of individual PHISTc proteins to deformability could be small, so we performed significant optimization of the filtration assay to increase reproducibility. Technical optimization included changes to fabrication of the bead matrix, synchronization and preparation of the parasite cultures, washing protocols during filtration, and measurement of output parasitemias (protocol described in depth in the Methods section of this chapter). We used this optimized assay to perform filtration time courses with wild type parasites to establish the dynamics of deformability changes. This experiment showed the expected decrease in asexual deformability during ring and early trophozoite stages, with minimal technical variability. However, after minimizing technical variability in our filtration system, we realized that slight differences in rate of asexual development were contributing to false differences in deformability of different strains. To account for this, we used DNA content to normalize parasites by developmental stage. With this additional step, our filtration assay shows significant technical and biological reproducibility (*Figure 3*A).

Using the optimized microsphere filtration assay, we measured deformability of each of the 6 3D7 knock out lines, 3D7Δ*MAL7P1.172*, 3D7Δ*PF08_0137,* 3D7Δ*PF11_0503*, 3D7Δ*PFB0105c*, 3D7Δ*PF10_0021-22*, and 3D7Δ*PF10_0161-3,* across the course of asexual development. Somewhat surprisingly, we found that there was no significant difference in deformability between the knock out and wild-type asexual parasites (*Figure 3*B). These data demonstrated that PHISTc proteins are not required for parasite-induced changes in infected red blood cell deformability and therefore may play a different role than PHISTb proteins in red blood cell remodeling.

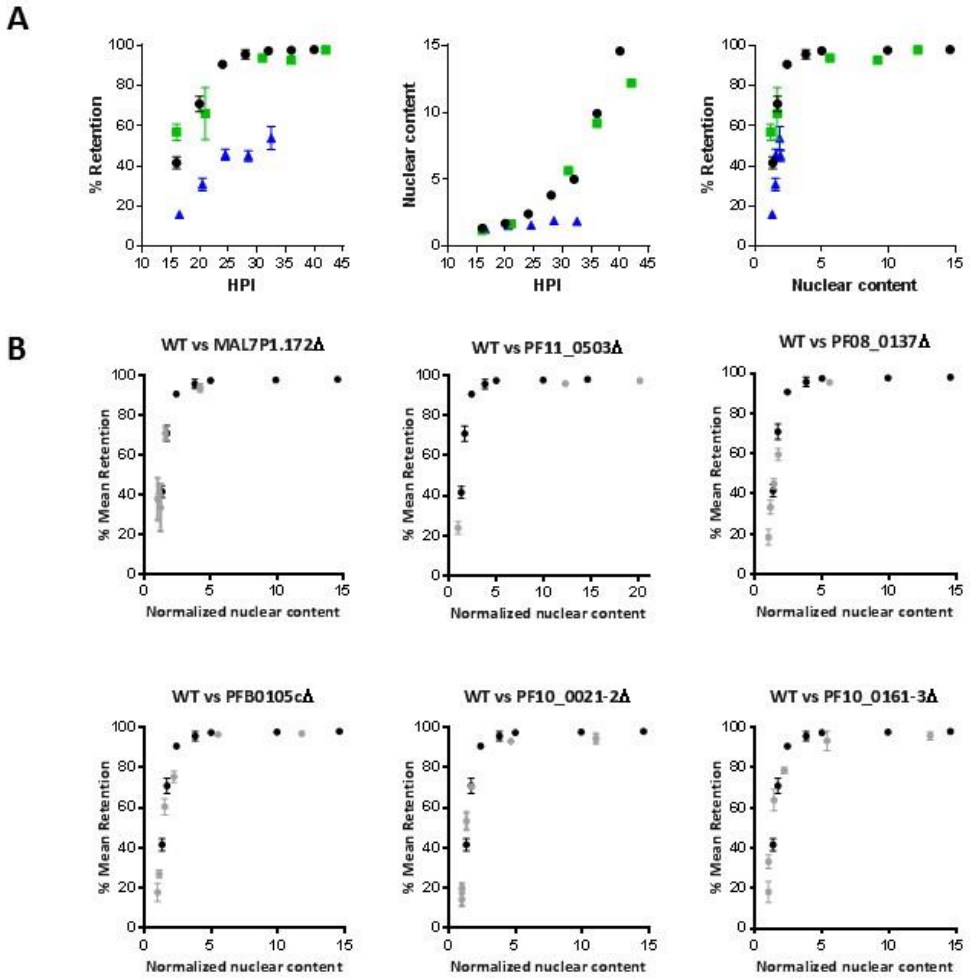

Figure 3. Contribution of PHISTc proteins to cellular rigidity. (A) Microsphere filtration was performed with wild type parasites in biological triplicate (represented in blue, green, or black). The three panels shown indicate that nuclear content can be used to "normalize" for parasite age. (B) Microsphere filtration to determine cellular rigidity of PHISTc knock out lines. Highly synchronous wild type or mutant parasites were harvested every 4 hours from 16-40 hours post invasion and assayed by microsphere filtration. Upstream and downstream populations were fixed and stained with SYBRgreen to measure parasitemia and nuclear content. Percent retention of 4 replicates was calculated for each time point and compared with nuclear content as a measure of parasite age. Wild type parasites are shown in black dots, and knock out parasites are shown in gray dots.

PHISTc proteins are not required for formation of export structures

Because we hypothesized that PHISTc proteins are involved in remodeling of the host red blood cell, we assessed whether disruption of these PHISTc proteins causes major alterations to parasite-derived structures in the host cell or relocalization of parasite-derived structural proteins. For this purpose, we used immunofluorescence (IFA) microscopy to localize i) the exported protein KAHRP, which forms the knob structure under the red blood cell membrane that displays PfEMP1 on the surface, and ii) MAHRP1, which resides in Maurer's clefts in the red blood cell cytoplasm. We found that KAHRP and MAHRP1 both had normal localization in each of the 6 knock out lines in 3D7 (Figure 4A,B), suggesting that these PHISTc genes are not necessary for formation of knobs or Maurer's clefts.

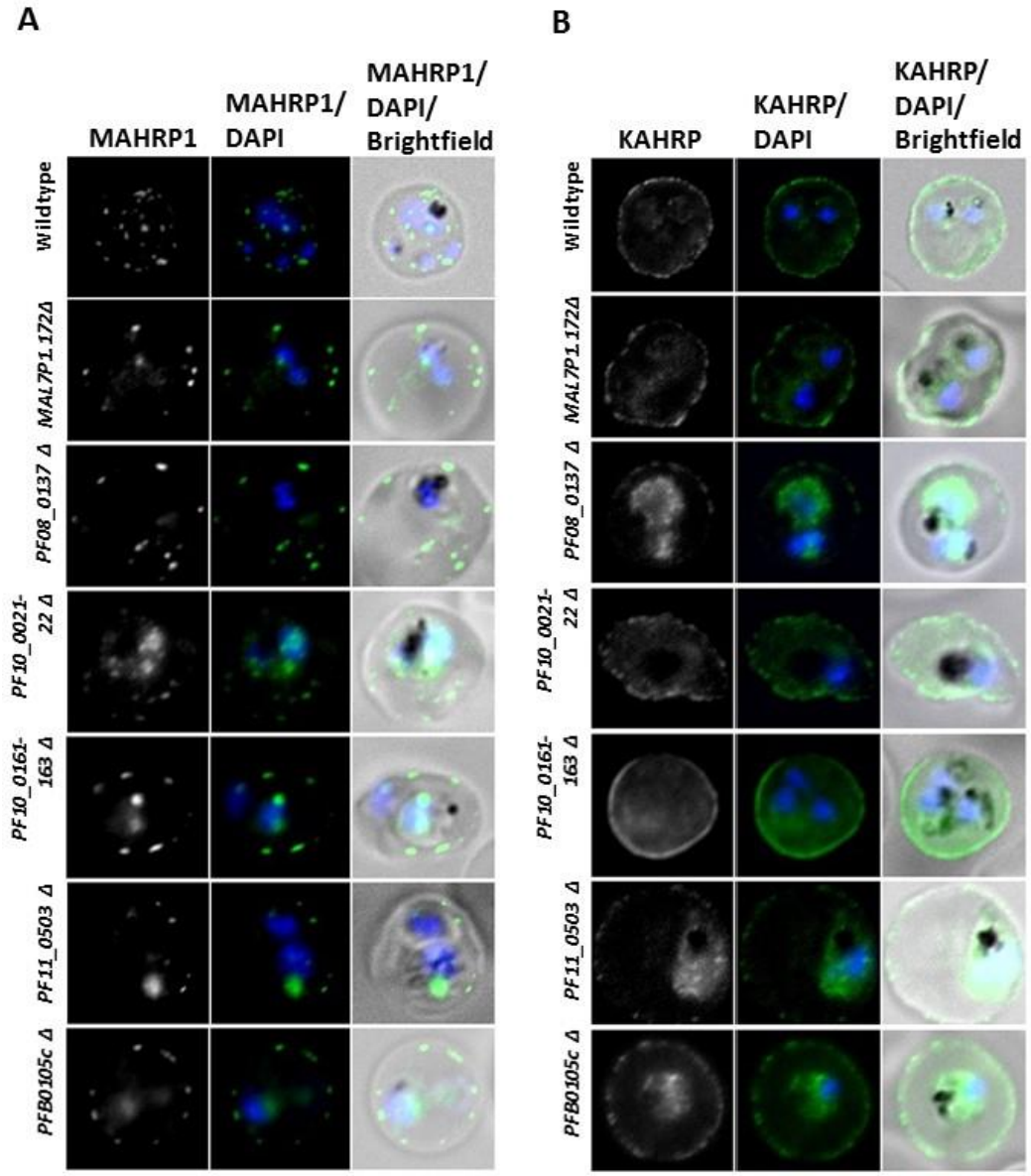

Figure 4. Contribution of PHISTc proteins to trafficking of export markers. Trophozoite stage parasites were paraformaldehyde/glutaraldehyde-fixed and Triton X-100 permeabilized. Parasites were then stained with primary antibodies against (A) MAHRP1 or (B) KAHRP and a DNA dye and analyzed by immunofluorescence microscopy. Both MAHRP1 and KAHRP appear to be exported to the host cell in all knock out lines.

PHISTc proteins are required for delivery of antigens to the surface of asexual-infected red blood cells

Because one PHISTc protein, MAL7P1.172*,* has previously been shown to play a role in antigen trafficking, we used several approaches to measure the contribution of our PHISTc proteins of interest to this process. To first broadly assess the contribution of PHISTc proteins to trafficking of asexual stage antigens to the surface of the infected red blood cell, we performed flow cytometry using immune sera collected from malaria patients in Malawi to measure reactivity against surface proteins on asexual cells. These sera have previously been used in a study in the lab and showed immune recognition of asexual and sexual stage parasites. We stained mid-trophozoite stage asexual parasites from each of the 6 3D7 knock out lines with naïve US sera and with immune sera from 6 patients. We compared median fluorescence intensity of infected parasites from each strain and compared the percent of infected parasites that were positive for surface reactivity. This showed that 3D7Δ*MAL7P1.172*, 3D7Δ*PF08_0137,* 3D7Δ*PF11_0503*, 3D7Δ*PFB0105c*, and 3D7Δ*PF10_0021-22* had significantly decreased surface reactivity, suggesting that they had decreased levels of parasite-derived antigens on their surface. One line, containing a triple knock out of *PF10_0161, PF10_0162, and PF10_0163,* showed wild-type levels of serum surface reactivity, suggesting that it had no defect in surface antigen trafficking (Figure 5A).

The major known variant surface antigens in asexual stages are PfEMP1, Rifins, and STEVORS. It has recently been demonstrated that immune responses are directed primarily against PfEMP1 (Chan et al., 2016; Chan et al., 2012), suggesting that we are detecting differences in PfEMP1 specifically. To determine whether PHISTc protein disruption specifically affects trafficking of PfEMP1, we performed IFAs and flow cytometry with the 4 CS2 knock out lines.

CS2 parasites dominantly express the VAR2CSA variant of PfEMP1 (Cooke et al., 1996), which means that specific antibodies against extracellular domains of PfEMP1 can used to detect surface expression of VAR2CSA. Using antisera against VAR2CSA to probe live asexual-infected cells (refered to as α-VAR2CSA JS), we show similar levels of VAR2CSA on the surface of CS2, CS2Δ*PF08_0137,* and CS2Δ*PFB0105c.* This suggests that *PF08_0137* and *PFB0105c* are not required for delivery of VAR2CSA to the infected cell surface. In contrast, we show that *CS2*Δ*PF11_0503* has no VAR2CSA on its surface, suggesting that *PF11_0503* is required for trafficking of VAR2CSA (Figure 5B).

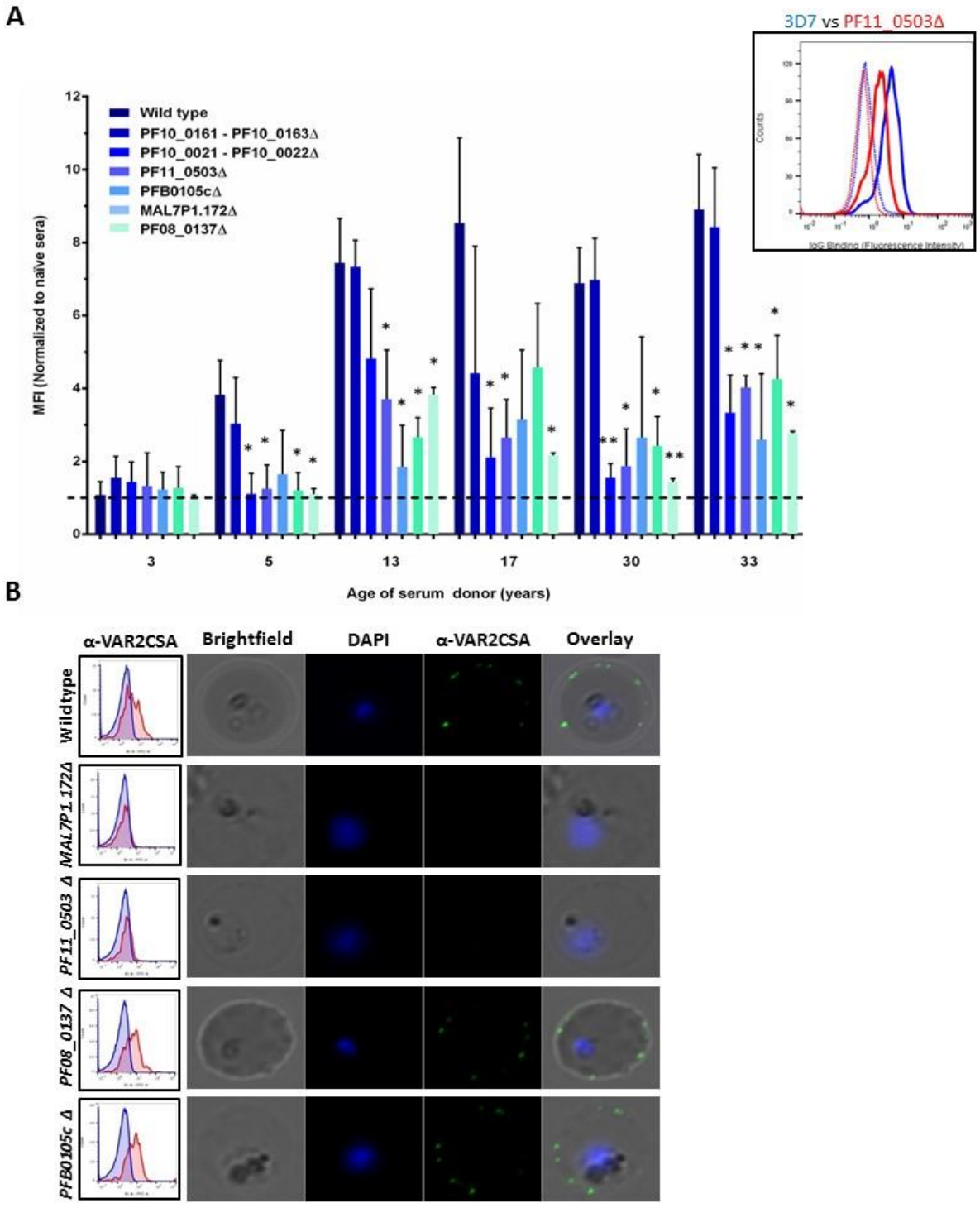

Figure 5. Contribution of PHISTc proteins to trafficking of surface antigens. (A) Immune serum surface reactivity of 3D7 wild type and PHISTc knock out asexual stages. Asexual stage parasites between 30-36 hours post invasion were stained with naïve (US) or immune (Malawian) sera and with a DNA dye (VybrantViolet). Surface reactivity was measured by flow cytometry, and median fluorescent intensity of infected cells was calculated for each sample. Data shown

Figure 5 (continued).
represents the mean of 2 technical replicates and 2 biological replicates. (* = $p<0.05$, ** = $p<0.01$). The inset shows sample histograms comparing 3D7 wild type (blue) and 3D7ΔPF11_0503 (red) parasites treated with naïve (dashed line) or immune serum (solid line). (B) PfEMP1 surface expression in CS2 wild type and knock out asexual stages. Live, unpermeablized trophozoite stage parasites (28 hours post invasion) were stained with antisera against the extracellular domain of VAR2CSA and were measured by flow cytometry and immunofluorescence microscopy. Left: Median fluorescence intensity of infected cells (red) versus uninfected cells (blue) was compared for each parasite line. Right: Representative images showing presence or absence of VAR2CSA on the surface of infected red blood cells.

To confirm that the lack of surface VAR2CSA expression in *CS2Δ*PF11_0503* is not due to an overall decrease in PfEMP1 expression or to expression of a different *var* gene, we measured RNA and protein expression of PfEMP1 in this clone. Although CS2 parasites rarely switch to expression of other *var* genes, it is possible and must be accounted for (Duffy et al., 2009). qRT-PCR analysis of ring–stage *CS2Δ*PF11_0503* from the same growth cycle as IFA and flow cytometry shows that total var gene expression levels are normal in this line and that about 50% of var gene transcripts come from *var2csa* (*Figure 6*A). This confirms that the complete absence of VAR2CSA staining is not simply due to an absence of *var2csa* mRNA expression. We also performed western blotting with trypsin treated and untreated asexual parasites using an antibody against the conserved cytoplasmic tail of PfEMP1 (refered to hereafter as α-ATS). We show that a PfEMP1 variant approximately the molecular weight of VAR2CSA is expressed in *CS2Δ*PF11_0503* (*Figure 6*B).

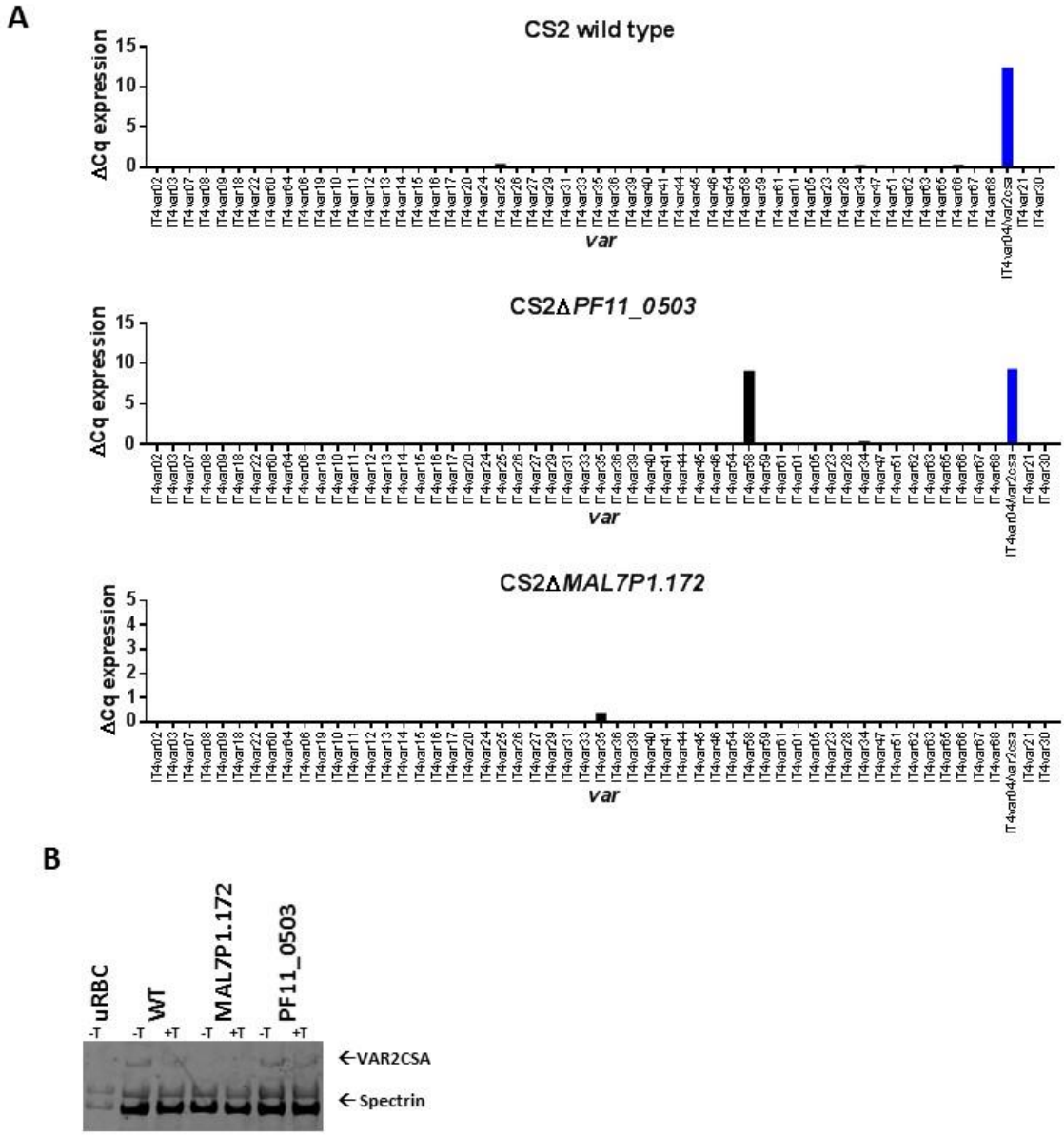

Figure 6. PfEMP1 expression of PHISTc wild-type and mutant lines. (A) qRT-PCR analysis of var gene expression of ring stage parasites from CS2 wild-type and knock out lines. VAR2CSA is indicated in blue, and other var genes are indicated in black. (B) Western blotting to show expression of PfEMP1. Trophozoite stage parasites were treated with or without trypsin (labeled –T or +T), extracted by Triton-X 100 and SDS, and probed by an anti-ATS antibody, which recognizes the intracellular domain of PfEMP1 and cross-reacts with host cell spectrin.

Although we have shown by IFA that export of Maurer's cleft and knob proteins are not disrupted by PHISTc deletion, we wanted to confirm that Maurer's clefts and knobs were truly intact in *CS2ΔPF11_0503,* where we see an absence of surface PfEMP1. To do so, we used scanning electron microscopy (SEM) and transmission electron microscopy (TEM) to show the presence of morphologically normal Maurer's cleft and knob structures in CS2 WT and *CS2ΔPF11_0503* (Figure 7A,B). This further suggests that the defect in PfEMP1 surface display is not due to a non-specific defect in remodeling of the host cell.

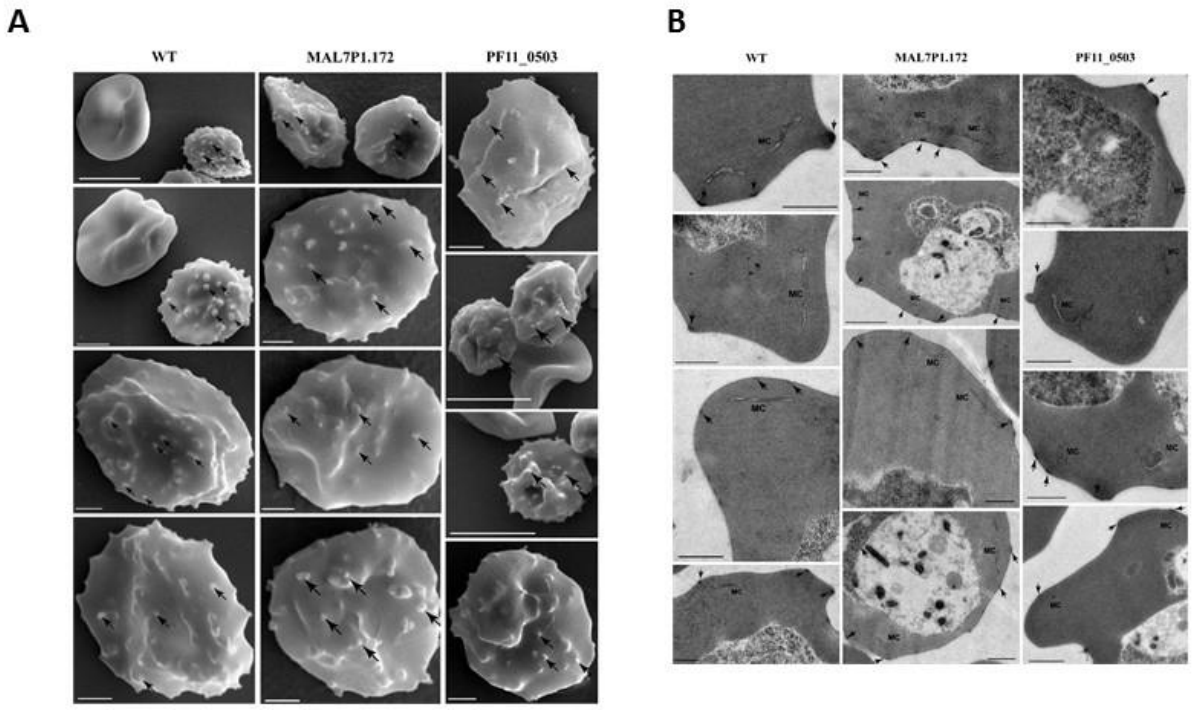

Figure 7. PF11_0503 and MAL7P1.172 contribution to infected cell ultrastructure. (A) Trophozoite stage parasite were fixed and imaged by scanning electron microscopy. Knob structures are indicated with black arrows. (B) Trophozoite stage parasite were fixed an imaged by transmission electron microscopy. Knob structures are again labeled with black arrows and Maurer's clefts are labeled "MC".

We were next interested in determining where VAR2CSA accumulates when PF11_0503 is disrupted. Maier et al (2008) previously showed an accumulation of PfEMP1 at Maurer's clefts when the PHISTc protein MAL7P1.172 was disrupted, so we hypothesized that PF11_0503 disruption might cause the same defect. To determine intracellular localization of PfEMP1 in *CS2Δ*PF11_0503*, we performed IFAs with fixed, permeabilized cells. Staining with the same VAR2CSA antibody used for analysis of live cells (α-VAR2CSA JS) showed punctate staining on or near the surface of CS2 WT cells but showed only staining of the parasitophorous vacuole (PV) and parasitophorous vacuole mebrane (PVM) in *CS2Δ*PF11_0503* asexual stage cells, suggesting accumulation of PfEMP1 within the PV/PVM (*Figure 8*A,B). However, because we suspected that this staining pattern might be due to the VAR2CSA antibody cross-reacting with another protein within the PV or PVM, we tried staining cells from a transgenic line that should have no expression of any PfEMP1 variant (Brancucci et al., 2012). We saw a similar PV/PVM staining pattern on this PfEMP1-knockdown line, suggesting to us that the VAR2CSA antibody does cross-react with proteins other than VAR2CSA within the parasite (*Figure 8*C). To overcome this technical limitation, we attempted staining of CS2 wild type and *CS2Δ*PF11_0503* parasites with three additional VAR2CSA antibodies, each of which recognize a different extracellular domain of VAR2CSA (refered to as α-VAR2CSA AS153, α-VAR2CSA AS27, and α-VAR2CSA AS37). With all three additional VAR2CSA antibodies, we obtained a similar PV/PVM staining pattern on *CS2Δ*PF11_0503 (Figure 8B).* We then tested these additional VAR2CSA antibodies and found that they also stained the PfEMP1-knockdown line (*Figure 8*C). As an alternative to these VAR2CSA antibodies, we attempted to stain CS2 WT and *CS2Δ*PF11_0503* with the α-ATS antibody against the PfEMP1 cytoplasmic domain but did not observe any signal by IFA. Although the validation of the VAR2CSA antibodies does show that they are sub-optimal for subcellular

localization studies of PfEMP1, the lack of staining at Maurer's clefts or other export structures and the presence of staining of the PV/PVM could suggest that PfEMP1 accumulates within the PV/PVM. Alternatively, PfEMP1 could accumulate in export structures but have altered permeability such that it is not visible by IFA.

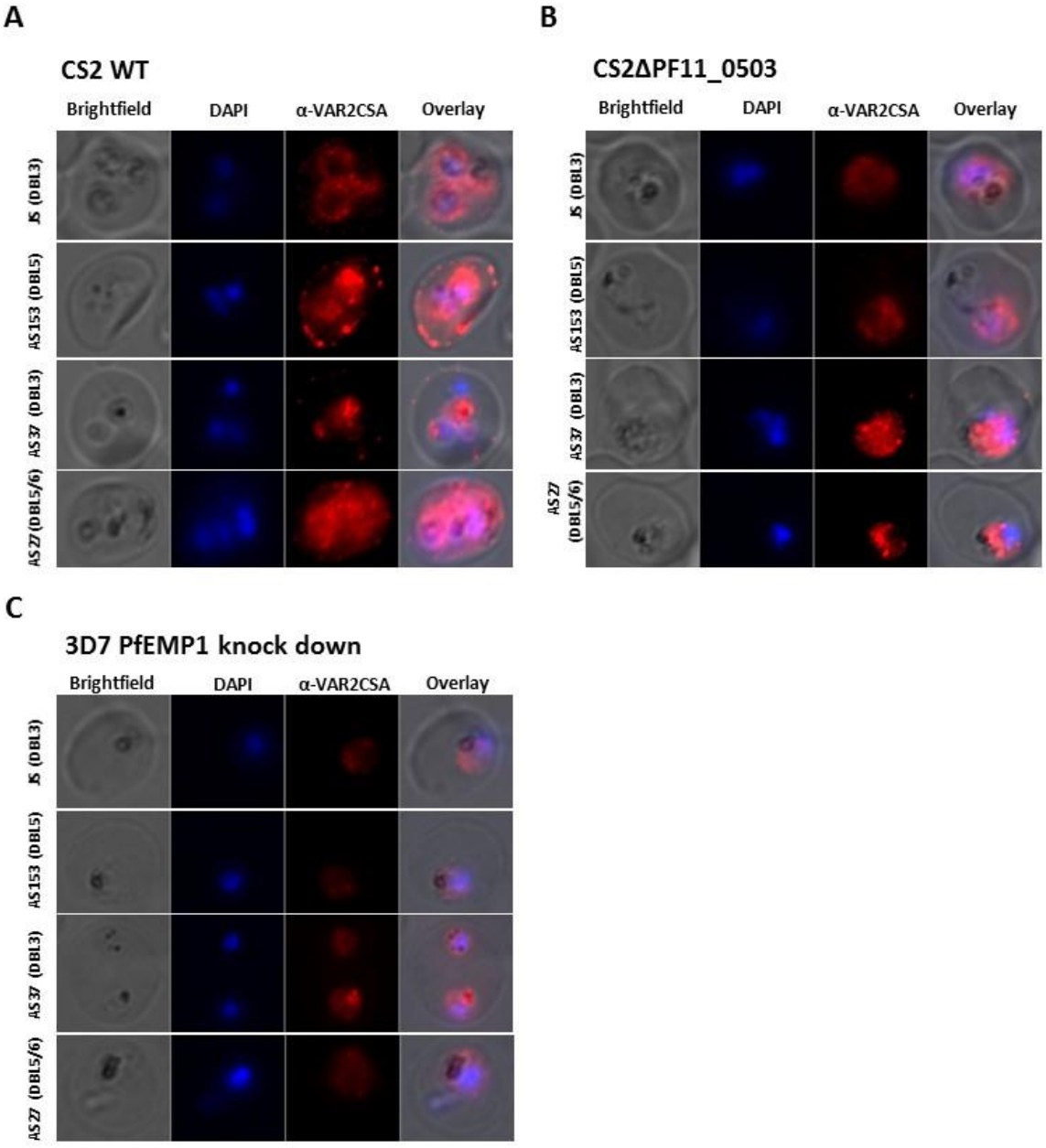

Figure 8. Localization of VAR2CSA in CS2ΔPF11_0503. Trophozoite stage parasites (32 hpi) were paraformaldehyde/glutaraldehyde-fixed and Triton X-100 permeabilized. Parasites were then stained with primary antibodies against VAR2CSA and a DNA dye and analyzed by immunofluorescence microscopy. (A) shows CS2 wild type parasites, (B) shows CS2ΔPF11_0503 parasites, and (C) shows 3D7/PfEMP1 knock down parasites.

We have also performed IFA and flow cytometry analysis to measure PfEMP1 surface expression of CS2Δ *MAL7P1.172* and observe a complete absence of surface PfEMP1 (Figure 5A), as shown previously (Maier et al., 2008). However, qRT-PCR analysis of this clone shows very low *var2csa* expression (**Figure 6**A), and we have been unable to observe VAR2CSA by western blotting (*Figure 6*B). In the original study that proposed a role for MAL7P1.172 in VAR2CSA trafficking, VAR2CSA was detected by IFA but not by western blotting (they suggested this was due to altered solubility characteristics). We are currently measuring VAR2CSA expression in additional clones of the CS2Δ *MAL7P1.172* transgenic line to identify a clone which can be used for further experiments.

To investigate whether trafficking of proteins from the Rifin or STEVOR families were disrupted by PHISTc deletion, we performed IFA analysis using antibodies against Rifins and STEVORS. Because these parasites do not express a single Rifin or STEVOR variant that can be recognized on unpermeabilized cells with an antibody against an extracellular domain (as could be done to analyze the VAR2CSA PfEMP1 variant), we used permeabilized cells and antibodies against the conserved C-terminal domains of Rifins or STEVORS. This means that we could not look specifically at surface expression of these proteins but could rather only determine whether they were still exported. We first stained live, Equinatoxin-permeabilized cells from 3D7Δ*MAL7P1.172*, 3D7Δ*PF08_0137,* 3D7Δ*PF11_0503*, 3D7Δ*PFB0105c*, 3D7Δ*PF10_0021-22*, and 3D7Δ*PF10_0161-3* with the anti-Rifin antibody*,* and we showed that all six knock out lines had the same staining at or near the red blood cell surface as wild type parasites (Figure 9). This suggests that Rifins are still exported to at or under the red blood cell surface when PHISTc proteins are disrupted. We also attempted to stain the same PHISTc knock out lines with two anti-STEVOR antibodies, but we could not detect staining on our wild-type or mutant parasites. This

is unsurprising given that unselected, culture-adapted parasites do not express high levels of STEVOR, and this anti-STEVOR antibody has been shown to give strong staining only on clones specifically selected for high STEVOR expression (Kripa Gopal Madnani, Peter Preiser lab, personal communication).

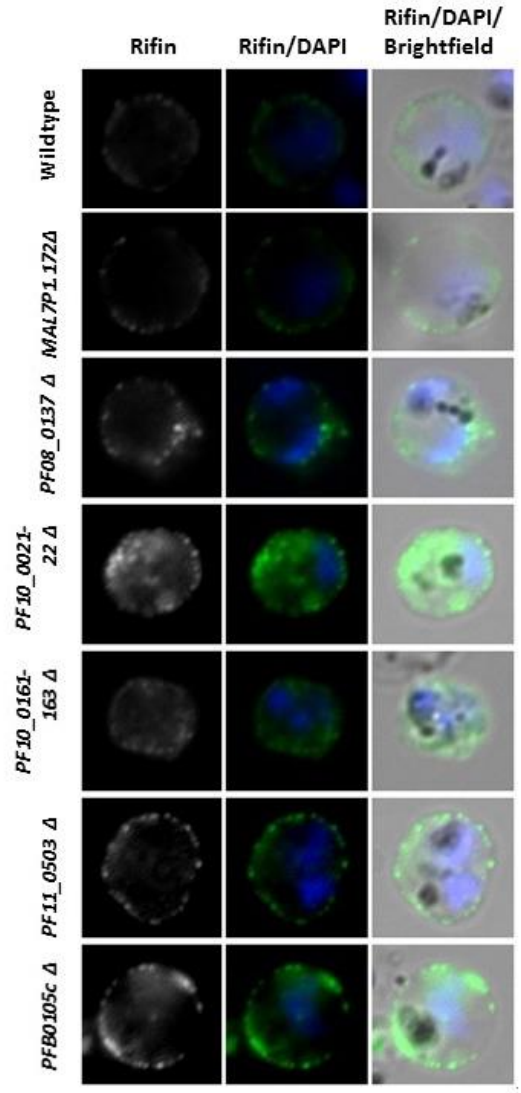

Figure 9. Contribution of PHISTc proteins to trafficking of Rifins. Live, trophozoite stage parasites were permeabilized with Equinatoxin II, probed with an antibody against the Rifin conserved C terminal domain, and analyzed by immunofluorescence microscopy.

To conclusively show that disruption of these PHISTc proteins causes the antigen trafficking defects outlined above, we have attempted to complement these phenotypes by overexpressing the full-length PHISTc proteins in the knock out lines. We aim to complement the VAR2CSA trafficking defect observed in *CS2Δ**PF11_0503,* and possibly in *CS2Δ**MAL7P1.172,* as well as the surface antigen trafficking defect observed in 3D7Δ*MAL7P1.172*, 3D7Δ*PF08_0137,* 3D7Δ*PF11_0503*, 3D7Δ*PFB0105c*, and 3D7Δ*PF10_0021-22.* We first generated overexpression vectors based on a construct that was previously used to complement the PfEMP1-mistrafficking phenotype caused by deletion of the exported parasite protein SBP-1 (Maier et al., 2007). In this vector, the gene of interest is flanked by the PFHSP86 5'UTR and a PbDT 3'UTR, and the vector contains a Blasticidin S deaminase (BSD) gene for use as a selectable marker (compatible with the knock out lines already containing a human dihydrofolate reductase selectable marker). This constuct had been further modified previously in our group to include an HA (hemagglutinin), TY (Ty1), and DD (destabilization domain) tag (Dvorin et al., 2010) at the C-terminal end of the overexpressed protein of interest (schematic shown in Figure 10A). We first used this vector to generate both tagged and untagged versions of each gene of interest. In the 3D7 background, we found that parasites expressing our MAL7P1.172 HA/TY/DD-tagged overexpression construct had significantly lower expression than parasites expressing 3' HA/TY/DD endogenously-tagged MAL7P1.172 (Figure 10B). We hypothesized that the low expression of the overexpression construct despite presence of a strong promoter could be caused by the presence of a truncated terminator sequence on this plasmid or recombination events between the two HSP86 promoters present on the plasmid. (We showed that presence of two copies of the HSP86 promoter caused significant recombination during bacterial cloning). Also, in the CS2 background, we found that all parasites obtained after transfection were the product of spontaneous blasticidin S resistance

rather than expression of the complementation plasmid; resistance was confirmed by a lack of sensitivity to sorbitol treatment (Sharma et al., 2013), poor growth, and absence of expression of the transfected construct (not shown).

To overcome these issues of low expression and resistance, we modified the overexpression construct. We first removed the DD-tag and corrected the truncated 3'UTR, and we then substituted the HSP86-BSD cassette with a CAM-DHODH cassette obtained from pUF-1 (Ganesan et al., 2011) (Figure 10C). Using this modified overexpression vector, we have so far generated three complemented lines: 3D7Δ*MAL7P1.172+MAL7P1.172-HA-TY*, 3D7Δ*PF11_0503+PF11_0503-HA-TY*, and 3D7Δ*PFB0105c+PFB0105c-HA-TY.* We have shown that MAL7P1.172-HA/TY and PF11_0503-HA/TY both have strong expression by western blot (Figure 10D), and we are now phenotyping these complemented lines using flow cytometry with immune sera. If rescue of antigen trafficking phenotypes cannot be achieved by overexpression of these PHISTc proteins, there are several alternative approaches available. The genes of interest could be reintroduced into the native locus of the knock out transgenic lines by CRISPR-Cas9 mediated gene editing, or new transgenic lines could be made with inducible knock down systems such as the GlmS riboswitch or knock-sideways approaches (Birnbaum et al., 2017; Elsworth et al., 2014).

In the CS2 background, we have had significant technical difficulty with transfection of the modified DHODH constructs. We have attempted to generate CS2Δ*MAL7P1.172+MAL7P1.172-HA-TY* and CS2Δ*PF11_0503+PF11_0503-HA-TY* transgenic lines several times using selection with the compound DSM-1 (as with the 3D7 transgenic lines). However, these transfections been unsuccessful or yielded parasites only two months post-transfection (compared to one month post-transfection in 3D7). Further, the parasites obtained two

months post-transfection appear to have little to no expression of the overexpression construct, suggesting that they are the product of spontaneous DSM-1 resistance. Confirmation of resistance is ongoing, along with transfection of CS2 parasites using an alternative method (Amaxa transfection of schizonts) (Moon et al., 2013). The status of generation of complementation lines is summarized in Figure 10E.

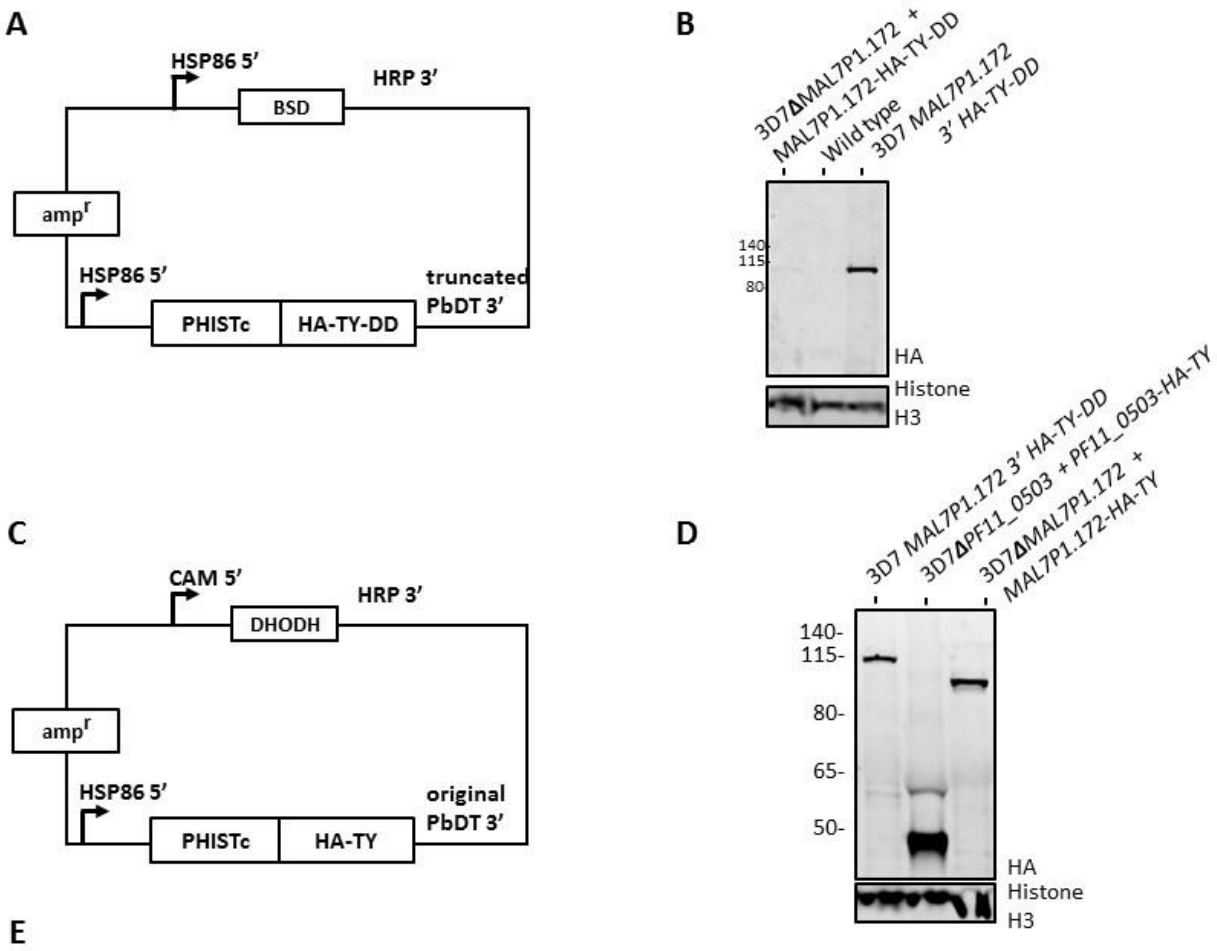

E

Gene	3D7 complementation (DHODH)	CS2 complementation (DHODH)
MAL7P1.172	• Transfected parasites have strong expression of HA/TY-tagged protein by western blot	• Ring transfections → parasites obtained 2 months post transfection, little or no detectable tagged protein • Schizont transfections → ongoing
PF11_0503	• Transfected parasites have strong expression of HA/TY-tagged protein by western blot	• Ring transfections → parasites obtained 2 months post transfection, little or no detectable tagged protein • Schizont transfections → ongoing
PFB0105c	• Transfected parasites with HA/TY construct obtained, western blotting pending	
PF08_0137 PF10_0021 PF10_0022	• Transfected parasites with untagged constructs obtained, cloning of HA-TY constructs ongoing	

Figure 10. Complementation of surface antigen trafficking defects. (A) Original vector used for complementation. The gene of interest was tagged with an HA/TY/DD sequence and flanked by an HSP86 promoter and PbDT terminator, and Blasticidin S deaminase was used as a selectable marker. (B) Western blotting to confirm expression of epitope-tagged overexpression constructs. Whole cell lysate from trophozoite stage parasites (cultured with Shield-1 to prevent DD-mediated

Figure 10 (continued).
degradation) from each line was probed with an anti-HA antibody and an anti-Histone H3 antibody for equal loading. (C) Modification of complementation vector used in this study. The DD tag sequence was removed from the vector, and the BSD selectable marker cassette (containing an HSP86 promoter) was replaced with a DHODH selectable marker cassette (containing a CAM promoter). (D) Western blotting to confirm expression of epitope-tagged overexpression constructs. Whole cell lysate from trophozoite stage parasites from each line was probed with an anti-HA antibody and an anti-Histone H3 antibody for equal loading. (E) Current status of genetic complementation of 3D7 and CS2 PHISTc knock out lines.

PHISTc proteins localize to punctate structures in the host cell during asexual and sexual development

To further understand the function of PHISTc proteins, we investigated the subcellular localization of a subset of our PHISTc proteins of interest. We endogenously tagged *MAL7P1.172, PF08_0137, PF11_0503,* and *PF10_0022* with a 3' HA-TY-DD tag in the 3D7 background using single crossover recombination. Tagging of *PFB0105c* was also attempted but was unsuccessful. Western blotting shows tagged protein product of the expected molecular weight for endogenously tagged MAL7P1.172-HA-TY-DD, PF08_0137-HA-TY-DD, and PF11_0503-HA-TY-DD. PF10_0022, which has been shown to have lower RNA and protein expression in asexual stages (López-Barragán et al., 2011), was not detected by western blotting (Figure 11A,B).

MAL7P1.172 was previously demonstrated by Maier et al to localize to the Maurer's cleft structures or vesicles budding from the Maurer's clefts in young trophozoite stage parasites (Maier et al., 2008; Regev-Rudzki et al., 2013). We stained our *MAL7P1.172*-HA-TY-DD transgenic line with an anti-HA antibody and could see specific staining only in late trophozoite and schizont stage parasites on methanol-fixed smears. We show that by this late trophozoite and early schizont stage, MAL7P1.172 is mostly found at punctate structures within the host cell that do not co-localize with MAHRP1 and are thus distinct from Maurer's clefts (Figure 11C). We also wanted to investigate the localization of PF11_0503 and PF08_0137. Although we could detect *PF11_0503*-HA-TY-DD by western blot, we could not detect it by immunofluorescence assay performed on methanol- or acetone-fixed smears of any asexual stage parasites. In the *PF08_0137*-HA-TY-DD line, we used an anti-HA antibody to show in late trophozoite and early schizont stages that PF08_0137 is mostly found at punctate structures distinct from Maurer's clefts, similar

to MAL7P1.172 (Figure 11C). As in our *MAL7P1.172*-HA-TY-DD line, the HA antibody does not detect PF08_0137-HA-TY-DD before the late trophozoite stage.

To investigate localization of MAL7P1.172 in younger stage parasites, we used a specific antibody against MAL7P1.172 (Maier et al., 2008) to stain both wild-type parasites and the *MAL7P1.172*-HA-TY-DD line. It is possible that the anti-MAL7P1.172 antibody detects an epitope that is accessible in both early and late stages, whereas the HA antibody detects an epitope detectable only in late stages. We show that in late ring and early trophozoite stage parasites, MAL7P1.172 does co-localize with a Maurer's cleft marker (Figure 11D), agreeing with the findings of Maier et al. (2008) and Regev-Rudzki et al. (2013). To next determine whether PF08_0137 co-localizes with MAL7P1.172, we also stained 3D7 *PF08_0137*-HA-TY-DD parasites with an HA antibody and the anti-MAL7P1.172 antibody. The anti-HA signal and anti-MAL7P1.172 signal do co-localize, suggesting that PF08_0137 co-localizes with MAL7P1.172 (Figure 11D).

Although the MAL7P1.172 antibody has been used in previously published immunofluorescence assays, and in our hands it does co-stain the *MAL7P1.172*-HA-TY-DD line with an HA antibody, we undertook additional validation of the antibody to confirm its specificity. Surprisingly, we show that the anti-MAL7P1.172 antibody gives a similar staining pattern on wild-type and MAL7P1.172Δ parasites, labeling punctate host cell structures that are also partially co-labeled with an anti-MAHRP1 antibody (Figure 11D). This suggests that the MAL7P1.172 antibody cross-reacts with another exported protein with similar localization to MAL7P1.172. BLAST analysis of the peptide against which the antibody was raised does not however reveal a likely target of cross-reactivity. Taken together, experiments using the anti-MAL7P1.172 antibody suggest that MAL7P1.172 does localize to Maurer's clefts in early trophozoite stage

parasites, although the antibody may be staining additional proteins also localized to the same site. Similarly, PF08_0137 likely co-localizes with MAL7P1.172 as well as the protein(s) that cross-react with the anti-MAL7P1.172 antibody.

Because we see only transient colocalization of MAL7P1.172 and PF08_0137 with Maurer's clefts, we were interested in determining whether they co-localize with some other known export structure. Recently, Zhang et al. (2017) used immunoprecipitation assays to show that PFE55 and PFHSP70-x, both protein components of J-dot structures hypothesized to play a role in PfEMP1 trafficking, interact with several exported proteins, including PF08_0137. This study showed a single example of partial colocalization between HSP70-x and PF08_0137, so we attempted to determine whether J-dots were the main site of function of PF08_0137 and other PHISTc proteins. We used an antibody against HSP70-x to stain 3D7 *PF08_0137*-HA-TY-DD and assess level of J-dot co-localization with PF08_0137. However, the timing of optimal HSP70-x IFA signal is significantly earlier than optimal staining of PF08_0137-HA-TY-DD using the HA antibody, making it rare to find cells stained with both antibodies. In rare cases, we can see some level of expression of both in mid trophozoie stage parasites, where we see only partial co-localization of HSP70-x with PF08_0137 (Figure 11E). However, the staining is too poor to be conclusive and will require further optimization. In addition, we wondered whether these PHISTc proteins co-localize with the tether structures that serve as a link between Maurer's clefts and the host cell. We stained *MAL7P1.172*-HA-TY-DD parasites with an anti-HA antibody as well as an antibody against the tether protein MAHRP2, and we showed that there is only minimal co-localization of MAL7P1.172 and tethers in mature asexual parasites (Figure 11E).

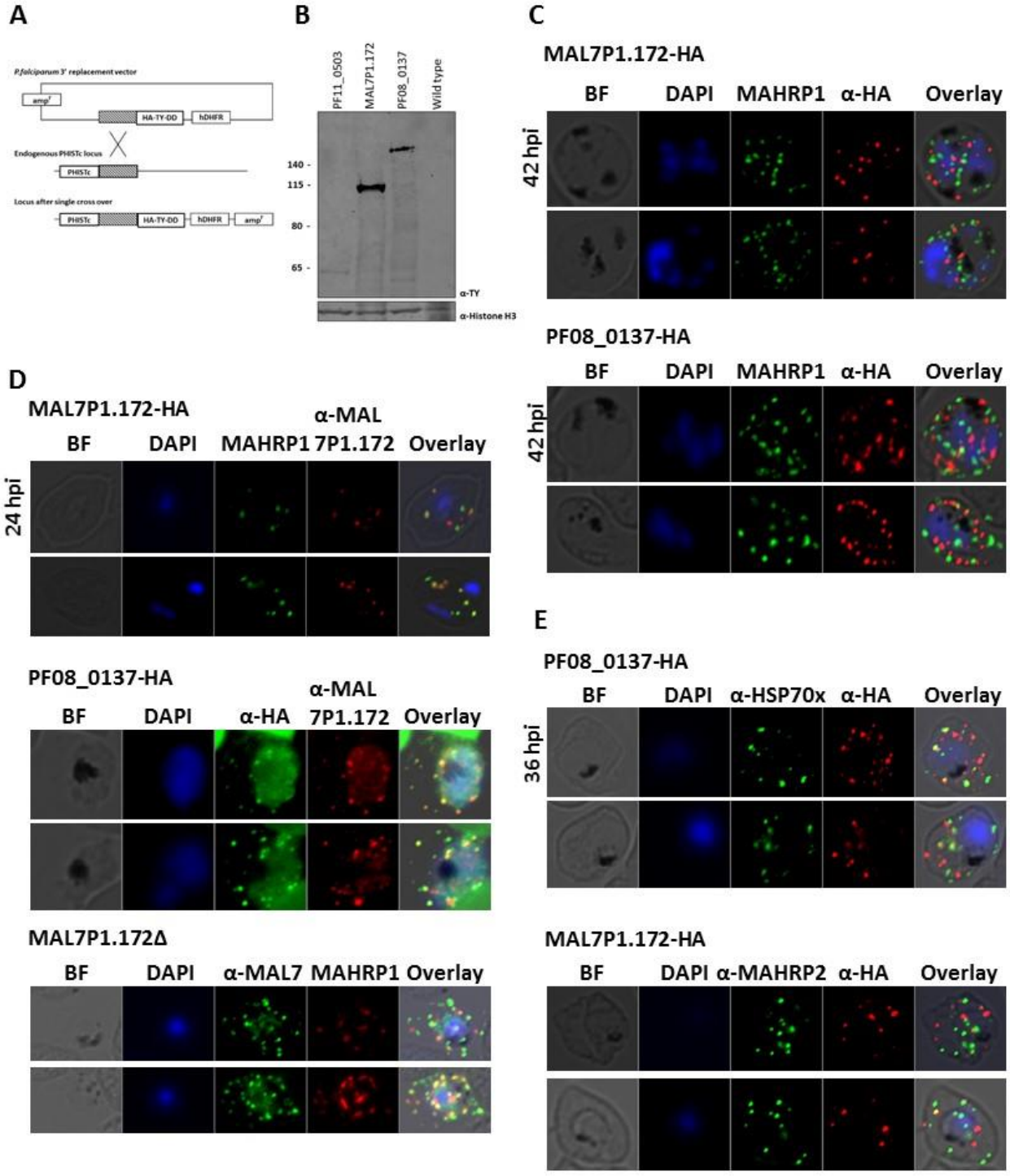

Figure 11. **Immunofluorescence localization of PHISTc proteins in asexual stage parasites.** (A) Strategy for generating PHISTc endogenously tagged lines. The 3' region of each gene of interest was modified by single cross over recombination with a triple HA tag followed by a double TY tag and a degradation domain (DD). (B) Western blotting to confirm epitope tagging. Whole cell lysate from trophozoite stage parasites (cultured with Shield-1 to prevent DD-mediated

Figure 11 (continued).
degradation) from each line was probed with an anti-TY antibody and an anti-Histone H3 antibody for equal loading. (C) Co-localization of MAL7P1.172 (top) and PF08_0137 (bottom) with a Maurer's cleft resident protein, MAHRP1, in asexual stage parasites. Parasites were synchronized to a four hour window and blood smears from 42 hours post invasion were fixed with methanol, permeablized with Triton-X 100, and probed with specific antibodies against HA and MAHRP1. (D) Co-localization of MAL7P1.172 with MAHRP1 and PF08_0137 using an anti-MAL7P1.172 antibody. Top: MAL7P1.172-HA-TY-DD parasites were synchronized to a four hour window and blood smears from 24 hours post invasion were fixed with methanol, permeablized with Triton-X 100, and probed with specific antibodies against MAL7P1.172 and MAHRP1. Middle: PF08_0137-HA-TY-DD parasites were similarly fixed and then stained with antibodies against HA and MAL7P1.172. Bottom: To test specificity of the MAL7P1.172 antibody, CS2Δ*MAL7P1.172* parasites were also methanol-fixed, Triton-X 100 permeablized, and probed with antibodies against MAL7P1.172 and MAHRP1. (E) Co-localization of PF08_0137 with J-dots and tethers in asexual stage parasites. Parasites were synchronized to a four hour window and blood smears from 36 hours post invasion were fixed with methanol, permeablized with Triton-X 100, and probed with antibodies against the HA epitope tag and HSP70-x (top) or MAHRP2 (bottom).

As an alternative approach to localize MAL7P1.172 and PF08_0137 in asexual stages, we performed cryo-immune electron microscopy. Preliminary imaging reveals localization of MAL7P1.172 and PF08_0137 at Maurer's clefts as well as at vesicle-like structures in the host cytoplasm (Figure 12A,B). Further cryo-immune EM analysis will investigate localization dynamics in these samples as well as co-localization of the HA-tagged PHISTc proteins with markers for other structures like J-dots.

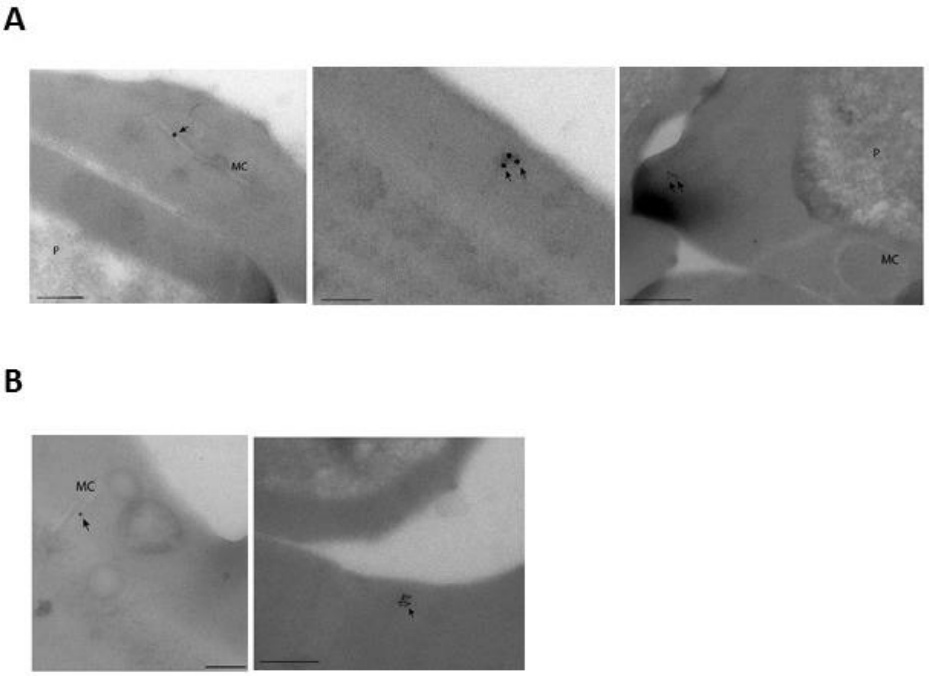

Figure 12. Cryo-immune electron microscopy localization of PHISTc proteins during asexual stages. (A) MAL7P1.172-HA-TY-DD trophozoite and schizonts stage parasites were magnet purified, fixed, stained with an anti-HA antibody, and imaged. (B) PF08_0137-HA-TY-DD trophozoite and schizonts stage parasites were magnet purified, fixed, stained with an anti-HA antibody, and imaged. Arrows indicate gold particles bound to the anti-HA antibody. MC indicates Maurer's clefts.

Finally, we show that endogenously tagged MAL7P1.172-HA-TY-DD, PF08_0137-HA-TY-DD, and PF11_0503-HA-TY-DD can also be detected by IFA on immature gametocytes. In Day 4 gametocytes (Stage II-III), we see that all three proteins are exported to punctate structures in the host cell (Figure 13A). We also use the anti-MAL7P1.172 antibody to show that PF11_0503 and MAL7P1.172 co-localize in Stage III gametocytes, although intepretation of this is again complicated by the cross-reactivity of the antibody (Figure 13B). We are currently investigating whether these PHISTc proteins partially co-localize with Maurer's clefts in gametocytes, as in asexual stages, or with other so far uncharacterized export structures present in these stages.

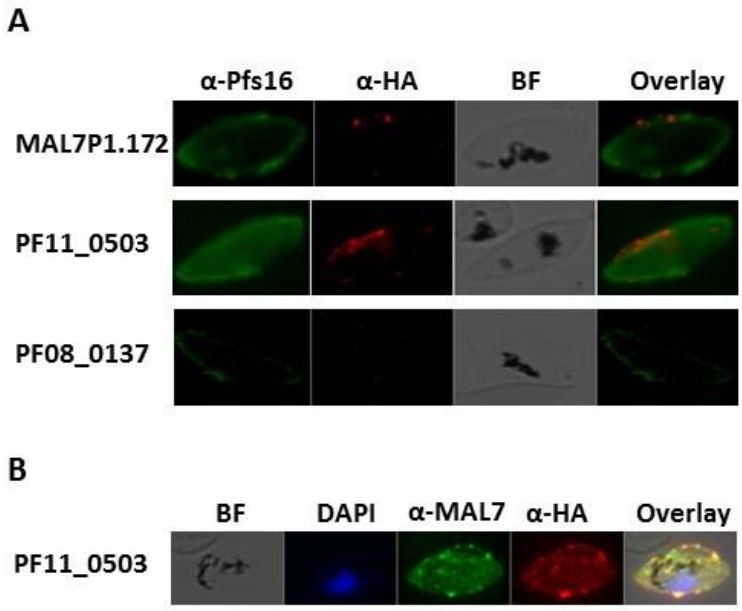

Figure 13. Localization of PHISTc proteins in gametocyte stages. (A) Immunofluorescence localization of PHISTc proteins in gametocyte stages. Day 4 gametocytes were methanol-fixed and probed with antibodies against the HA epitope tag and Pfs16, a marker of sexual development. Shown are MAL7P1.172-HA-TY-DD (top), PF11_0503-HA-TY-DD (middle), and PF08_0137-HA-TY-DD (bottom). (B) Co-localization of PHISTc proteins in gametocytes. Day 3 PF11_0503-HA-TY-DD gametocytes were methanol-fixed, Triton-X 100 permeablized, and probed with antibodies against the HA epitope tag and MAL7P1.172.

2.4. Discussion

Although trafficking of parasite antigens to the red blood cell surface is necessary for cytoadherence, and thus malaria pathogenesis, the mechanisms underlying this process still remain only partially understood. Here, we have used a reverse genetic approach to show that several PHISTc proteins contribute to this process of surface antigen trafficking in *P. falciparum*. In contrast to proteins from the PHISTb family, they are not required for changes in cellular deformability. Further, PHISTc proteins are required for correct export of asexual surface antigens but not for formation of the major export structures, Maurer's clefts and knobs. Localization of a subset of PHISTc proteins shows that they are exported to the host cell in both asexual and sexual stages, and in asexual stages they localize first to the Maurer's clefts and then to a distinct compartment in the host cell. Many open questions remain, particularly: (1) "Which surface antigens are trafficked by PHISTc proteins?," (2) "By what mechanism do PHISTc proteins mediate trafficking of blood stage antigens?", and (3) "To what extent is the function of PHISTc proteins conserved across life cycle stage and *Plasmodium* species?"

In this study, we aimed to determine whether PHISTc proteins are required for delivery of antigens to the red blood cell surface. 3D7Δ*MAL7P1.172*, 3D7Δ*PF08_0137,* 3D7Δ*PF11_0503*, 3D7Δ*PFB0105c*, and 3D7Δ*PF10_0021-22* had significantly decreased surface reactivity to immune serum, suggesting that they lack surface expression of major antigens. We then showed that *CS2ΔPF11_0503* lacks VAR2CSA surface expression, complementing the previous finding by Maier et al that CS2Δ*MAL7P1.172* also lacks VAR2CSA surface expression. Because it has been shown that the majority of the human immune response to *P. falciparum* asexual stages is directed towards PfEMP1 (Chan et al., 2012), it is most likely that the serum reactivity defects observed in the 3D7 PHISTc knock out lines are due to an absence of surface PfEMP1. The role

of PF11_0503 and MAL7P1.172 in trafficking of the PfEMP1 variant VAR2CSA support this hypothesis. Interestingly, 3D7Δ*PF08_0137* and 3D7Δ*PFB0105c* have reduced serum surface reactivity, but CS2Δ*PF08_0137* and CS2Δ*PFB0105c* have normal levels of surface VAR2CSA. We hypothesize that PHISTc proteins may each differentially contribute to the trafficking of specific PfEMP1 variants; therefore, PF08_0137 and PFB0105c could be required for surface expression of non-VAR2CSA variants of PfEMP1 but not the VAR2CSA variant. This is supported by the observation that PFE1605w, a PHISTb protein, binds PfEMP1 and selectively contributes to cytoadherence to CD36 but not other endothelial receptors, suggesting a role in cytoadherence mediated by only a subset of PfEMP1 variants (Oberli et al., 2016). Alternatively, these PHISTc proteins (*PFB0105c, PF08_0137*) could be involved in trafficking of STEVORS, Rifins, or other invariant surface antigens.

To determine which surface antigens are trafficked by PHISTc proteins, several possible avenues of research could be used. With the 3D7 knock out lines presented in this study, surface proteomics or flow cytometry with a broader panel of antibodies against putative surface antigens could be performed. To determine whether each PHISTc contributes differentially to trafficking of PfEMP1 variants, inducible PHISTc knock down transgenic lines could be generated. As in the study by Oberli et al. (2016), these lines could be panned on different endothelial receptors to select for expression of specific PfEMP1 variants, and then trafficking of each variant with and without PHISTc knock down could be assessed.

PHISTc proteins could contribute to trafficking of VAR2CSA, or other PfEMP1 variants, by several possible mechanisms. To reach the red blood cell surface, parasite-encoded proteins must be secreted out of the parasite and then transported across the PVM. After this, PfEMP1 must then be transported to the Maurer's clefts and finally to the red blood cell surface; it is during these

steps that PHISTc proteins, which localize to the host cell, likely mediate PfEMP1 trafficking. Trafficking of PfEMP1, as well as some other proteins, to the Maurer's clefts is thought to occur by diffusion of chaperone-associated complexes rather than by vesicular transport (Knuepfer et al., 2005a, b). PfEMP1 has been shown to associate with J-dot structures, which contain parasite-encoded chaperone proteins and are likely involved with trafficking of PfEMP1 from the PVM to the Maurer's clefts (Kulzer et al., 2012). Further, PF08_0137 has been shown to physically interact with J-dot resident proteins and to at least transiently co-localize with the J-dot protein HSP70-x(Zhang et al., 2017) (Figure 11E). This suggests that PF08_0137, and possibly other PHISTc proteins, could act at J-dot or other chaperone complexes to transport PfEMP1. Alternatively, PF08_0137 and other PHISTc proteins could just be transported alongside PfEMP1 to Maurer's clefts as part of J-dot complexes but actually play a functional role outside of J-dots. After reaching Maurer's clefts, PfEMP1 has been shown to associate with electron-dense vesicles as well as tether structures that connect Maurer's clefts to the erythrocyte cytoskeleton (McMillan et al., 2013; Trelka et al., 2000). Previous studies have shown that MAL7P1.172 co-localizes with Maurer's clefts and vesicles budding from Maurer's clefts (Maier et al., 2008; Regev-Rudzki et al., 2013), and our study shows that both MAL7P1.172 and PF08_0137 both move from Maurer's clefts to distinct host cell strucures (Figure 11C,D). We have shown that these distinct structures are not tethers, but it is possible that they are J-dots or another uncharacterized structure. Because we see that disruption of several PHISTc proteins leads to a substantial defect in surface antigen trafficking, and because we have preliminary evidence showing that some PHISTc proteins co-localize with eachother outside of Maurer's clefts, we hypothesize that these proteins may non-redundantly act in a complex and/or mediate trafficking of different antigen families or variants.

To determine the mechanism by which PHISTc proteins mediate trafficking of blood stage antigens, future work must first identify the site of PfEMP1, and possibly other antigen, accumulation after PHISTc disruption and then investigate physical interaction between PHISTc proteins at this and downstream sites. Although technical hurdles have so far prevented this (*Figure 8*), we will use immuno-electron microscopy and alternative immunofluoresence microscopy approaches to tackle these questions. Combining information about the localization of these PHISTc proteins with information about the relocalization of surface antigens caused by disruption of PHISTc proteins will allow us to create a model of how they direct trafficking of PfEMP1 and/or other surface antigens. Depending on where we see surface antigens stuck in the cell, or what we identify as the final localization of PHISTc proteins, we can then perform higher resolution imaging and biochemical analyses at the correct time points to probe mechanism.

Finally, this study introduces questions about the extent to which the function of PHISTc proteins is conserved across life cycle stages and *Plasmodium* species. We show that MAL7P1.172, PF11_0503, and PF08_0137 are all involved in trafficking of surface antigens in asexual stages (Figure 5) and that they are exported to the host cell in sexual stages (Figure 13). Further, deletion of the PHISTc genes included in this study does not prevent formation of morphologically normal immature and mature gametocytes (not shown). Recently, our group has shown that immature sexual stage parasites are the target of natural immune responses and has identified several putative surface antigens on sexual stage parasites (Dantzler, 2017). By using the same approaches we used to characterize asexual antigen trafficking in Figure 5 (combination of patient immune serum and specific antibodies), we will investigate whether PHISTc deletion disrupts surface antigen trafficking in sexual stages. If PHISTc proteins are shown to play a role in this process, then detailed investigation of where PHISTc proteins localize within the host cell

of sexual stages combined with where the sexual stage antigens accumulate will allow us to probe PHISTc mechanism of action.

The contribution of PHISTc proteins to trafficking of surface antigens, but not to cytoskeletal remodeling, in *P. falciparum* also leads us to speculate that PHISTc proteins could play a role in cytoadherence of other *Plasmodium* species. As mentioned previously, PHISTc proteins are ancestral, with significant conservation across primate malarias and orthologs in rodent and avian malarias. Although cytoadherence and vascular sequestration was previously considered to be primarily a feature of *P. falciparum,* there is much recent evidence for sequestration in *P. vivax* as well as *P. berghei* (De Niz et al., 2016; Lopes et al., 2014). Interestingly, the *P. vivax* PHIST protein PVX_093680, or CVC-8195, localizes to erythrocyte membrane inward extensions (called calveola-vesicle complexes or Schuffner's dots) in *P. vivax*-infected cells (Akinyi et al., 2012) (Anderson et al., 2015), suggesting that it could be a candidate for mediating sequestration. Also, a recent genetic study in *P. berghei* showed that two *P. berghei* PHIST proteins, PBANKA_114540 and PBANKA_122900, co-localize with each other at punctate structures in the host cell. Interestingly, BLAST analysis showed that PVX_093680, PBANKA_114540 and PBANKA_122900 have highest homology to PF08_0137, particularly suggesting a conserved role for this PHISTc (Moreira et al., 2016). As additional *Plasmodium spp.* become genetically tractable and as their cytoadherence characteristics and surface antigen repertoires become better understood, we expect that further investigation of PHISTc proteins in these species will reveal a conserved functional role.

In summary, we have shown that several PHISTc proteins are required for trafficking of antigens to the surface of *P. falciparum* asexual stages and that they do this without altering the

deformability or overall architecture of the infected cell. This study further introduces many new questions regarding the mechanism and conservation of PHISTc-mediated trafficking of antigens.

2.5. Materials and Methods

General notes

Parasite maintenance was performed according to protocols published in the sixth edition of the Methods in Malaria Research handbook (Moll et al., 2013). Protocols followed included sorbitol synchronization ("Sorbitol-synchronization of Plasmodium falciparum-infected erythrocytes"), freezing ("Stockholm sorbitol method"), thawing ("Thawing of glycerolyte-frozen parasites with NaCl"), transfection ("Transfection of Plasmodium falciparum within human red blood cells"), and gelatin selection ("Enrichment of knob-infected erythrocytes using gelatin sedimentation").

All experiments were performed at room temperature unless otherwise indicated. Centrifugation of live or fixed uninfected and infected red blood cells was always performed at a relative centrifugal force less than 550 x g. Magnet purification was performed using MACS CS and LD columns (Miltenyi Biotec). For all assays that required highly synchronous parasites, cultures containing late schizonts were MACS purified, allowed to reinvade into fresh blood for 2-4 hours while shaking at 55 rpm, and then sorbitol synchronized to remove unruptured schizonts.

Plasmodium falciparum in vitro culture

Plasmodium falciparum blood stage parasites were cultured as published previously with slight modifications (Trager and Jensen, 1976). Briefly, cultures were grown at 4% hematocrit in O+ human red blood cells (Research Blood Components, Boston, MA, USA; Interstate Blood

Bank, Memphis, TN, USA); culture media consisted of RPMI 1640 supplemented with 25 mM HEPES (EMD Biosciences), sodium bicarbonate (Sigma), gentamycin, 50mg/l hypoxanthine, and either 10% O+ human serum or 0.5% Albumax (Thermo Fisher Scientific). O+ human serum was obtained from Caucasian male donors (Interstate Blood Bank, Memphis, TN, USA). Cultures were kept at 37°C in a modular incubation chamber (Billups-Rothenberg) gassed with 5% CO_2, 1% O_2, and balanced nitrogen (Med-Tech Gases; Airgas).

Several wild-type and transgenic parasite strains were used for this work. CS2 parasites are a clone of the It reference strain and were obtained from Alan Cowman and from Patrick Duffy. P2G12 is a clone of the 3D7 reference strain generated by our lab (Buchholz et al., 2011).

Transgenic parasites expressing proteins tagged with a DD destabilization domain require the addition of 625 nM Shield-1. These parasites were cultured in media complemented with 0.5% Albumax (rather than human serum) to avoid depletion of Shield-1. Transgenic parasites containing a hDHFR resistance allele were cultured in media supplemented with 4 nM WR99210 (Jacobus Pharmaceuticals). Transgenic parasites containing a BSD allele were cultured in media supplemented with 2.5 µg/ml Blasticidin S. Blasticidin potency against parasites seems to differ between sources; for this work, we used Blasticidin isolated from *Streptomyces griseochromogenes* from both Sigma-Aldrich (Catalog number 203350) and from Invivogen (Catalog number ant-bl-10p). Finally, transgenic parasites containing a DHODH allele were cultured in media supplemented with 1.5 µM DSM-1 (obtained from Pradip Rathod, University of Washington, Seattle, WA, USA).

Molecular cloning

All primers used in this thesis are listed in *Table 2*.

Table 2. Primers used in this study.

Purpose	Name	Sequence
To confirm PHISTc knock out lines	PFB0105c 3' F	GGAGAAAGGCATTAAGTAC
	PFB0105c 3' R	CTTGTACCTTATTCCTTGAG
	PFB0105c 5' F	CCTGCAAGTATAACTAAAGG
	PFB0105c 5' R	TCATCTAGACTTCTGGAAAG
	PF110503 3' F	CAAGACTTTGAAAGTGACAC
	PF110503 3' R	AGTCTCAGAGTGCTGTAAAC
	PF110503 5' F	TTAAATACCCCACTACCC
	PF110503 5' R	GTCTTCTTACCCATAATCAC
To replace HSP86-BSD cassette with CAM-DHODH cassette	DBR70_pHBSDBSDtoDHODH_F	GATCCCTCACTTAGGGTACGAAGATCTGTCTTAAGC
	DBR71_pHBSDBSDtoDHODH_F	CTAG**GCTTAGC**TTAAATGCTGTTCAACTTCCCAC
To make complementation plasmids	DBR99_MAL7P1.172comptag_F	GATC**GCGGCCGC**ATGCTTCTTTTTAAGGATCCCC
	DBR100_MAL7P1.172comptag_R	CTAG**GCTAGC**TTATTCACCCATGGTTATAGCCAAAG
	DBR27_PF080137comptag_F	GATC**GCGGCCGC**ATGATATTTGTTAAGAGTAAGATTTTATATTTCC
	DBR95_PF080137comptag_R	CTAG**GCTAGC**TGCTCCACTATATTTTCTCATTTTATAAG
	DBR33_PF110503comptag_F	GATC**GCGGCCGC**ATGAAGCAACATATAACCTTTAAGAAG
	DBR94_PF110503comptag_R	CTAG**GCTAGC**TTTGCTTGGTAATCTTTTTTTTTCTTTTTTATC
	DBR35_PFB0105ccomptag_F	GATC**GCGGCCGC**ATGTGGTTATGCAAAAGGGGACT
	DBR96_PFB0105ccomptag_R	CTAG**GCTAGC**ATTTGTAACATTTCTCATGTTATTTTC
	DBR29_PF100021comptag_F	GATC**GCGGCCGC**ATGCAACCAAGACCATGTGC
	DBR97_ PF100021comptag_R	CTAG**GCTAGC**TTGTGATCGTAATTTTCTTTTTCTTTTG
	DBR31_PF100022comptag_F	GATC**GCGGCCGC**ATGGATAAGACAAATTATAGTATAAAG
	DBR98_PF100022comptag_R	CTAG**GCTAGC**TAATCTCTGATTTAATGCCTTTTTTAATT

To generate knock out transgenic lines, PHISTc 3' and 5' homology regions were cloned into the pCC-1 vector (Maier et al., 2008). For overexpression, PHISTc coding sequences were cloned into the pCC-4 vector (Maier et al., 2007) using NEB restriction enzymes and NEB ligation or Gibson cloning. PHISTc coding sequences were amplified from gDNA from wild type P2G12 parasites. A resistance marker cassette containing a calmodulin promoter sequence and a DHODH coding sequence was amplified from the pUF-1 vector and used to replace the HSP86 promoter-BSD cassette in pCC-4. Confirmatory sequencing was performed by Genewiz and Macrogen. Primer design, sequence analysis, and plasmid map generation was performed using the software Geneious (Geneious). Primers were synthesized with standard desalting by IDT and Invitrogen.

DNA manipulation was performed with the following reagents and kits: PCR: Phusion DNA polymerase (New England Biolabs) and iProof High Fidelity DNA polymerase (Biorad); Digestion: Restriction enzymes from New England Biolabs; Ligation: T4 ligase (New England Biolabs and Promega; Transformation: XL10-Gold Ultracompetent cells (Agilent); DNA purification: Plasmid miniprep kit, Plasmid maxiprep kit, DNeasy blood and tissue kit, PCR purification kit, gel extraction kit (all from Qiagen)

Gametocyte culture

Transgenic P2G12 parasites used for immunofluorescence analysis were cultured in media supplemented with Albumax and Shield-1 to prevent degradation of DD-tagged proteins. Under these culture conditions, these parasites do not significantly increase gametocyte production in response to stress or nutrient depletion, so gametocytes were obtained as follows: Parasites were synchronized using consecutive sorbitol treatments and allowed to grow to a high ring stage parasitemia (>5%); this ring stage culture is referred to as Day 0. Media was changed daily, and 50 mM N-Acetylglucosamine (GlcNAc) (Sigma-Aldrich) was added to the gametocyte culture

from Day 0-4 to prevent reinvasion and growth of asexual stage parasites. Gametocytes were then purified by MACS enrichment.

Microsphere filtration

Microsphere filtration was performed as published with some modifications (Deplaine et al., 2011; Lavazec et al., 2013). To fabricate the filter, 400 mg of "Type 5" beads and 400 mg of "Type 6" beads were weighed and combined in an eppendorf tube (Gesick MPM – Sn 96.5%, Ag 3%, Cu 0.5%; Type 5: 15-25 um; Type 6: 5-15 um). 800 ul of pre-warmed, complete RPMI was then added to the eppendorf containing the beads; beads were always resuspended in the same media as cells (complete RPMI supplemented with Albumax or human serum). Beads and media were then quickly resuspended in the shortened filter tip, and the filter tip was inverted to allow the beads to settle on top of the filter. Beads were allowed to settle for at least two minutes, and the tip was then filled with complete media using a needle and syringe.

Parasite culture was diluted to $\leq$2% hematocrit and $\leq$5% parasitemia in pre-warmed, complete media. When the culture contained signficant amounts of debris, cells were gently washed prior to dilution. An aliquot of this culture was collected pre-filtration to serve as the "upstream" sample (for smear or flow cytometry).

For asexual stage assays, all steps were performed with media pre-warmed to 37ºC in a lab space at room temperature. For gametocyte assays, all steps were performed with media pre-warmed to 37ºC in a warm room maintained at 37ºC.

For filtration, the filter tip and a 10 ml syringe were connected to a 3 way stop cock, and the 10 ml syringe was filled with 9 ml of pre-warmed, complete media (again, the same media as cells and beads were resuspended in). With the port to the 10 ml syringe closed, a 1 ml syringe

was used to inject 1 ml of culture into the filter tip through the stop cock at a rate of ~100 ul/second. A syringe pump was then used to wash the filter through the stop cock with 7 ml of complete media at 1 ml/minute, and the flow through was collected as the "downstream" sample. To collect parasites retained in the filter, the beads and parasites in the filter tip were resuspended and ejoected into an eppendorf tupe. The beads were allowed to settle for 1-2 minutes, and the supernatant (still containing parasites) was collected. This process was repeated 2-4 times depending on desired purity.

Upstream and downstream samples were washed 1X in PBS and fixed for 40 minutes at room temperature in 1X PBS containing 4% Paraformaldehyde and 0.01% Glutaraldehyde. Cells were again washed 1 X in PBS and were then stored at 4ºC until processing. To measure parasitemia of these samples by flow cytometry, fixed cells were washed once in PBS and incubated with PBS containing 1:5000 SybrGreen DNA dye for twenty minutes in the dark. Samples were then run on a MACSQuant VYB flow cytometer, with at least 200,000 events counted per samples. Parasitemia of upstream and downstream samples were calculated, and the retention rate was calculated as 100 * (1-(downstream parasitemia/upstream parasitemia)).

Immunofluorescence assays and flow cytometry

Concentrations for all primary antibodies used in this thesis are listed in *Table 3*

Table 3. Antibodies used in this study.

Antibody	Source	Concentration (Live)	Concentration (PFA/Glu)	Concentration (MeOH)
Rabbit α-VAR2CSA JS (IT4-DBL3)	Joe Smith	1:100	1:100	
Rabbit α-VAR2CSA AS27	Ali Salanti	1:100	1:100	
Rabbit α-VAR2CSA AS37	Ali Salanti	1:100	1:100	
Rabbit α-VAR2CSA AS153	Ali Salanti	1:100	1:100	
Rabbit Rifin IgG (raised against conserved peptide from Rifin C-terminus)	Mats Wahlgren	1:190 (10 ug/ml)		
STEVOR S1	Peter Preiser	1:400 recommended (never saw signal with titration)		
STEVOR S2	Peter Preiser	1:400 recommended (never saw signal with titration)		
Mouse α-MAHRP1	Hans-Peter Beck		1:500	1:2000
Rabbit α-MAHRP1	Hans-Peter Beck		1:500	1:2000
Rabbit α-MAHRP2	Hans-Peter Beck			1:500
Mouse α-KAHRP ("mAb89")	Diane Taylor		1:500	1:500
Rabbit α-Hsp70-x	Paul Gilson		1:100	1:100
Rabbit α-PTP2 ("R883")	Alan Cowman			1:250
Rabbit α-PF08_0137	Alan Cowman			1:200
Rabbit α-Pfs16	Matthias Marti			1:5000
Mouse α-Pfs16	Kim Williamson			1:500
Rat α-HA ("3F10")	Roche			1:50

a) Live IFAs with specific antibodies:

Infected cells for live, unpermeabilized immunofluorescence assays were harvested, washed one time in PBS, and blocked for one hour in blocking buffer (3% Bovine Serum Albumin in PBS) on a rotator. Primary antibody was then diluted in at least 50 µl of blocking buffer, and cells were resuspended in this primary antibody dilution and incubated for one hour on a rotator. Cells were then washed three times in blocking buffer. Secondary antibody (AlexaFluor 488) was diluted 1:500 in blocking buffer, and cells were resuspended in this mix and incubated for one hour on a rotator in the dark.

Cells to be used for microscopy were then centrifuged and resuspended in 1:10000 Hoechst DNA dye in blocking buffer and incubated for ten minutes on a rotator in the dark. Cells were then washed twice in blocking buffer and once in PBS. Cells were mounted on Poly-L-Lysine coated slides (Electron Microscopy Services) with Vectashield (Vector Labs), covered with a 1.5 mm coverslip, and sealed with nail polish. Slides were allowed to set for at least twenty minutes before imaging. All imaging was performed using a Zeiss Observer.Z1 inverted fluorescent microscope, and images were acquired using a Zeiss AxioCam MRm camera and Zeiss ZEN software. Images were processed directly in Zen or in ImageJ.

Cells to be used for flow cytometry were centrifuged after secondary incubation washed 3 times in blocking buffer. VybrantViolet DNA dye was then diluted 1:500 in Hanks Buffered Salt Solution, and cells were resuspended in this mix and incubated for thirty minutes at 37°C. Cells were then diluted in HBSS to a final hematocrit of no higher than 0.4%. Flow cytometry was performed using a MACSQuant VYB flow cytometer and a MACSQuant Analyzer 10 flow cytometer (Miltenyi Biotec). Analysis was then performed using the software FlowJo (FlowJo LLC).

b) Paraformaldehyde/glutaraldehyde (PFA-G)-fixed IFAs with specific antibodies:

Cells were prepared as in (a) above with the following additional steps prior to blocking (Tonkin et al., 2004):

Cells were resuspended in PBS containing 4% Paraformaldehyde and 0.01% glutaraldehyde, and they were fixed for forty minutes on a rotator. Cells were then washed three times in PBS and resuspended in PBS containing 0.01% Triton X-100. Cells were permeabilized for ten minutes on a rotator and then washed three times in PBS prior to blocking.

c) Live, equinatoxin-permeabilized IFAs

Cells were prepared as in (a) above with the following additional steps prior to blocking (Jackson et al., 2007):

200,000,000 cells/sample were washed three times in PBS and then incubated for 12 minutes in PBS containing 0.008 µg/µl Equinatoxin2. After permeabilization, cells were washed 3 times in PBS before proceeding with blocking.

d) Live cell flow cytometry with human sera

Immediately before use, serum samples were pre-incubated with uninfected red blood cells (20:1) for one hour on a rotator. Infected cell samples and uninfected cell controls were washed three times in blocking buffer (PBS containing 1% heat-inactivated Fetal Bovine Serum). Wells of a U-bottom 96 well microtiter plate were also pre-coated with blocking buffer for 30 minutes and then drained well. Pre-incubated serum samples were aliquoted into wells (2.5 µl each), and parasites were separately resuspended in blocking buffer at a hematocrit of 0.4%. 50 µl of parasite suspension was added to each well to obtain a serum concentration of 1:20, and cells were

incubated for 90 minutes, with mixing every thirty minutes. Cells were then washed three times in blocking buffer and resuspended in blocking buffer containing a 1:500 dilution of AlexaFluor secondary antibody (anti-human IgG). Cells were incubated with the secondary antibody for thirty minutes in the dark and then washed three times with blocking buffer. They were then resuspended in Hanks balanced salt solution containing a 1:500 dilution of Vybrant DyeCycle Violet and incubated for thirty minutes at 37°C in the dark. Stained samples were analyzed by flow cytometry using a MACSQuant VYB flow cytometer and a MACSQuant Analyzer 10 flow cytometer (Milteny Biotec).

e) Methanol-fixed IFAs

Parasites were synchronized to a four-hour window by MACS/sorbitol treatment and were harvested at several time points post invasion. Thin blood smears were made for each sample and allowed to air dry for at least one hour at room temperature. If cell culture media contained serum, cells were washed twice in albumax media or blocking buffer before smears were made to reduce background binding. Dried blood smears were fixed in ice cold 100% methanol for 15 minutes and then allowed to dry at room temperature for at least one hour. Dried, fixed smears were either used immediately or were frozen at -80C in a sealed bag with desiccant for future use. After drying, a hydrophobic pen (Dako) was used to draw a well on each smear, and wells were allowed to dry for at least one hour before staining.

Smears were placed in a humidification chamber (made by placing wet paper towels in a slide box), and wells were washed in PBS three times for five minutes each; wells were never allowed to dry after the first wash. Samples were permeabilized in 0.1% Triton X-100 for three minutes (Absalon et al., 2016) and then washed three times more. The samples were then blocked

in PBS containing 3% BSA for one hour at room temperature or overnight at 4°C. Primary antibodies were diluted into blocking buffer and were added to samples for one hour at room temperature or overnight at 4°C. After washing wells three times in blocking buffer, they were incubated with PBS containing a 1:500 dilution of AlexaFluor secondary antibodies (488, 594, or 647) for one hour at room temperature in the dark. Wells were washed two times in blocking buffer and then once in PBS. After removing remaining PBS, 2 µl of VectaShield was added to each well and covered with a coverslip (VWR micro coverglass, No. 1.5). Slides were sealed with nail polish, allowed to set for at least 20 minutes prior to imaging, and stored at 4°C in the dark.

All imaging was performed using a Zeiss Observer.Z1 inverted fluorescent microscope, and images were acquired using a Zeiss AxioCam MRm camera and Zeiss ZEN software. Images were processed directly in Zen or in ImageJ.

Electron microscopy

a) Cryo-immune electron microscopy (immunoEM)

Parasites were synchronized to a four-hour window by MACS/sorbitol treatment and were harvested at ~28, 34, and 40 hours post invasion. Cultures were washed one time in PBS and resuspended in PBS containing 4% paraformaldehyde and 0.2% glutaraldehyde. Fixed cells were stored at 4°C until further processing.

After several washes in fixation buffer, cells were embedded in 10% gelatin at 37ºC for 30 minutes. The material was spun down and the samples were left on ice for 30 minutes. After confirming the gelatin was solid, the pellet was removed from the eppendorfs and infiltrated overnight in 2.1 M sucrose and rapidly frozen by immersion in liquid nitrogen. Cryo-sections (70 nm thick) of the frozen material were obtained at −120ºC using an Ultracut cryo-ultramicrotome

(Leica Microsystems). The cryo-sections were collected on formvar-coated nickel grids, thawed, and put on a cushion of 2% gelatin. The grids were left for 20 minutes at 37ºC and then blocked in PBS containing 3% bovine serum albumin for 1 hour. After this time, they were incubated in the presence of primary antibody (anti-HA, 1:200 dilution). Then they were washed several times in blocking buffer, and incubated with 15 nm gold-conjugated Protein A (Aurion). The grids were washed several times in the blocking buffer, dried and contrasted in a mixture of methylcellulose/uranyl acetate, and then observed using a Jeol 1200 EX transmission electron microscope.

b) Scanning electron microscopy (SEM)

Parasites were synchronized to a four-hour window by MACS/sorbitol treatment and were harvested at 32 hours post invasion. Cultures were washed one time in PBS and resuspended in PBS containing 4% paraformaldehyde and 2% glutaraldehyde. Fixed cells were stored at 4°C until further processing.

Following serial washes in 0.1M phosphate buffer, the material was let to adhere onto glass coverslips coated with poly-l- lysine. After 20 minutes, serial washes with phosphate buffer were performed, followed by dehydration in ascending series of ethanol, and critical point dried (Tousimis, USA). The dried coverslips were coated with gold/palladium (5 nm thick layer) and imaged in a JEOL IT-100 scanning electron microscope (Jeol, Japan).

c) Transmission electron microscopy (TEM)

Parasites were prepared and fixed as in (b) above.

Following serial washes in 0.1M phosphate buffer, the material was post-fixed in 1% OsO4 (vol:vol) in the same buffer for 1 hour on ice in the dark, and contrasted en bloc with 0.5% aqueous uranyl acetate for 1 hour at room temperature in the dark. The samples were then dehydrated in acetone ascending series and embedded in epoxy resin. Ultra-thin sections (60nm) were observed in a Jeol 1200 transmission electron microscope (Jeol, Japan).

Western blotting

Western blotting to detect epitope-tagged PHISTc proteins was performed using whole cell lysate from MACS-purified late stage parasites. Infected red blood cells were lysed in NuPAGE LDS sample buffer complemented with 2-Mercaptoethanol, boiled for three minutes at 105C, centrifuged at 15,000 rpm for five minutes, and the supernatant was frozen. Protein from 2.5 million cells were run in each lane of a 15 well 4-12% Bis-Tris gel (Invitrogen) at 100V at room temperature in MOPS buffer. Proteins were then transferred in Tris-glycine buffer supplemented with 10% methanol to a charged PVDF membrane using an XCell Sure-Lock wet transfer chamber (Thermo Fisher Scientific) for one hour at 100V or 30V overnight (both at 4°C).

Western blotting to detect PfEMP1 was performed as published (Van Schravendijk et al., 1993). For trypsin cleavage assays, trophozoite stage parasites were MACS purified, washed once in PBS-S (PBS containing 10% sucrose), and incubated with PBS-S or PBS-S supplemented with 1 mg/ml trypsin (Sigma, Catalog number T1426) for one hour at 37°C on a rotator. Cells were then washed twice in PBS-S supplemented with EDTA-free protease inhibitors and washed once in PBS. RBC pellets were lysed in PBS containing 1% Triton X-100 and 1 mM DTT and incubated for five minutes on ice. They were then washed twice in PBS containing 1% Triton X-100 and 1 mM DTT. To extract PfEMP1, the pellet was resuspended in PBS containing 2% SDS and 10 mM

DTT and vortexed for thirty minutes at room temperature; cells were extracted in a ratio of 500,000,000 infected cells/100 µl PBS/SDS/DTT. Samples were centrifuged at full speed (21000 x g), and the supernatant was collected and stored at -20C. Prior to use, samples were then diluted in a 1:1 ratio with 4X NU-PAGE LDS supplemented with 25 mM DTT. Sample in loading buffer was heated at 80C for three minutes. 20 µl of sample in LDS was run in each lane of a 10 well 3-8% Tris-Acetate gel for 3.75 hours at 105 V in Tris-Acetate buffer.

Proteins were then transferred in Tris-glycine buffer supplemented with 10% methanol to a charged PVDF membrane using XCell Sure-Lock wet transfer chamber (Thermo Fisher Scientific) for one hour at 100V or 30V overnight (both at 4°C). Proteins were fixed to the membrane with methanol, and the membrane was then blocked in Odyssey Blocking Buffer PBS (Li-Cor). Primary antibodies were diluted in blocking buffer and incubated with the membrane with agitation for one hour at room temperature or overnight at 4°C. Membranes were washed in PBS with 0.5% Tween 20 three times for five minutes each and were then incubated for one hour in the dark at room temperature with secondary antibody diluted 1:3000 in Licor blocking buffer (IRDye 800CW or 680CW). Membranes were again washed three times in PBS with 0.5% Tween 20 and were detected using the Odyssey CLx system (LI-COR Biosciences).

Southern blotting

Genomic DNA was isolated from parasites by either phenol-chloroform extraction or using the Qiagen DNeasy blood and tissue kit. 2 µg of DNA per sample was restriction enzyme digested overnight and run overnight on a 0.7% agarose gel. The gel was soaked in 0.25M HCl to depurinate the DNA, washed twice in ddH2O, and soaked twice in alkaline transfer buffer (0.4M NaOH) to denature the DNA. DNA was transferred to an Amersham Hybond-N+ nylon membrane (GE

healthcare) by passive transfer and UV cross-linked (UV Stratalinker 800, Stratagene). The membrane was then washed in 2X SSPE buffer and pre-incubated for one hour in hybridization buffer at 60C while rotating. ^{32}P-labeled DNA probe was then generated from 10 ng of PCR-amplified hDHFR fragment using the RadPrime DNA labeling system (Invitrogen) according to the manufacturer's instructions. The probe was denatured by incubating it for five minutes at 95C and then added to hybridization buffer for overnight incubation at 60C. The membrane was then washed briefly twice with 2X SSPE buffer containing 0.1% SDS at 60C and washed for 30-60 minutes with 0.2X SSPE buffer containing 0.1% SDS. Membranes were then exposed to Carestream Kodak BioMax MS film (Sigma-Aldrich).

qRT-PCR

5 ml of blood stage culture containing at least 5% parasitemia at 4% hematocrit was harvested for each sample. The culture was washed one time in PBS and incubated for five minutes at room temperature in 1 ml of Trizol reagent. Trizol-preserved parasites were then frozen at -80C until RNA extraction.

RNA extraction was performed using a PureLink RNA isolation kit according to the manufacturer's instructions. cDNA was then synthesized from 1 µg of input RNA for each sample using random hexamers and M-MLV reverse transcriptase (Sigma) according to the manufacturer's instructions. RNA quality was assessed by gel electrophoresis, and RNA concentration was measured using the Qubit RNA HS kit (Thermo Fisher Scientific).

Var gene transcriptional profile of parasitized red blood cell was then assessed as previously described (Nunes-Silva et al., 2015). The quantitative real-time PCR was performed in 20µL using Universal SYBR Green Supermix (BioRad), specific primer pairs for each IT4 *var* gene (Rask et

al., 2010) and the prepared cDNA. The reactions were assessed on a CFX96 thermocycler (BioRad). Relative transcription was determined by normalization with the housekeeping control gene seryl-tRNA synthetase [PlasmoDB: PF07_0073] and converted to relative copy numbers.

2.6. Acknowledgements

We thank the following people for providing crucial antibodies for this study: Joe Smith for VAR2CSA antibody (PfEMP1), Ali Salanti for VAR2CSA antibodies (PfEMP1), Diane Taylor for mAb89 (KAHRP), Hans-Peter Beck for MAHRP1 and MAHRP2 antibodies, Michael Duffy for mAb 6H1 (PfEMP1 ATS), Mats Wahlgren for antibodies against Rifins, Peter Preiser for antibodies against STEVORS (S1 and S2), Alan Cowman for antibodies against PF08_0137 and MAL7P1.172, and Paul Gilson for antibodies against HSP70-x. For patient immune sera, we thank Drs. Terrie Taylor, Karl Seydel, and Miriam Laufer, the Blantyre Malaria Project staff, especially Nelson Chimbiya, Chiledso Mlangali, and Andy Bauleni, and Blantyre ICEMR facility-based surveillance team, led by Dr. Atupele Kapito-Tembo, for their invaluable help in sample collection. We also thank the patients and their families who participated in the study. We would like to thank Flaminia Catteruccia and Robert Shaw for use of their microscope and thank Sabrina Absalon, Markus Ganter, and Sandra Nilsson for advice concerning immunofluorescence assays. Finally, we thank the Wirth, Duraisingh, Dvorin, Catteruccia, and Burleigh labs at HSPH for helpful feedback. Funding for this work was provided by the U.S. National Institute of Health (5R01AI077558) and a U.S. National Science Foundation Graduate Research Fellowship (DGE1144152).

CHAPTER 3: TRANSCRIPTIONAL PROFILING TO DEFINE *PLASMODIUM FALCIPARUM* DEFORMABILITY AND INFECTIOUSNESS

Deepali Ravel[1], Lisette Meerstein-Kessel[2], Sanna Rijpma[2], Geert-Jan van Gemert[2], Wouter Graumans[2], Marga van der Vegte-Bolmer[2], Rianne Siebelink-Stoter[2], Priscilla Ngotho[3], Daniel Neafsey[4], Martijn Huijnen[2], Teun Bousema[2, 5], Matthias Marti[1,3]

[1]Department of Immunology and Infectious Disease, Harvard T.H.Chan School of Public Health, Boston, MA, USA
[2]Department of Medical Microbiology, Radboud University Medical Centre, Nijmegen, The Netherlands
[3] Wellcome Trust Centre for Molecular Parasitology, Univ. of Glasgow, Glasgow, UK
[4]Broad Institute of MIT and Harvard, Cambridge, MA, 02142, USA.
[5]Department of Immunology & Infection, London School of Hygiene and Tropical Medicine, London, UK

Author contributions:

D. Ravel designed and performed optimization of gametocyte deformability assays (Table 4) and gametocyte deformability time courses for RNA sampling (Table 5) and prepared RNA samples for sequencing, all under the mentorship of M. Marti. T. Bousema and S. Rijpma planned experiments relating to mosquito infection, and S. Rijpma performed gametocyte infection time courses presented in Table 9 and Figure 16 with assistance from G. van Gemert, W. Graumans, M. van der Vegte-Bolmer, and R. Siebelink-Stoter.

L. Meerstein-Kessel performed all initial read mapping, normalization, and differential expression analysis included in this study. D. Ravel then performed further analysis included in Figure 14, Table 6, Table 7, Table 8, and Table 10. L. Meerstein-Kessel also performed principle component analysis included in Figure 15 and Figure 17. D. Neafsey provided advice regarding RNA sequencing.

D. Ravel wrote the text and generated all figures and tables included in this chapter, with the exception of Figure 16 (adapted from S. Rijpma).

3.1. Abstract

Despite progress in understanding the development of malaria transmission stages, there remain many unanswered questions about how these gametocytes progress from being immature to infectious. In *P. falciparum,* immature gametocytes are rigid and sequester outside of circulation in host tissues, while deformable, mature stages are found in circulation and then transmitted to mosquitoes. Key remaining questions about this process include: (1) What factors mediate the deformability switch separating sequestering and circulating gametocytes? and (2) Are there specific markers for deformable, circulating gametocytes that are capable of infecting mosquitos? Here, we developed a combination of biomechanical and transcriptional signatures to define the transition from immature non-infectious to mature infectious gametocyte. Aiming to identify markers of deformable mature gametocytes, we first correlated deformability, as measured by microsphere filtration, with RNA profiles across gametocyte development. We used microsphere filtration to separate highly synchronous gametocyte populations by rigidity every 24 hours from day 6 to 12 of gametocyte development. This time frame spans the transition in gametocyte deformability and infectivity, including activation to gametes. RNA samples of deformable and non-deformable populations at each time point were analyzed by RNA sequencing, and we identified genes that were enriched or depleted in deformable gametocytes. Based on functional annotation of these genes, we expect that some act by remodeling the parasite cytoskeleton while others act by remodeling the red blood cell cytoskeleton. In parallel, we performed RNA sequencing with *in vitro* and *in vivo* gametocyte samples that were assayed for infectiousness through controlled mosquito infections. We identified a preliminary set of markers for deformable, infectious gametocytes and expect that further integration of the deformability and infectivity data sets will enable identification of a transcriptional signature for deformable,

infectious gametocytes found in circulation *in vivo*. Candidate genes from this study could be genetically disrupted to functionally validate their potential as targets of transmission-blocking interventions and could also be pursued as diagnostic biomarkers to measure the human infectious reservoir.

3.2. Introduction

In this study, we are investigating the mechanisms underlying deformability changes in *P. falciparum* gametocytes and assessing the contribution of these changes to sequestration and infectivity. Despite progress in understanding the development of malaria transmission stages, there remain many unanswered questions about how these gametocytes progress from being immature to infectious. Answering these questions will be important for transmission-blocking interventions and diagnostics to measure infectiousness.

In *P. falciparum,* immature gametocytes (stages I-IV) sequester in host tissues, primarily bone marrow, while mature stages (stage V) are found in circulation (Aguilar et al., 2014; Joice et al., 2014). During maturation, they undergo a marked change in morphology and deformability. Beginning as a round form indistinguishable from asexual stages (termed Stage I), they then develop through several transition stages (Stages II/III) to an elongated spindle form (Stage IV) and finally, the curved sausage-like mature form seen in circulation (Stage V) (Hawking et al., 1971; Sinden et al., 1978)**.** Three groups have recently characterized the mechanical properties of these distinct morphological stages, using several methods to show decreased gametocyte deformability during Stage I-IV and restored deformability during Stage V (Aingaran et al., 2012; Dearnley et al., 2012; Tiburcio et al., 2012a). Aingaran et al. (2012) show specifically that deformability of both the parasite and the host red blood cell undergo this process of deformability

decrease and restoration. Computational modeling based on infected red blood cell deformability predicts that immature gametocytes cannot pass through sinusoidal slits during splenic filtration (Aingaran et al., 2012), agreeing with observations of immature gametocytes being sequestered. Deformability restoration in stage V gametocytes thus allows them to circulate in the blood stream before being taken up in a mosquito blood meal, egressing from the host cell and successfully concluding the sexual cycle.

Significant progress has been made in recent years to understand the mechanisms that drive red blood cell deformability changes during malaria infection. Deformability of red blood cells infected by asexual stage malaria parasites has been extensively characterized, and many proteins that alter deformability in these stages have been identified. Erythrocytes infected with early asexual ring-stages have slightly lowered deformability compared to uninfected cells, and erythrocytes infected with mature asexual stages have 20-fold lower deformability (Aingaran et al., 2012). Several well-studied parasite genes, including RESA, PfEMP3, and KAHRP, associate with the red blood cell cytoskeleton and membrane to decrease deformability (Glenister, 2002; Mills et al., 2007), and numerous other exported proteins that control asexual deformability have also been identified (Maier et al., 2008).

In gametocytes, the parasite cytoskeleton has been implicated in deformability changes, although the parasite proteins that mediate these changes remain largely unknown. Fluorescence microscopy experiments probing the mechanism for gametocyte morphological and mechanical changes revealed that microtubules within the parasite elongate from Stage I to IV, forming a structure reminiscent of the inner membrane complex of other stages, and then collapse from Stage IV to Stage V (Dearnley et al., 2012; Dixon et al., 2012). However, treatment of Stage III gametocytes with a microtubule-destabilizing compound disrupted morphology but did not restore

deformability (Dearnley et al., 2016), suggesting that microtubules are not solely required for the reduction in deformability observed in immature gametocytes. An actin cytoskeleton within the parasite has also been shown to be present primarily at the gametocyte poles, and it dissociates during the transition to Stage V (Hliscs et al., 2015).

Changes to the host red blood cell have also been implicated in gametocyte deformability. Dearnley et al. (2016) recently showed that the size of the red blood cell cytoskeleton meshwork gets larger in immature gametocytes and then contracts in Stage V gametocytes, with actin moving from the red blood cell membrane to Maurer's clefts at the same time as the meshwork contraction. The membrane cytoskeleton also becomes more closely coupled to the plasma membrane during early gametocyte development and then becomes more loosely coupled in mature gametocytes; stage III gametocytes treated with an actin-destabilizing compound had decreased membrane cytoskeleton and plasma membrane coupling and increased deformability. In addition, members of the polymorphic STEVOR protein family have been proposed to change stiffness of the host cell during gametocyte development (Tiburcio et al., 2012a). STEVOR proteins bind the red blood cell ankyrin complex and are required for stiffness of immature gametocytes, and the dephosphorylation and dissociation of STEVOR proteins from the red blood cell membrane correlates with the rigidity switch from Stage IV to V. Further, cAMP and protein kinase A signaling has been shown to be required for stiffness of immature gametocytes, with phophodiesterase activity then required for deformability of mature gametocytes (Naissant et al., 2016; Ramdani et al., 2015; Tiburcio et al., 2012a). Overall, these observations suggest that, as in asexual stages, parasite-encoded factors alter the deformability of the host cell during gametocyte development.

In addition to not knowing all of the mechanisms underlying changes in gametocyte deformability, it is also not clear at which point during or after this transition the gametocytes are released into the blood stream and therefore accessible to mosquitoes. Also, it is not known whether all deformable, circulating gametocytes are infective to mosquitoes. Previous *in vivo* studies have shown a poor correlation between numbers of circulating stage V gametocytes and infectivity to mosquitos, suggesting heterogeneity in the stage V population (Churcher et al., 2013). This is a crucial knowledge gap as biomarkers for infective gametocytes may be key diagnostic tools to determine the human infectious reservoir and assess the efficacy of transmission-blocking interventions.

We seek to answer two major questions: (1) What factors mediate the deformability switch separating sequestering and circulating gametocytes? and (2) Are there specific markers for deformable, circulating gametocytes that are capable of infecting mosquitos? In this study, we optimized a biophysical assay to measure and separate gametocyte populations based on deformability, and we used this assay to separate deformable and stiff gametocyte over the course of gametocyte development. We combined biomechanical and transcriptional signatures to define the transition from immature non-infectious to mature infectious gametocyte. Using RNAseq of both in vitro and ex vivo samples, we aim to identify an intersecting set of genes that drive or delineate this transition.

3.3. Results

Optimization of gametocyte deformability assay

In order to study the stage IV to V transition in *P. falciparum,* we performed significant optimization of gametocyte induction and growth protocols to increase population synchrony and

gametocyte conversion rate (see Methods). We have optimized these approaches for four strains – P2G12 (3D7 clone), Pf2004, HB3, and NF54 – and selected NF54 for use in future experiments due to its status as a reference strain and its ability to reliably produce high levels of deformable late-stage gametocytes. To optimize microsphere filtration assays, we first focused on *P. falciparum* asexual stages (as discussed in Chapter 2). However, despite successful optimization with asexual stages, we still could not reliably measure the expected restoration of deformability in stage V gametocytes. Rather than observing high retention rates of early gametocytes in the bead matrix and low retention rates of late gametocytes, we consistently observed high retention of both early and late gametocytes.

We attempted to alter several parameters at the level of gametocyte culture and filtration, and we identified the bead source/batch used in the filtration as the problem. Optimization parameters and results are summarized in Table 4. In the original studies that used microsphere filtration to measure deformability of *P. falciparum* asexual and sexual stages (Deplaine et al., 2011; Sanyal et al., 2012; Tiburcio et al., 2012a), they used Type 5 (15-25 μm diameter) and Type 6 (5-15 μm in diameter) solder powder beads that were 96.50% tin, 3.00% silver, and 0.50% copper (Industrie des Poudres Sphériques, France). Because beads from this manufacturer could not be sourced in the United States, the beads we used for all asexual deformability assays and initial gametocyte deformability assays were of the same size and composition but from a domestic supplier (Amtech Advanced SMT Solder Products, division of SMT International, LLC, USA). To determine whether the bead source was causing the unexpected late gametocyte retention in our assays, we obtained beads from a lot used successfully for gametocyte deformability assays by the group of Leann Tilley and Matthew Dixon (Dearnley et al., 2016). These beads were manufactured by Heraeus Electronics and were the same composition (96.50% tin, 3.00% silver,

and 0.50% copper) and almost same size (Type 5: 10-25 mm diameter, Type 6: 5-15 mm in diameter) as used in the original gametocyte filtration study (Tiburcio et al., 2012a). Using these beads, we found that all of our gametocyte lines tested showed expected retention rates of early and late gametocytes, suggesting that the beads were the problem. However, when we obtained a new lot of the same beads directly from the same company, Heraeus, we found that gametocytes did not show expected retention rates (almost all late gametocytes were still retained in the bead matrix). Lot-to-lot variability in suitability of microspheres for gametocyte filtration has also been observed by others (Catherine Lavazec, personal communication). We expect that slight variations in bead size (below quality control thresholds) or chemical impurities from the manufacturing process could contribute to such variability. For all further assays, we used Heraeus beads from the original lot obtained from the Dixon/Tilley groups, but future use of this assay will require investigation into lot-to-lot variability or identification of alternative bead sources.

Table 4. Optimization of gametocyte microsphere filtration assay. Microsphere filtration was performed with Stage II-IV gametocytes (early to mid stage) and Stage V gametocytes (late stage). Baseline culture and filtration conditions were as follows, except where indicated otherwise: Hypoxanthine concentration = 367 uM, Glucose concentration = 11 mM, MACS purification = none, Filtration temperature = Room temperature, Assay hematocrit = 2%, Bead source = Amtech.

Culture or filtration condition altered	Early-mid gametocyte retention	Late gametocyte retention
Hypoxanthine – 367 uM	80-100%	80-100%
Hypoxanthine – 200 uM	80-100%	80-100%
Hypoxanthine – 100 uM	80-100%	80-100%
Glucose concentration – 21 mM	80-100%	80-100%
Glucose concentration –11 mM	80-100%	80-100%
MACS purification	80-100%	80-100%
No MACS purification	80-100%	80-100%
Temperature during filtration – RT	80-100%	80-100%
Temperature during filtration – 37°C	80-100%	80-100%
Assay hematocrit – 2%	80-100%	80-100%
Assay hematocrit – 1%	80-100%	80-100%
Assay hematocrit – 0.5%	80-100%	80-100%
Filtration beads – Amtech	80-100%	80-100%
Filtration beads (Heraeus, Dixon/Tilley lab lot)	80-100%	40-60%
Filtration beads (Heraeus, Marti lab 9/2015 lot)	80-100%	80-100%

Sampling of gametocyte deformability

Using the microsphere filtration assay, we harvested parasites for transcriptional profiling during the stage IV to V transition and stage V maturation. We harvested NF54 gametocytes (termed the "Upstream" sample) every 24 hours from Day 6 to 12 of gametocyte development, and we performed microsphere filtration at each time point. In this assay, both stiff and deformable gametocytes are present in the starting "upstream" sample, whereas only deformable gametocytes are present in the filtered "downstream" sample. For each time point, we performed at least 3 filtration replicates. Starting on Day 9, the filtration "Downstream" sample contained enough gametocytes to be harvested for RNA sequencing, therefore we additionally harvested "Downstream" samples on Day 9-12. At each time point, we made giemsa-stained smears of parasites to analyze morphology and quantify deformability, and we performed exflagellation assays to quantify *in vitro* activation of male gametocytes as an additional measure of maturity. A summary of samples harvested in this time course is presented in Table *5*.

Table 5. Summary of gametocyte deformability time course. Microsphere filtration was performed from Day 6 – 12 of gametocyte development. Upstream samples were harvested at each time point, and downstream samples were harvested at time point where low bead retention was observed. Exflagellation of male gametocytes was additionally measured in the upstream sample at each time point.

	Day 6	**Day 7**	**Day 8**	**Day 9**	**Day 10**	**Day 11**	**Day 12**
Samples collected	3 Up	3 Up	3 Up	3 Up, 4 Down	3 Up, 4 Down	3 Up, 4 Down	3 Up, 4 Down
Exflagellation (centers/ml)	0	0	0	20,000	100,000	370,000	200,000
Bead retention	High	High	Slightly decreased	Low	Low	Low	Low

Sequencing

RNA was extracted for each time point of the deformability assays and was submitted for SmartSeq2 (Illumina) sequencing at the Broad Institute (see Methods for detail). Upon sequencing, initial analysis of the results showed sufficient sequencing quality as approximately 85% of the reads aligned to the reference genome, with more than 1,000,000 unique reads identified for each sample.

The first round of sequencing was performed using 25 base pair read lengths (standard for the SmartSeq2 protocol), but we found that only about 30% of reads mapped to unique sites in the *P. falciparum* genome. To increase the proportion of unique reads, the libraries were resequenced using 37 base pair read lengths. With the 37 base pair reads, 84.9% of forward reads and 87.7% of reverse reads were mapped to the reference genome, and 48% of all reads were mapped uniquely. This was surprising given that it had been predicted previously that read lengths of at least 36 base pairs would yield greater than 90% uniquely mapped reads (Hoeijmakers et al., 2013). It is possible that the high expression of transcripts from variable genes families during blood stages contributed in part to the lower percentage of uniquely mapped reads in these samples.

Transcriptional changes associated with deformability

To begin identifying genes correlated with high or low deformability, we have compared gene expression between the total population ("Upstream") and the filtered, deformable population ("Downstream"). We expect genes that have higher expression in the downstream, filtered population as compared to the upstream, total population to be associated with deformability, and conversely we expect genes depleted in the downstream, filtered population to be associated with rigid parasites. We find over 200 genes significantly upregulated and downregulated in the downstream samples at each time point, with many genes upregulated or downregulated by more

than two-fold (Figure 14A,B). Because there are hundreds of genes that are significantly enriched or depleted in the downstream samples at different time points, we have taken multiple approaches to filter them further.

A

	Day 9	Day 10	Day 11	Day 12
p<.05, log2(fold change) > 0	558	538	430	767
p<.05, log2(fold change) > 1	31	86	6	198
p<.05, log2(fold change) < 0	426	507	296	779
p<.05, log2(fold change) < 1	55	207	14	476

B

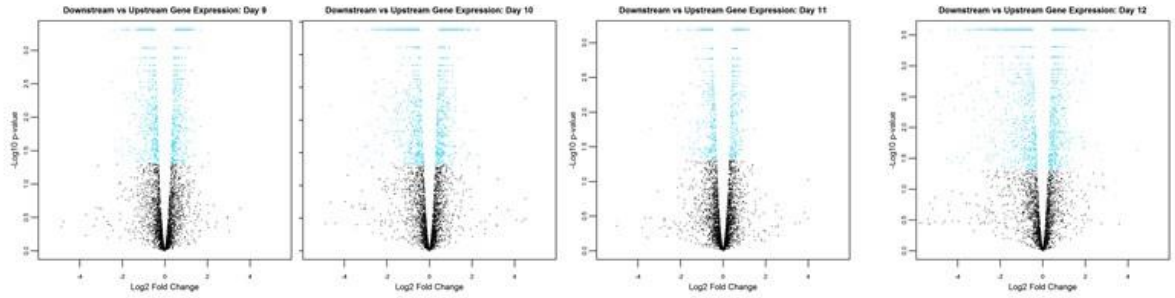

Figure 14. Differentially expressed genes between upstream and downstream samples. (A) Number of genes enriched or depleted in upstream samples per time point. (B) Comparison of upstream and downstream samples at each time point. Blue dots indicate differentially expressed genes with an adjusted p-value of ≤ 0.05.

First, we identified 6 genes that have a consistently significant (adjusted p-value ≤ 0.05), at least two-fold increase in expression in the downstream, deformable sample at all four time points, Day 9, 10, 11, and 12, and we find 17 genes with a significant (adjusted p-value ≤ 0.05), at least two-fold increase in at least 3 of the 4 timepoints (Table *6*). All of these genes have been shown previously to have highest RNA expression in late gametocytes (López-Barragán et al., 2011), which supports the hypothesis that they are drivers or markers of mature gametocyte deformability. Most of these genes have not been functionally characterized, so we performed a gene ontology (GO) analysis and correlated each gene with *P. falciparum* functional transcriptional clusters that have been described previously (Pelle et al., 2015). We identified a transcriptional cluster that is overrepresented in the consistently upregulated gene set. This cluster, termed Cluster 49, was previously annotated as a mature gametocyte cluster.

Table 6. Genes highly and consistently enriched in deformable gametocytes. All genes shown were significantly enriched by at least two fold in downstream samples at 3/4 time points (adjusted p-value ≤ 0.05: Wald test, adjusted for multiple testing by Benjamini and Hochberg method). Gene description and Curated GO terms were accessed from Plasmodb.org. Transcriptional clusters were accessed from Pelle et al. (2015).

Gene ID	Gene Description	Curated GO Function/Component/Process	Transcriptional Cluster/Annotation
PF3D7_0604400	conserved Plasmodium protein, unknown function	apicoplast; null; null	252
PF3D7_0616600	conserved Plasmodium protein, unknown function	null; null; null	216
PF3D7_0618900	NA	null; phosphatidylinositol N-acetylglucosaminyltransferase activity; GPI anchor biosynthetic process	216
PF3D7_0630200	secreted ookinete protein, putative (PSOP6)	null; null; null	5
PF3D7_0825800	conserved Plasmodium protein, unknown function	null; null; null	49 - Mature Gametocyte
PF3D7_0907800	apicoplast ribosomal protein L35 precursor, putative	apicoplast; null; null	227
PF3D7_1020200	conserved Plasmodium protein, unknown function	null; null; null	49 - Mature Gametocyte
PF3D7_1103500	CPW-WPC family protein	apicoplast; null; null	67 – Mature Gametocyte
PF3D7_1129600	phosphatidylinositol-4-phosphate 5-kinase, putative	apicoplast; phosphatidylinositol phosphate kinase activity; phosphatidylinositol phosphorylation, phosphatidylinositol-mediated signaling	49 - Mature Gametocyte
PF3D7_1141900	inner membrane complex protein 1b, putative (IMC1b)	inner membrane complex, subpellicular network; structural constituent of cytoskeleton; null	49 - Mature Gametocyte
PF3D7_1204200	conserved Plasmodium protein, unknown function	apicoplast; null; null	170
PF3D7_1207700	blood stage antigen 41-3 precursor	null; null; null	49 - Mature Gametocyte
PF3D7_1321000	conserved Plasmodium protein, unknown function	null; null; null	49 - Mature Gametocyte
PF3D7_1356000	conserved Plasmodium protein, unknown function	null; null; null	10
PF3D7_1421800	conserved Plasmodium protein, unknown function	null; null; null	49 - Mature Gametocyte
PF3D7_1447400	conserved Plasmodium protein, unknown function	null; null; null	133
PF3D7_1465700	plasmepsin VIII	null; null; cell gliding, exit from host cell	84 – Immature Gametocyte

Next, we identified 4 genes that have a significant (adjusted p-value ≤ 0.05), at least two-fold decrease in expression in the downstream samples at Day 9, 10, 11, and 12, and we identified 35 genes that have a significant, at least two-fold decrease in at least 3 of the 4 timepoints (Table *7*). The majority of these genes have highest RNA expression in early gametocytes. Several genes are also members of gametocyte clusters annotated by Pelle et al, and some have GO functions relating to motility or cytoskeletal structure.

Table 7. Genes highly and consistently depleted in deformable gametocytes. All genes shown were significantly depleted by at least two fold in downstream samples at 3/4 time points (adjusted p-value ≤ 0.05: Wald test, adjusted for multiple testing by Benjamini and Hochberg method). Gene descriptions and Curated GO terms were accessed from Plasmodb.org. Transcriptional clusters were accessed from Pelle et al. (2015).

Gene ID	Gene Description	Curated GO Function/Component/Process	Transcriptional Cluster/Annotation
PF3D7_0219600	replication factor C subunit 1, putative (RFC1)	DNA replication factor C complex; null; DNA replication	182
PF3D7_0309500	asparagine synthetase, putative	null; null; null	79
PF3D7_0320400	oocyst capsule protein (Cap380)	null; null; null	131
PF3D7_0422300	alpha tubulin 2	microtubule; null; microtubule-based movement	240 – Mature Gametocyte
PF3D7_0509000	SNAP protein (soluble N-ethylmaleimide-sensitive factor attachment protein), putative	Golgi apparatus, endoplasmic reticulum; soluble NSF attachment protein activity, transporter activity; null	159
PF3D7_0531800	5.8S ribosomal RNA	null; null; null	NA
PF3D7_0605400	calcium-binding protein, putative	null; null; null	216
PF3D7_0610800	transketolase (TK)	cytoplasm, nucleus; transketolase activity; pentose-phosphate shunt	106
PF3D7_0620000	conserved Plasmodium protein, unknown function	cell surface; null; entry into host cell	278 – Immature Gametocyte
PF3D7_0725800	5.8S ribosomal RNA	null; null; null	NA
PF3D7_0801200	5.8S ribosomal RNA	null; null; null	NA
PF3D7_0911900	falstatin (ICP)	cytosol, host cell cytoplasm, vesicle; cysteine-type endopeptidase inhibitor activity; cell motility, entry into host cell	26
PF3D7_0923600	lipoate-protein ligase 2 (LipL2)	apicoplast, mitochondrion; lipoate-protein ligase activity; null	195
PF3D7_1006800	RNA-binding protein, putative	food vacuole; mRNA binding, single-stranded telomeric DNA binding; telomere maintenance	70
PF3D7_1007700	transcription factor with AP2 domain(s) (ApiAP2)	null; sequence-specific DNA binding; null	141
PF3D7_1011900	heme oxygenase (HO)	apicoplast; heme oxygenase (decyclizing) activity; null	239
PF3D7_1016900	early transcribed membrane protein 10.3 (ETRAMP10.3)	symbiont-containing vacuole membrane; null; null	NA
PF3D7_1030000	transcription elongation factor SPT4, putative (SPT4)	null; rDNA binding; mRNA splicing, via spliceosome, regulation of transcription, DNA-templated	37
PF3D7_1033400	haloacid dehalogenase-like hydrolase (HAD1)	cytoplasm; sugar-phosphatase activity; dephosphorylation, negative regulation of isopentenyl diphosphate biosynthetic process, methylerythritol 4-phosphate pathway	86
PF3D7_1123200	leucine-rich repeat protein (LRR11)	null; null; null	239

Gene ID	Gene Description	Curated GO Function/Component/Process	Transcriptional Cluster/Annotation
PF3D7_1222700	glideosome-associated protein 45 (GAP45)	extrinsic component of membrane, host cell membrane, inner membrane complex; protein binding; null	266 – Sexual commitment
PF3D7_1235000	PIH1 domain-containing protein, putative (PIH1)	R2TP complex; null; box C/D snoRNP assembly	254
PF3D7_1243000	syntaxin, Qa-SNARE family (SYN16)	SNARE complex, trans-Golgi network; SNAP receptor activity, protein transporter activity; intracellular protein transport, regulation of vesicle fusion	192
PF3D7_1304100	DNA ligase I (LigI)	apicoplast, replication fork; DNA ligase (ATP) activity, calcium ion binding, magnesium ion binding, manganese ion binding; lagging strand elongation	NA
PF3D7_1314400	conserved Plasmodium protein, unknown function	null; null; null	202 – Immature Gametocyte
PF3D7_1341500	inner membrane complex suture component, putative (ISC1)	inner membrane complex; null; null	272 – Sexual Commitment
PF3D7_1346700	6-cysteine protein (P48/45)	anchored component of plasma membrane; protein binding; null	36 – Immature Gametocyte
PF3D7_1350800	conserved Plasmodium protein, unknown function	null; null; null	257
PF3D7_1361900	proliferating cell nuclear antigen 1 (PCNA1)	nucleus; null; null	212
PF3D7_1418300	calmodulin, putative	null; calcium ion binding; null	159
PF3D7_1426300	dynein-associated protein, putative	cytoskeleton; microtubule motor activity; microtubule-based movement	30 – Immature Gametocyte
PF3D7_1449000	gamete egress and sporozoite traversal protein, putative (GEST)	endoplasmic reticulum, microneme, osmiophilic body; null; exit from host cell	36 – Immature Gametocyte
PF3D7_1454500	nifU protein, putative (IscU1)	mitochondrion; iron ion binding; cellular iron ion homeostasis	28
PF3D7_1458700	exonuclease V, mitochondrial, putative	null; null; null	239
PF3D7_1462800	glyceraldehyde-3-phosphate dehydrogenase (GAPDH)	cell surface, cytosol, membrane; glyceraldehyde-3-phosphate dehydrogenase (NAD+) (phosphorylating) activity, protein binding; entry into host cell, gluconeogenesis, glycolytic process	106

As an alternative method to identify genes associated with deformability, we performed a principle component analysis. We show that upstream and downstream samples can be separated well and that there is additional separation between the downstream, deformable samples at each time point (Figure 15). This suggests that deformable gametocytes have a distinct transcriptional signature but also that transcriptional changes still occur as deformable parasites mature further. Two transcriptional clusters were significantly enriched in PC1, suggesting that they are correlated with deformability. The first cluster, Cluster 49 (FWER p-value = 0), is the mature gametocyte cluster also found to be correlated with deformability by fold change analysis. A second cluster, Cluster 241 (FWER p-value = 0.08), was also enriched in PC1.

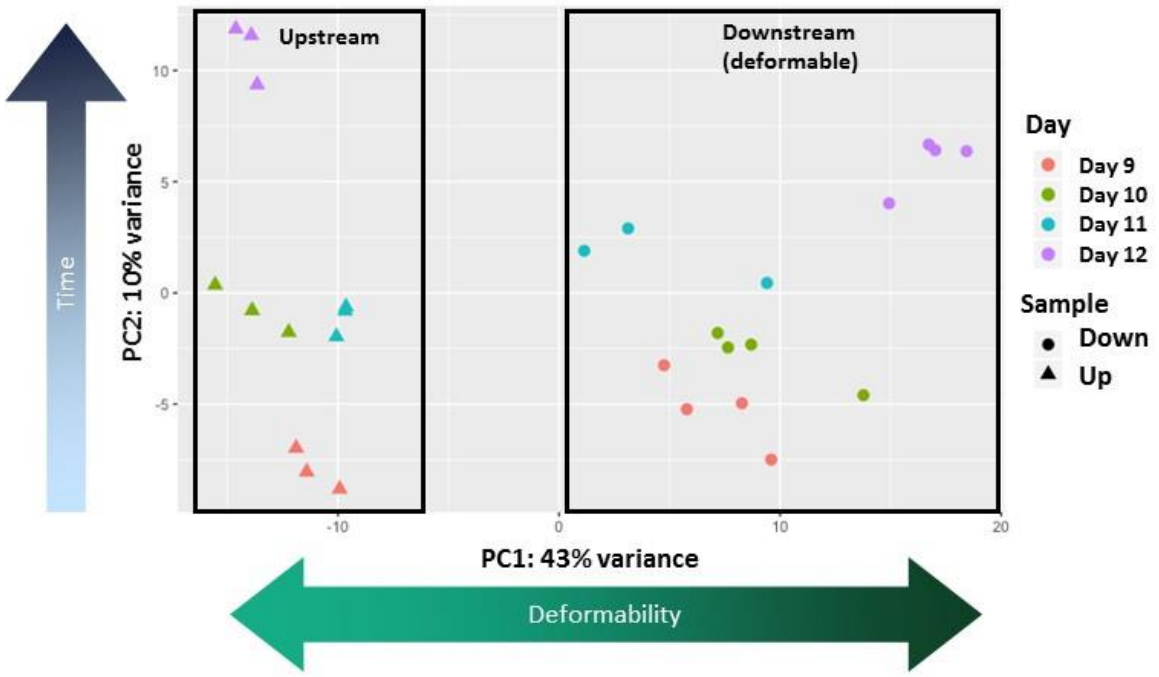

Figure 15. Principle component analysis of upstream and downstream samples from deformability time course. Comparison of upstream and downstream samples from Day 9, 10, 11, and 12. PC1 = Principle component 1, PC2 = Principle component 2.

To complement our filtering approaches based on degree or consistency of enrichment/depletion, we took a targeted approach to investigate transcriptional profiles of genes involved in cellular processes previously implicated in gametocyte deformability changes. We focused on genes putatively involved in cytoskeleton remodeling as well as cAMP-signaling, including genes that were putatively labeled as being related to actin, tubulin, dynein, myosin, protein kinase A, or phosphodiesterases. Table *8* presents all genes that included these terms and were either significantly enriched or depleted (adjusted p-value ≤ 0.05) in deformable gametocytes at *any* of the four time points assayed. Notably, many of these genes fall just under the fold change thresholds we applied previously.

Given that STEVOR expression has been shown to contribute to gametocyte deformability in a cAMP-dependent manner, we also attempted to determine whether STEVORs were upregulated or downregulated in any of our samples. However, the C-terminal sequence of STEVORs are highly conserved, making it so that most 37 base pair reads identified in this studied mapped to non-unique locations in the genome. In these cases, only the best scoring alignment was kept, making analysis of STEVORS arbitrary and inconclusive. Future transcriptional analysis would benefit from longer read lengths in order to provide better resolution for variable gene families such as these.

Table 8. Curated cytoskeleton remodeling or cAMP-signaling genes enriched or depleted in deformable gametocytes. Genes shown were significantly enriched or depleted in deformable gametocytes at least one time point. Genes are ordered according to degree of enrichment in the downstream sample (log2FC??) on Day 9. Gene descriptions were accessed from Plasmodb.org, and cluster annotations were accessed from Pelle et al, 2015. L2FC = $\log_2$(Downstream expression/Upstream expression); so, positive values indicated enrichment in the downstream, deformable sample. P-val = P-value (Wald test, adjusted for multiple testing by Benjamini and Hochberg method). D9 = Day 9, D10 = Day 10, D11 = Day 11, D12 = Day 12. MG = mature gametocyte, IG = immature gametocyte, SC = sexual commitment.

Gene ID	Gene Description	Cluster/ Annot.	D9 L2FC	p-val	D10 L2FC	p-val	D11 L2FC	p-val	D12 L2FC	p-val
PF3D7_1118700	myosin light chain B (MLC-B)	261	1.00	0.0000	0.36	0.1620	0.63	0.0001	0.57	0.0013
PF3D7_0514000	tubulin--tyrosine ligase, putative (TTL)	252	0.73	0.0001	0.70	0.0023	-0.02	0.9555	0.17	0.5890
PF3D7_0906400	dynein light intermediate chain 2, cytosolic	240 – MG	0.62	0.0001	0.70	0.0025	0.16	0.5923	1.15	0.0000
PF3D7_1321600	phosphodiesterase gamma, putative (PDEgamma)	239	0.62	0.0399	-0.07	0.9070	0.85	0.0011	0.13	0.7951
PF3D7_1145400	dynamin-like protein (DYN1)	246	0.61	0.0000	0.52	0.0000	0.68	0.0000	0.75	0.0000
PF3D7_1453100	dynactin subunit 4, putative	244	0.53	0.0965	-0.21	0.6535	-0.01	0.9895	0.94	0.0117
PF3D7_0503400	actin-depolymerizing factor 1 (ADF1)	273	0.53	0.0000	0.69	0.0000	0.48	0.0005	0.93	0.0000
PF3D7_1147200	tubulin--tyrosine ligase, putative	49 – MG	0.50	0.0002	0.60	0.0001	0.56	0.0000	1.09	0.0000
PF3D7_0909500	subpellicular microtubule protein 1, putative (SPM1)	148	0.49	0.0130	0.18	0.5369	0.48	0.0078	0.78	0.0002
PF3D7_0528500	F-actin-capping protein subunit alpha, putative (CPalpha)	202 – IG	0.46	0.0240	0.35	0.1453	0.25	0.3289	0.39	0.0573
PF3D7_1246400	myosin A tail domain interacting protein (MTIP)	275	0.45	0.0022	0.73	0.0000	0.66	0.0000	0.77	0.0000
PF3D7_0933500	gamma-tubulin complex component, putative	182	0.42	0.0013	0.49	0.0001	0.19	0.3220	0.79	0.0000

Gene ID	Gene Description	Cluster/ Annot.	D9 L2FC	p-val	D10 L2FC	p-val	D11 L2FC	p-val	D12 L2FC	p-val
PF3D7_1342600	myosin A (MyoA)	275	0.41	0.0190	0.01	0.9739	0.30	0.0170	0.03	0.8984
PF3D7_0818300	dynactin subunit 6, putative	NA	0.40	0.1224	0.50	0.0346	0.12	0.6910	0.60	0.0022
PF3D7_1118800	actin-related protein 2/3 complex subunit 1, putative (ARC40)	240 – MG	0.35	0.0672	0.39	0.0816	0.00	0.9888	0.61	0.0062
PF3D7_1009700	tubulin--tyrosine ligase, putative	266 – SC	0.16	0.5626	0.45	0.1768	0.31	0.2584	0.58	0.0058
PF3D7_0729900	dynein heavy chain, putative	30 – IGe	0.03	0.8974	0.13	0.4213	0.18	0.2535	0.51	0.0000
PF3D7_1140500	myosin F, putative (MyoF)	263 – MG	-0.18	0.2842	0.15	0.4588	-0.41	0.0054	0.15	0.4025
PF3D7_1412500	actin II (ACT2)	96	-0.23	0.5906	-0.87	0.0000	0.04	0.8915	-1.33	0.0000
PF3D7_0927500	dynein light chain, putative	262 – IG	-0.23	0.6713	-0.91	0.0449	-0.18	0.7249	-0.72	0.1546
PF3D7_1246200	actin I (ACT1)	273	-0.23	0.3241	-1.45	0.0000	0.04	0.9409	-1.46	0.0000
PF3D7_1230300	subpellicular microtubule protein 2, putative (SPM2)	NA	-0.27	0.6128	-0.41	0.5463	-0.75	NA	-1.90	0.0000
PF3D7_1229800	myosin D (MyoD)	266 – SC	-0.28	0.2993	0.23	0.3358	0.19	0.4264	0.57	0.0008
PF3D7_1223100	cAMP-dependent protein kinase regulatory subunit (PKAr)	272 – SC	-0.36	0.0291	-0.11	0.7245	-0.53	0.0016	-0.25	0.3569
PF3D7_0903700	alpha tubulin 1	213	-0.36	0.2161	-0.77	0.0003	-0.08	0.8097	-0.56	0.0147
PF3D7_1122900	dynein heavy chain, putative	209	-0.36	0.0092	-0.32	0.0255	-0.56	0.0000	-0.54	0.0000
PF3D7_0321700	microtubule and actin binding protein, putative	216	-0.37	0.1030	-0.24	0.3384	-0.47	0.0085	-0.36	0.0751
PF3D7_1008700	tubulin beta chain	212	-0.40	0.0129	-0.52	0.0063	-0.33	0.0373	-0.77	0.0000
PF3D7_1023100	dynein heavy chain, putative	254	-0.40	0.0024	-0.32	0.0137	-0.56	0.0000	-0.47	0.0000
PF3D7_1361400	actin-depolymerizing factor 2 (ADF2)	270	-0.40	0.0450	0.14	0.6774	-0.30	0.2740	0.03	0.9258
PF3D7_0718000	dynein heavy chain, putative	30 – IG	-0.42	0.0003	-0.32	0.0140	-0.56	0.0000	-0.62	0.0000

Gene ID	Gene Description	Cluster/ Annot.	D9 L2FC	p-val	D10 L2FC	p-val	D11 L2FC	p-val	D12 L2FC	p-val
PF3D7_1420800	dynein-associated protein, putative	NA	-0.43	0.1012	-0.26	0.5576	-0.17	0.6469	-0.85	0.0091
PF3D7_1346000	dynactin subunit 2, putative	210 – IG	-0.44	0.4110	0.19	0.7988	0.31	NA	1.32	0.0043
PF3D7_0905300	dynein heavy chain, putative	135	-0.47	0.0003	-0.43	0.0002	-0.57	0.0000	-0.56	0.0000
PF3D7_1114000	dynein light chain type 2, putative	7	-0.47	0.1405	-0.73	0.0077	-0.29	0.4375	-1.72	0.0000
PF3D7_0922000	dynein intermediate chain, putative	210 – IG	-0.48	0.0019	-0.37	0.0699	-0.28	0.1290	-0.53	0.0124
PF3D7_1465800	dynein beta chain, putative	84 – IG	-0.51	0.0010	-0.39	0.0116	-0.63	0.0000	-0.69	0.0000
PF3D7_1202300	dynein heavy chain, putative	30 – IG	-0.52	0.0002	-0.30	0.0394	-0.44	0.0030	-0.42	0.0071
PF3D7_1475700	tubulin epsilon chain, putative	209	-0.52	0.0009	-0.66	0.0000	-0.93	0.0000	-1.15	0.0000
PF3D7_0933800	delta tubulin, putative	30 – IG	-0.54	0.0001	-0.43	0.0077	-0.75	0.0000	-0.78	0.0000
PF3D7_1037500	dynamin-like protein (DYN2)	272 – SC	-0.64	0.0005	-0.75	0.0016	-0.15	0.5304	-1.60	0.0000
PF3D7_1470500	phosphodiesterase delta, putative (PDEdelta)	240 – MG	-0.74	0.0000	-1.14	0.0000	-0.17	0.4724	-1.26	0.0000
PF3D7_0613900	myosin E, putative (myoE)	277 – SC	-0.83	0.0068	-0.01	0.9922	-0.24	0.6307	-0.81	0.0231
PF3D7_0409900	actin-like protein, putative (ALP5b)	252	-1.03	0.0031	-0.72	0.1701	-0.40	0.3423	-0.77	0.1289
PF3D7_0422300	alpha tubulin 2	240 – MG	-1.23	0.0000	-2.15	0.0000	-0.86	0.0000	-2.55	0.0000
PF3D7_1426300	dynein-associated protein, putative	30 – IG	-1.43	0.0000	-1.75	0.0000	-0.52	0.0631	-1.57	0.0000

Sampling of in vitro and in vivo infectious gametocytes

We also harvested samples from gametocytes used in mosquito infection assays in order to identify targets associated with parasite maturation and infectiousness. At Radboud University, mosquito infections were performed at several time points during gametocyte maturation, and RNA samples were collected at each time point. Figure 16 shows a sample time course of gametocyte infectiousness.

First, highly synchronous gametocytes were harvested daily around the time point of activation (Day 7 – Day 10), and at each time point, the gametocyte infectivity was characterized through analysis of male/ female ratio, exflagellation intensity and degree of mosquito infectiousness in the standard membrane feeding assay (SMFA) (Table 9). This was done primarily with NF54 WT parasites, with a subset of time points collected for the additional *P. falciparum* strains NF135 and NF166. Samples were also harvested from an NF54 line in which males and females were differentially tagged with GFP and mCherry markers (Lasonder et al., 2016), respectively, and separated by FACS sorting.

Finally, RNA samples were also collected in Cameroon from over 40 infectious and non-infectious patients who had matched gametocyte densities. For each patient, direct membrane feeding experiments were performed to measure infectiousness. RNA was extracted and sequenced from all samples, and suitable sequencing quality was obtained.

Because the deformability and infectiousness time courses were performed with the same NF54 strain but in different labs, we wanted to compare transcriptional profiles of samples from each time course. We performed a principle component analysis including samples from Day 9 to 12 of the deformability time course and from Day 4 to 16 of the infectiousness time courses (including the Day 6 – 10 samples that were used in mosquito infection assays). This analysis

shows clustering of samples by time point (Figure 17). Importantly, many of the deformability and infectiousness samples cluster together according to developmental age.

A

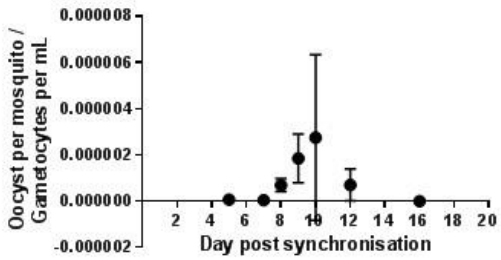

Figure 16. Sample time course of in vitro gametocyte infectiousness. (A) Dynamics of gametocyte infectiousness. NF54 gametocytes were tightly synchronized, and mosquito infections were performed from Day 5 to 16 of infection to establish the timing of peak infectiousness.

Table 9. Summary of gametocyte infectiousness time course. Highly synchronous gametocyte cultures were fed to mosquitos in standard membrane feeding assays from Day 6-10 of development. On each day, prevalence of mosquito infection was measured (indicated here as degree of infectiousness), and RNA samples were collected. X = sample collected for RNAseq.

	Day 6	**Day 7**	**Day 8**	**Day 9**	**Day 10**
Degree of infectiousness	None	None	Low	Medium	Peak
Sample harvested: NF54		**X**	**X**	**X**	**X**
Sample harvested: NF54 males		X	X	X	X
Sample harvested: NF54 females		X	X	X	X
Sample harvested: NF135	X			X	
Sample harvested: NF166	X	X	X	X	X

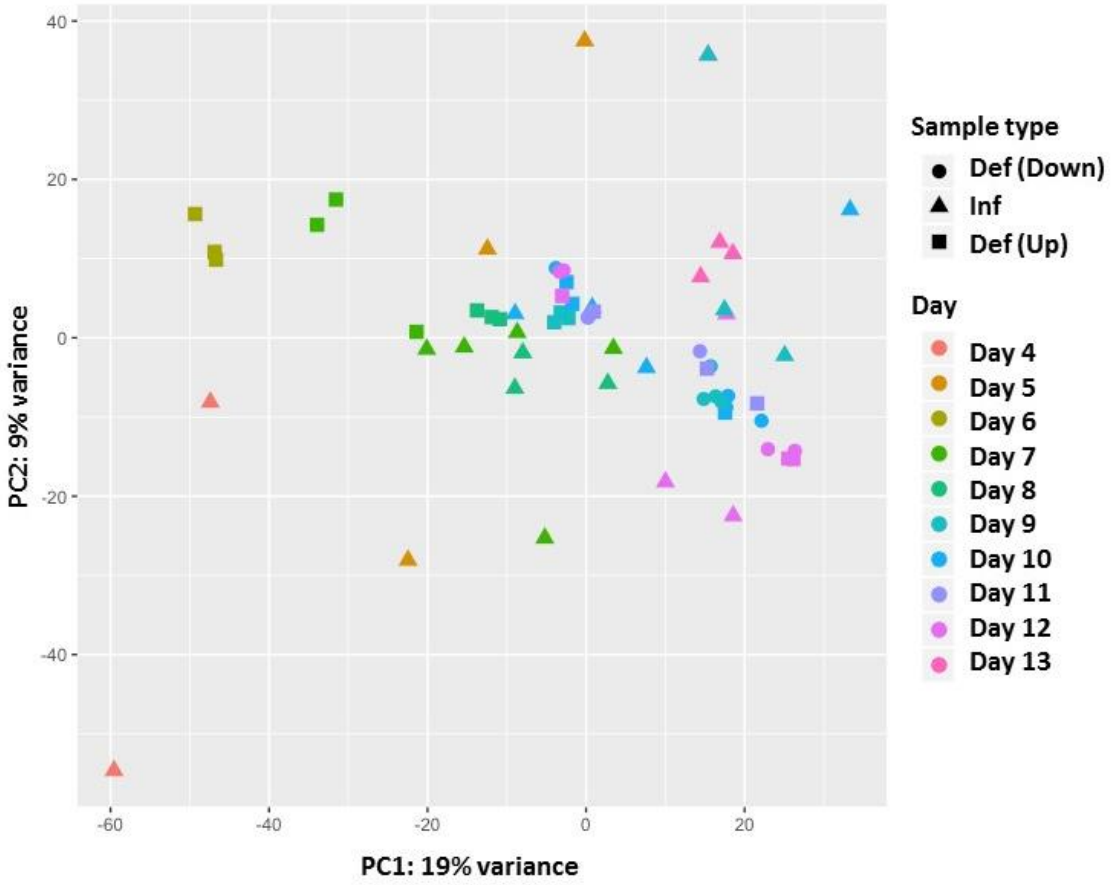

Figure 17. Principle component analysis of samples from deformability and infectiousness time courses. NF54 parasites were induced to become gametocytes and subjected to deformability assays (Boston) or infection assays (Nijmegen). RNA samples were harvested from each and overall transcriptional signatures compared. Def (Down) = Downstream samples from deformability time course. Def (Up) = Upstream samples from deformability time course. Inf = Samples from infectiousness time course. PC1 = Principle component 1, PC2 = Principle component 2.

Transcriptional changes associated with deformability and infectiousness in vitro

To identify genes that are markers of deformable, infectious gametocytes, we compared genes enriched in *in vitro* deformable gametocyte samples with those enriched in *in vitro* infectious gametocyte samples. Analysis of mosquito prevalence (defined as the percentage of mosquitos that were infected in the standard membrane feeding assays at each time point) allowed identification of several gametocyte samples that were highly infectious (ranging from Day 8 to 12 of gametocyte development) and several samples that were not infectious. We identified 107 genes that were significantly enriched (adjusted p-value $\leq$ 0.05) in the infectious samples compared to the non-infectious samples, and we found that 32 of these genes were also significantly enriched (adjusted p-value $\leq$ 0.05) in deformable gametocytes from Day 9-12 (Table 10). These genes represent a preliminary set of markers for deformable, infectious gametocytes.

Table 10. Genes significantly enriched in infectious and deformable samples. Genes shown were significantly enriched in deformable gametocytes from Day 9-12, and they were significantly enriched in infectious samples versus non-infectious samples (p-value ≤ 0.05). Genes are ordered according to degree of enrichment in infectious samples. Gene descriptions were accessed from Plasmodb.org, and cluster annotations were accessed from Pelle et al. (2015). L2FC(Inf) = $\log_2$(Infectious sample/Non-infectious sample). L2FC(DefD9) = $\log_2$(Day 9 Upstream sample/Day 9 Downstream sample). p-val = P-value (Wald test, adjusted for multiple testing by Benjamini and Hochberg method). MG = mature gametocyte, IG = immature gametocyte, SC = sexual commitment.

Gene ID	Gene Description	Cluster/ Annot.	L2FC (Inf)	p-val	L2FC (Def D9)	p-val
PF3D7_0810400	aquaporin, putative (AQP2)	136/MG	2.105548	0.000862	0.628917	0.000002
PF3D7_1331400	CPW-WPC family protein	5	1.845933	0.000243	1.064809	0.000000
PF3D7_1141100	conserved Plasmodium protein, unknown function	55	1.778001	0.003435	0.553108	0.000008
PF3D7_1204200	conserved Plasmodium protein, unknown function	170	1.773852	0.01938	1.003688	0.000000
PF3D7_0507200	subtilisin-like protease 3 (SUB3)	242	1.765632	0.009303	0.355126	0.037954
PF3D7_1013100	U3 small nucleolar RNA-associated protein 13, putative (UTP13)	39	1.749331	0.02279	0.585158	0.001796
PF3D7_0903800	LCCL domain-containing protein (CCp4)	241/MG	1.700889	0.004524	0.614183	0.000000
PF3D7_1034300	thioredoxin-like associated protein 2, putative (TLAP2)	193/IG	1.680839	0.044888	0.893087	0.000000
PF3D7_1353300	conserved Plasmodium protein, unknown function	230	1.560021	0.012226	0.378623	0.009203
PF3D7_1471800	conserved Plasmodium protein, unknown function	49/MG	1.536162	0.00062	0.452658	0.004234
PF3D7_0717800	conserved Plasmodium protein, unknown function	254	1.520281	0.033864	0.649345	0.000055
PF3D7_0320200	CPW-WPC family protein	49/MG	1.514309	9.39E-05	0.666862	0.000400
PF3D7_1221300	conserved Plasmodium protein, unknown function	257	1.508958	0.019108	0.549079	0.000017
PF3D7_1435600	conserved Plasmodium protein, unknown function	275	1.501252	0.000481	0.627115	0.000002
PF3D7_1316700	conserved Plasmodium protein, unknown function	36/IG	1.462143	0.029622	0.626337	0.000000
PF3D7_0922300	conserved Plasmodium protein, unknown function	263/MG	1.448445	0.017337	0.989904	0.000000
PF3D7_1441300	serine/threonine protein kinase, putative	257	1.427548	0.016889	0.731764	0.000000
PF3D7_1214500	conserved Plasmodium protein, unknown function	240/MG	1.420968	0.030222	0.747735	0.000000
PF3D7_1356800	serine/threonine protein kinase, putative (ARK3)	275	1.341699	0.048194	0.641628	0.000001
PF3D7_1107900	mechanosensitive ion channel protein	263/MG	1.252372	0.00659	0.507214	0.000507
PF3D7_1145200	serine/threonine protein kinase, putative	261	1.251437	0.00659	0.424332	0.000222
PF3D7_1011800	PRE-binding protein (PREBP)	100	1.246583	0.02279	0.526258	0.000001

Gene ID	Gene Description	Cluster/ Annot.	L2FC (Inf)	p-val	L2FC (Def D9)	p-val
PF3D7_0924600	conserved Plasmodium protein, unknown function	257	1.235905	0.021549	0.757946	0.000000
PF3D7_1109100	conserved Plasmodium protein, unknown function	NA	1.210704	0.044254	0.757534	0.000000
PF3D7_1327100	conserved Plasmodium protein, unknown function	263/MG	1.17749	0.028492	0.552558	0.000010
PF3D7_0403800	alpha/beta hydrolase, putative	276	1.0271	0.04353	1.106047	0.000000
PF3D7_0804700	conserved Plasmodium protein, unknown function	67/MG	0.997089	0.025525	0.538738	0.000000
PF3D7_0407800	conserved Plasmodium protein, unknown function	266/SC	0.990975	0.039231	0.692347	0.000000
PF3D7_1471500	conserved Plasmodium membrane protein, unknown function	240/MG	0.974884	0.032308	0.500493	0.000019
PF3D7_1147200	tubulin--tyrosine ligase, putative	49/MG	0.953108	0.027247	0.641107	0.000000
PF3D7_1004300	E3 ubiquitin-protein ligase, putative	31	0.902423	0.049893	0.500949	0.000237
PF3D7_1208800	zinc finger protein, putative	31	0.792376	0.048194	0.577041	0.000000

3.4. Discussion

With renewed interest in transmission-blocking interventions comes a need to better understand the biology of gametocyte maturation. Here, we took a biomechanical and transcriptional approach to identify genes that drive or delineate deformability changes in gametocytes. We optimized a biomechanical assay by which deformable and stiff gametocytes could be separated, and we used this assay to perform transcriptional profiling of deformable and stiff gametocyte samples during the course of gametocyte maturation. We identified genes that were significantly and consistently enriched in deformable gametocyte populations, suggesting that they either play a role in deformability changes or are biomarkers of deformable gametocytes capable of circulating and mediating transmission. Genes that restore the deformability of mature gametocytes could do so by reversing stiffness changes induced in immature gametocytes as well as inducing new changes to the parasite and infected red blood cell. We also identified genes that

were depleted in deformable gametocyte populations, suggesting that they play a role in maintaining the stiffness of immature gametocytes.

We first identified genes that were significantly and consistently enriched in deformable gametocyte populations. Of the genes with a greater than two-fold increase in the deformable samples for at least 3/4 time points, the majority do not yet have a described function or annotated functional domains, while a subset have known or suggested functions relating to motility or cellular remodeling (Table 6). Several of these genes were also previously assigned to mature gametocyte function transcriptional clusters (Pelle et al., 2015). However, we observed that most of these candidates have high RNA but low protein expression in mature gametocytes, suggesting that they could indeed serve as useful biomarkers of mature gametocytes but are unlikely to mediate the deformability increase observed during the stage IV to V transition. For example, IMC1b, or inner membrane complex protein 1b, has been shown to be a member of the ookinete inner membrane complex, playing an essential role in motility, cell shape, and infectiousness (Tremp et al., 2008). Although it is tempting to speculate that IMC1b could play a similar role in mature gametocytes, the lack of evidence for IMC1b protein expression during gametocyte stages (Tremp et al., 2008) suggests that while the transcript may be upregulated in mature gametocytes, it is not functional until the mosquito stages. Similarly, PF3D7_1103500, which codes for a member of the CPW-WPC family and has been shown to be expressed at the ookinete surface, is transcriptionally upregulated in our deformable gametocytes but does not have protein expression in gametocytes (Kangwanrangsan et al., 2013). Finally, PF3D7_1465700 codes for Plasmepsin VIII and has a *P. berghei* ortholog that is required for sporozoite gliding motility (Mastan et al., 2017), suggesting that this protease could play a role in cytoskeletal alteration during the deformability switch. However, there is no evidence for Plasmepsin VIII protein expression in

gametocytes, again suggesting that it is unlikely to play a functional role before the mosquito stages. Based on these observations, we expect that many of the genes with the highest transcriptional upregulation in mature, deformable gametocytes are functional primarily in the mosquito stages but could present excellent targets of diagnostics to measure density of mature gametocytes in humans.

In addition to the genes that were highly and consistently enriched in deformable gametocyte populations, we identified hundreds of additional genes that were significantly enriched in deformable populations, although with slightly lower enrichment. To filter these genes, we focused on genes with known or putative functions in processes previously shown to be involved in gametocyte deformability changes, such as cytoskeletal remodeling and cAMP-signaling (Table *8*). We propose that these candidates represent likely drivers of deformability changes. For example, we see significant enrichment of actin-depolymerizing factor 1 (ADF1, PF3D7_0503400) in the deformable gametocyte population at all 4 time points. ADF1 is expressed as a protein in late gametocytes and has been shown to sequester monomeric actin and sever actin filaments in *P. falciparum* (Wong et al., 2011), suggesting that it could play a role in the actin cytoskeleton dismantling shown to occur during the stage IV to V transition. Several other proteins involved in cytoskeletal architecture and movement are similarly enriched in our deformable gametocyte samples and known to have protein expression in late gametocytes; these proteins include: MyoA (myosin A, PF3D7_1342600), MTIP (myosin A tail domain interacting protein, PF3D7_1246400), DYN1 (dynamin-like protein, PF3D7_1145400), a putative dynactin subunit (PF3D7_1453100), dynein light intermediate chain 2 (PF3D7_0906400), a putative tubulin-tyrosine ligase (PF3D7_0514000), and a putative gamma-tubulin complex component (PF3D7_0933500). Because remodeling of actin filaments and microtubules is known to play a

role in the stage IV to V transition, we propose that these genes could mediate this remodeling and present strong candidates for follow up in reverse genetic studies.

We also identified hundreds of genes that were depleted in mature gametocytes, including several genes that had a greater than two-fold depletion in deformable gametocytes during at least three time points. Many of these genes could contribute to the increased stiffness of immature gametocytes, and as shown in Table *7* and Table *8*, many have known roles in cytoskeletal remodeling. For example, we see a significant depletion in mature gametocytes of alpha tubulin 2 (PF3D7_0422300), a core component of microtubules, which have been shown to mediate lengthening and stiffness of immature gametocytes. We also see depletion of an inner membrane complex suture component, ISC1 (PF3D7_1341500), which agrees with the previously shown role for the inner membrane complex in maintaining immature gametocyte stiffness (Dearnley et al., 2012). Depletion of GAP45 (PF3D7_1222700), a protein associated with the inner membrane complex and involved in merozoite invasion of red blood cells (Angrisano et al., 2012; Baum et al., 2006), points again toward inner membrane complex proteins involved in other stages of parasite motility also contributing to gametocyte stiffness. Depletion of PF3D7_1426300, a putative dynein-associated protein, similarly supports the role for cytoskeletal proteins in deformability changes. One interesting candidate is GEST, the gamete egress and sporozoite traversal protein (PF3D7_1449000) (Talman et al., 2011). As implied by its name, GEST is required for gamete egress and sporozoite motility, but its depletion in mature gametocytes suggests that this protein could play an additional host-parasite interaction role during immature gametocyte development.

Interestingly, one of the non-cytoskeletal genes that was most significantly downregulated in deformable gametocyte populations is a member of the ApiAP2 transcription factor family,

PF3D7_1007700, and thus could serve as a regulator of gametocyte deformability. ApiAP2 proteins have been shown to regulate several life cycle transitions in *P. falciparum,* including the decision to switch from asexual to gametocyte development (Kafsack et al., 2014; Modrzynska et al., 2017; Sinha et al., 2014). PF3D7_1007700, also referred to as ApiAP2-I, has recently been shown to play a role in invasion. However, it also binds upstream of several genes involved in host cell remodeling (Santos et al., 2017). Deletion of PF3D7_1007700 and its homolog in *P. berghei,* PBANKA_1205900, has so far been unsuccessful, and its functional role in gametocytes has not been characterized (Modrzynska et al., 2017; Santos et al., 2017). It is therefore possible that in addition to playing a role in red blood cell invasion, PF3D7_1007700 could control expression of genes that increase stiffness in immature gametocytes and would therefore be repressed in mature, deformable gametocytes.

In this study, we sought to answer two major questions: (1) What factors mediate the deformability switch separating sequestering and circulating gametocytes?, and (2) Are there specific markers for deformable, circulating, gametocytes that are capable of infecting mosquitos? Our initial analysis of these gametocyte transcriptomes has identified several putative markers of deformable, infectious gametocytes and has introduced several genes that could drive immature gametocyte stiffness or mature gametocyte deformability. This analysis has also introduced many new questions for bioinformatic and experimental follow up. To answer the first question, further bioinformatic analysis will be useful to differentiate between genes that specifically play a role in gametocyte deformability versus those that are upregulated (or downregulated) in mature gametocytes but simply co-regulated with deformability. Systematically filtering genes based on level of gametocyte protein expression (as measured by Lasonder et al. (2016), for example) as well as further gene ontology analysis will be useful for prioritizing genes most likely to be

functional in mature gametocytes. We also hypothesize that genes that drive deformability changes should be most enriched in deformable populations during the earlier time points where deformable gametocytes are detected (Day 9 and 10, in this study). Principle component analysis showed that although deformable (downstream) samples could be separated well from unfiltered (upstream samples), the deformable gametocytes at each time point are not identical (Figure 15). So, we propose to perform additional systematic investigation of transcriptional differences between younger deformable gametocytes (Day 9, for example) and older deformable gametocytes (Day 12, for example). We expect that genes that are significantly enriched in older deformable gametocytes compared to younger ones are likely to be involved in aspects of gametocyte infectiousness that are unrelated to deformability. Candidate genes proposed to drive deformability changes could then be genetically disrupted in *P. falciparum* as well as in *P. berghei.* In *P. falciparum*, deformability of transgenic lines could be measured by microsphere filtration as in this study, and in *P. berghei*, sequestration of gametocytes in host tissues could be measured during infection.

To answer our second question ("Are there specific markers for deformable, circulating, gametocytes that are capable of infecting mosquitos?"), we will perform further bioinformatic integration of these *in vitro* and *in vivo*-generated data sets. We have so far identified a preliminary union set of genes that are significantly enriched in *in vitro* deformable and infectious gametocytes (Table 10), and future work should focus on identifying which of these genes are also highly expressed in *in vivo* infectious gametocyte samples. These genes present the most promising targets for diagnostics aimed at measuring the human infectious reservoir. Combining these data sets will also enable us to better understand correlations between deformability and infectiousness. At present, it remains unclear whether all deformable gametocytes are present in circulation and

whether all deformable, circulating gametocytes are infectious. Correlating transcriptional profiles between the *in vitro* and *in vivo* data sets will be useful in answering these questions. To determine whether all deformable gametocytes are present in circulation, the profiles of deformable *in vitro* gametocytes can be compared to the profiles of *in vivo* gametocytes (from both infectious and non-infectious patients). These comparisons could include GSEA analysis and analysis of enrichment of the Pelle et al. (2015) functional transcriptional clusters as well as principle component analysis to measure relatedness of the samples. To determine whether all deformable gametocytes are infectious, similar comparisons could be made between the *in vitro* deformable samples and the *in vitro* and *in vivo* infectious samples. This study has been part of a larger Malaria Vaccines Initiative project focused on designing a field-deployable qRT-PCR-based diagnostic to measure human infectiousness, so markers identified here could be used in this diagnostic platform (Taylor et al., 2017).

Together, this study has identified several new candidate proteins that could mediate changes in gametocyte deformability or serve as markers of deformable, circulating gametocytes. The transcriptomic data sets generated in this study also provide many opportunities to answer new questions relating to genetic correlations between deformability and infectiousness of mature gametocytes. We anticipate that genes identified in this study could serve as targets of novel transmission-blocking interventions and diagnostics.

3.5. Materials and Methods

Plasmodium falciparum in vitro asexual and gametocyte culture

Blood stage parasites were cultured as described in chapter 2 of this thesis. Several wild-type and transgenic parasite strains were used for this work. For optimization of gametocyte

deformability assays, we used transgenic Pf2004 and HB3 strains that overexpress a TandemTomato construct in gametocytes (Brancucci et al., 2015). These lines were cultured in media supplemented with 4 nM WR99210 (Jacobus Pharmaceuticals) to maintain the episome. NF54 parasites, obtained from Teun Bousema (Radboud University, Nijmegen, the Netherlands), were used for the transcriptional profiling experiment. All parasites used for gametocyte production were cultured in media containing 10% human serum.

Gametocytes used for optimization of deformability assays were induced according to Fivelman et al. (2007). Briefly, parasites were grown to high ring stage parasitemia, incubated with partially spent media until schizont stage, and then split to 2% parasitemia before reinvasion occurred. Fresh media containing 50 mM GlcNac was then added to the resulting "Day 0" culture containing asexual and gametocyte rings. Media was then changed daily thereafter, with GlcNac added from Day 0-5. To prevent exflagellation of mature gametocytes, media changes were performed on a 37°C slide warmer beginning on Day 6.

Gametocytes used for transcriptional profiling were induced according to Brancucci et al. (2015) with slight modifications. Parasites were sorbitol synchronized twice 18 hours apart to obtain synchronous cultures. At 24 hours post invasion, media containing serum was replaced with media containing 0.5 % Albumax to induce formation of gametocytes. Media containing serum was added back at 44 hours post invasion, and parasites were allowed to reinvade under shaking conditions (55 rpm). After reinvasion, magnet purification was performed to collect ring stage parasites and remove late asexual stages or any gametocyte stages already present in the culture; this culture is referred to as "Day 0". Serum media was changed daily from Day 0 onwards and was supplemented with 50 mM GlcNac from Day 0-5 to prevent asexual growth. To minimize

perturbation and prevent exflagellation of mature gametocytes, media changes were performed on a 37°C slide warmer beginning on Day 0.

Microsphere filtration

Beads used for filtration assays were calibrated microspheres used for soldering and are composed of 96.50% tin, 3.00% silver, and 0.50% copper. Initial optimization of gametocyte deformability assays was performed using beads of the same composition and size as published by Deplaine et al. (2011), obtained from Gesick MPM (Type 5: 15 to 25 µ m, Type 6: 5 to 15 µ m). Further optimization and filtration for transcriptional profiling was then performed using beads of the same composition (Sn 96.5%, Ag 3%, Cu 0.5%;) and similar size (Heraeus; Type 5: 10-25 um, Type 6: 5-15 um) (Dearnley et al., 2016). These beads were a generous gift from Matthew Dixon and Leann Tilley (University of Melbourne, Melbourne, Australia).

Filtration was performed as described in Chapter 2 of this thesis. To minimize perturbation of cultures, gametocyte-containing cultures were not washed prior to filtration, and all steps were performed with media pre-warmed to 37ºC in a warm room maintained at 37ºC. After filtration, upstream and downstream parasites were collected and pelleted in a pre-warmed centrifuge (37°C) for five minutes at 500 *x g*. Giemsa smears were made for each sample. For the samples used for transcriptional profiling, supernatant was removed and parasites were then resuspended in 1 ml of Buffer RLT (Qiagen) supplemented with 1% b-mercaptoethanol. Samples were then quickly frozen at -80C.

Exflagellation assays

To measure exflagellation, 40 µl of a 2% hematocrit gametocyte culture was centrifuged and resuspended in 20 µl of media containing 50% serum. This sample was then incubated at 23

°C in a heat block. 10 µl of the sample was then placed in a hemacytometer and the number of exflagellation centers per 1 mm^2 was counted.

RNA preparation

RNA extractions were performed as published (Hoeijmakers et al., 2013). Samples preserved in Buffer RLT were extracted using the Qiagen RNeasy Mini kit. They were then incubated for 30 minutes with TURBO DNase (Thermo Fisher Scientific) and purified/concentrated using a Qiagen RNeasy Micro kit.

RNA concentration and quality was then measured at the Harvard Medical School Biopolymers Facility (Boston, MA) by RNA 6000 Pico Bioanalyzer (Agilent). Concentrations were confirmed by Qubit RNA HS assay (Thermo Fisher Scientific).

Sequencing and analysis

RNA samples were diluted to 2 ug/ul in nuclease-free ddH20 (Ambion). 10 ul of each sample was placed in a 96 well plate to obtain a final concentration of 20 ng RNA/well.
The SmartSeq2 libraries were prepared according to the SmartSeq2 protocol (Picelli et al., 2013; Picelli et al., 2014) with some modifications (Trombetta et al., 2014). Briefly, total RNA was purified using RNA-SPRI beads. Poly(A)+ mRNA was converted to cDNA which was then amplified. cDNA was subject to transposon-based fragmentation that used dual-indexing to barcode each fragment of each converted transcript with a combination of barcodes specific to each sample. In the case of single cell sequencing, each cell was given its own combination of barcodes. Barcoded cDNA fragments were then pooled prior to sequencing. Sequencing was carried out as paired-end 2x25bp with an additional 8 cycles for each index.

For library re-sequencing, sequencing was carried out as paired-end 2x37bp with an additional 8 cycles for each index.

Paired reads were checked for general quality by FastQC(Andrews). Mapping of the reads to the 3D7 reference genome (version 3, retrieved from PlasmoDB version 28) was performed with the Tuxedo Tools suite (Bowtie 2 version 2.2.6 and TopHat v2.0.14)(Kim et al., 2013; Langmead and Salzberg, 2012), and read counts per gene were calculated with HTseqcount (Anders et al., 2015). If mapping was not unique, best scoring alignment was kept. Alignment score was determined by base quality of the reads, number and positions of mismatches in the alignment, and whether forward and reverse reads could be mapped concordantly. Normalization of the read counts for library size, accounting for batch effects, differential expression analysis and principle component analysis were then performed with the DEseq2 package for R (Love et al., 2014).

3.5. Acknowledgements

We thank Dr. Matthew Dixon and Dr. Leann Tilley for the kind gift of Heraeus beads used for filtration. We thank the Broad Technologies Lab and Broad Sequencing Platform for performing the SmartSeq2 work. We thank Ping Lui for help with exflagellation assays, Elias Gerrick, Dr. Richard Bartfai, and Dr. Wieteke Hoeijmakers for advice regarding RNA preparation ans sequencing, and Dr. Elamaran Meibalan and Dr. Nicolas Brancucci for help with final sequencing sample prep. Finally, we thank PATH MVI and the U.S. National Science Foundation Graduate Research Fellowship Program (DGE1144152) for funding.

CHAPTER 4: DISCUSSION

Deepali Ravel[1], Kathleen Dantzler[1], Matthias Marti[1, 2]

[1]Department of Immunology and Infectious Disease, Harvard T.H. Chan School of Public Health, Boston, MA, USA
[2]Wellcome Centre for Molecular Parasitology, Institute of Infection, Immunity & Inflammation, University of Glasgow, Glasgow, UK

Author contributions

D. Ravel wrote sections 4.1. and 4.2. The discussion of recently developed tools included in section 4.2 was originally written by D. Ravel , with input from K. Dantzler and M. Marti, as part of a review article published in 2015 in Current Opinions in Microbiology (Dantzler et al., 2015). D. Ravel adapted this discussion for inclusion in this thesis.

4.1. Summary

Despite significant progress in global malaria control, *Plasmodium falciparum* remains a major cause of morbidity and mortality world-wide, demanding new interventions based on a better understanding of the underlying cellular mechanisms that mediate parasite survival and transmission. In this thesis, we focus on improving understanding of the cellular processes involved in remodeling and sequestration of malaria parasites during asexual and sexual development. Using both reverse and forward genetic approaches, we have identified new genes involved in these key processes.

In Chapter 2, we investigated red blood cell remodeling and sequestration during blood stage development by focusing specifically on the *Plasmodium* helical interspersed sub-telomeric c (PHISTc) protein family. PHIST proteins are exported and contain a helical core domain shared by all PHIST paralogs. Members of the PHISTc subfamily are conserved across primate malarias, and several are expressed in both asexual and sexual blood stages (Sargeant et al., 2006; Warncke

et al., 2016). Due to this conservation, they are appealing candidates for mediating remodeling and sequestration changes across species and life cycle stages. Prior to this thesis, several PHIST domain-containing proteins from the PHISTb family had been shown to play a role in cellular rigidity or cytoskeletal architecture (Diez-Silva et al., 2012; Maier et al., 2008; Parish et al., 2013). One PHISTc protein, MAL7P1.172, was also shown to play a role in trafficking of PfEMP1 to the red blood cell surface (Maier et al., 2008).

To investigate the role of PHISTc proteins in asexual and sexual stage remodeling, we genetically disrupted 9 of the 16 *P. falciparum* paralogs in the reference line 3D7 and knocked out a subset of these in a second line, CS2. Using flow cytometry, we showed that 6 of the 9 PHISTc knock outs have decreased asexual surface reactivity to serum from malaria patients, suggesting that they are required for trafficking of antigens to the surface of the asexual infected red blood cell. Disruption of one of these genes, PF11_0503, in CS2 parasites also showed a complete absence of the VAR2CSA PfEMP1 variant at the erythrocyte surface, while disruption of two other genes, PF08_0137 and PFB0105c, did not disrupt VAR2CSA surface display. These data show that PF11_0503 is required for trafficking of VAR2CSA to the red blood cell surface, and they also suggest differential specificity for surface antigen delivery between PHISTc proteins. It is important to note that although the majority of antigen trafficking studies have focused on PfEMP1, particularly the VAR2CSA variant, these findings emphasize the importance of further investigation into trafficking of other variant surface antigens and other PfEMP1 variants. To determine whether PHISTc proteins are required for deformability changes in the infected cell, we used filtration through a bead matrix to show that none of the 9 PHISTc genes studied affects cellular rigidity of asexual stages. Immunofluorescence and electron microscopy further confirmed that PHISTc disruption also does not affect trafficking of knob or Maurer's clefts markers. Finally,

we used immunofluorescence and cryo-immune electron microscopy of epitope-tagged PHISTc proteins to show that they are exported to punctate structures in the host cells during asexual and sexual stages. So far, our observations suggest that PHISTc proteins play a specialized role in antigen delivery to the host cell surface without drastically altering cellular architecture and that this role may be conserved across asexual and sexual stage development. Interestingly, this suggests partitioning between the functional roles of proteins in the PHIST b and c subfamilies.

In Chapter 3, we investigated remodeling during sequestration and transmission by focusing on the molecular processes involved in transition of stiff, sequestered gametocytes to deformable, circulating gametocytes. In the past decade, there has been significant progress in understanding sequestration and remodeling of gametocytes. Our group and others have shown that immature gametocytes are rigid and sequester outside of circulation in host tissues, while mature stages are deformable and found in circulation, where they can be transmitted to mosquitoes (Aguilar et al., 2014; Aingaran et al., 2012; Dearnley et al., 2012; Joice et al., 2014; Tiburcio et al., 2012a). These observations led us to ask what factors mediate the deformability switch separating sequestering and circulating gametocytes and to ask if there are specific markers for deformable, circulating gametocytes that are capable of infecting mosquitos.

To answer these questions, we optimized a biomechanical assay by which deformable and stiff gametocytes could be separated, and we used this assay to perform transcriptional profiling of deformable and stiff gametocyte samples during the course of gametocyte maturation. We sampled gametocytes during a time frame spanning the transition in gametocyte deformability and infectivity, and these populations were analyzed by RNA sequencing. We identified genes that were significantly enriched in deformable gametocyte populations, suggesting that they either play a role in deformability changes or are biomarkers of deformable gametocytes capable of circulating

and mediating transmission, and we identified genes that were depleted in deformable gametocyte populations, suggesting that they play a role in maintaining the stiffness of immature gametocytes. As expected, many of the genes correlated with deformability changes are known or predicted to play a role in cytoskeletal remodeling. We also identified many genes of unknown function, supporting the potential for this forward genetic method to reveal new players involved in gametocyte deformability changes. In parallel to deformability sampling, we performed RNA sequencing with *in vitro* and *in vivo* gametocyte samples that were assayed for infectiousness through controlled mosquito infections. This has so far enabled us to generate an initial set of markers for deformable, infectious gametocytes, and we anticipate that these data sets will provide rich opportunities to identify a transcriptional signature for deformable, infectious gametocytes and delve further into the biology of remodeling and infectiousness.

4.2. Future Directions

The major studies in this dissertation have focused on different aspects of remodeling and sequestration, and they point toward the existence of both conserved and stage-specific mechanisms involved in these processes. Our investigation of PHISTc proteins focuses primarily on asexual stages, but extending these studies to include gametocytes will be important for understanding PHISTc protein biology and potentially introducing conserved targets for transmission-blocking intervention. Surface proteomic profiling of asexual and gametocyte stage parasites from transgenic lines lacking PHISTc proteins will be useful for determining stage overlap in PHISTc-trafficked proteins. Such studies will also elucidate the contribution of PHISTc proteins to the trafficking of antigens other than PfEMP1 and indicate whether PHISTc proteins play a role in remodeling and sequestration outside of PfEMP1-mediated cytoadherence. Finally,

further localization studies of PHISTc proteins in asexual stages and gametocytes will be important for understanding conservation of trafficking machinery between asexual and gametocyte stages. Ultimately, these insights may be relevant for the design of interventions that are capable of simultaneously targeting pathogenic and transmissible stages of the parasite.

Our transcriptional investigation of deformability, and its links to transmission, has so far focused entirely on gametocytes, and future work should pursue gametocyte-specific and more conserved candidates identified in this study. As mentioned previously, we identified many genes that may mediate stiffening or deformability restoration in gametocytes. Many of the proteins that correlate with gametocyte deformability have been shown to have a role in inner membrane complex formation or migration of other *P. falciparum* stages (such as merozoites, sporozoites, or ookinetes) and thus may play conserved roles across these stages. Drugs that target such components could therefore be effective against not only gametocytes but also other life cycle stages. Similarly, proteins identified in this study that may contribute to changes to the host cell cytoskeleton could play a role in altering both asexual stages and gametocytes. For example, we identified a protein from the PHISTb family, PF3D7_1252700, that was significantly depleted in mature, deformable gametocytes and was previously shown to be exported to the host cell periphery in asexual stages (Tarr et al., 2014); given previous evidence for PHISTb-mediated deformability changes, this gene could be involved in deformability of both asexual and sexual stages. Finally, biomarkers of infectiousness identified in this study could be combined with current biomarkers in order to create diagnostics that dually measure total parasite burden and the reservoir of infectiousness in patient populations.

During the time frame of this thesis, the malaria research community has made significant progress in developing molecular, imaging, and drug/vaccine screening tools that present exciting

opportunities to pursue observations and questions introduced by our studies. First, the development of systems for CRISPR-Cas-mediated genetic disruption (Ghorbal et al., 2014; Wagner et al., 2014) in *P. falciparum* will enable targeted much higher throughput investigation of the candidate deformability-related genes identified in Chapter 3. Similarly, such genetic tools will make it practical to perform follow up investigation of the PHISTc genes from Chapter 2 in recently-adapted field isolates or in additional lines particularly amenable to gametocyte studies. In addition, advances in *in vivo* live imaging of *Plasmodium* infections in rodent and non-human primate models will enable the study of asexual and gametocyte sequestration in the context of the host organism (Beignon et al., 2014; Claser et al., 2014). Given that remodeling and sequestration are more important for parasite survival and virulence *in vivo* than *in vitro*, such tools will be essential for validating the true functional roles of genes introduced in our studies. Several new platforms for high throughput screening of drugs that target gametocytes in addition to asexual stages could be used to test drugs that target remodeling-related processes. Some of these assays enable monitoring of gametocyte-specific drug activity (Cevenini et al., 2014; Wang et al., 2014), while others allow screening of parasite lines including field isolates (Brancucci et al., 2015; D'Alessandro et al., 2013; Duffy and Avery, 2013; Sanders et al., 2014; Tanaka et al., 2013). In addition, new readouts for transmission-blocking activity will increase throughput of drug and vaccine testing (Ruecker et al., 2014; Stone et al., 2014). Finally, additional transcriptomic and proteomic studies (Lasonder et al., 2016; Pelle et al., 2015; Tao et al., 2014) will complement the transcriptomes presented in this work and may help identify stage-specific biomarkers.

In conclusion, the malaria elimination agenda has driven a renewed focus on understanding the molecular underpinnings of parasite biology and survival. In this dissertation, we have

presented two studies that reveal new components and processes involved in the remodeling and sequestration of *P. falciparum* parasites during malaria infection and transmission.

REFERENCES

Absalon, S., Robbins, J.A., and Dvorin, J.D. (2016). An essential malaria protein defines the architecture of blood-stage and transmission-stage parasites. Nature Communications *7*, 11449.

Aguilar, R., Magallon-Tejada, A., Achtman, A.H., Moraleda, C., Joice, R., Cistero, P., Li Wai Suen, C.S., Nhabomba, A., Macete, E., Mueller, I.*, et al.* (2014). Molecular evidence for the localization of Plasmodium falciparum immature gametocytes in bone marrow. Blood *123*, 959-966.

Aingaran, M., Zhang, R., Law, S.K., Peng, Z., Undisz, A., Meyer, E., Diez-Silva, M., Burke, T.A., Spielmann, T., Lim, C.T.*, et al.* (2012). Host cell deformability is linked to transmission in the human malaria parasite Plasmodium falciparum. Cell Microbiol *14*, 983-993.

Akinyi, S., Hanssen, E., Meyer, E.V., Jiang, J., Korir, C.C., Singh, B., Lapp, S., Barnwell, J.W., Tilley, L., and Galinski, M.R. (2012). A 95 kDa protein of Plasmodium vivax and P. cynomolgi visualized by three-dimensional tomography in the caveola-vesicle complexes (Schuffner's dots) of infected erythrocytes is a member of the PHIST family. Mol Microbiol *84*, 816-831.

Alano, P. (2007). Plasmodium falciparum gametocytes: still many secrets of a hidden life. Mol Microbiol *66*, 291-302.

Alonso, P.L., Brown, G., Arevalo-Herrera, M., Binka, F., Chitnis, C., Collins, F., Doumbo, O.K., Greenwood, B., Hall, B.F., Levine, M.M.*, et al.* (2011). A research agenda to underpin malaria eradication. PLoS Med *8*, e1000406.

Anders, S., Pyl, P.T., and Huber, W. (2015). HTSeq--a Python framework to work with high-throughput sequencing data. Bioinformatics (Oxford, England) *31*, 166-169.

Anderson, D.C., Lapp, S.A., Akinyi, S., Meyer, E.V.S., Barnwell, J.W., Korir-Morrison, C., and Galinski, M.R. (2015). Plasmodium vivax trophozoite-stage proteomes. Journal of proteomics *115*, 157-176.

Andrews, S. FastQC A Quality Control tool for High Throughput Sequence Data.

Angrisano, F., Riglar, D.T., Sturm, A., Volz, J.C., Delves, M.J., Zuccala, E.S., Turnbull, L., Dekiwadia, C., Olshina, M.A., Marapana, D.S.*, et al.* (2012). Spatial localisation of actin filaments across developmental stages of the malaria parasite. PLoS One *7*, e32188.

Bannister, L.H., Margos, G., and Hopkins, J.M. (2005). Making a home for Plasmodium post-genomics: ultrastructural organization of the blood stages. Molecular Approaches to Malaria, ASM Press, Chapter 3.

Baum, J., Richard, D., Healer, J., Rug, M., Krnajski, Z., Gilberger, T.W., Green, J.L., Holder, A.A., and Cowman, A.F. (2006). A conserved molecular motor drives cell invasion and gliding motility across malaria life cycle stages and other apicomplexan parasites. J Biol Chem *281*, 5197-5208.

Beck, J.R., Muralidharan, V., Oksman, A., and Goldberg, D.E. (2014). PTEX component HSP101 mediates export of diverse malaria effectors into host erythrocytes. Nature *511*, 592-595.

Beignon, A.S., Le Grand, R., and Chapon, C. (2014). In vivo imaging in NHP models of malaria: challenges, progress and outlooks. Parasitol Int *63*, 206-215.

Birnbaum, J., Flemming, S., Reichard, N., Soares, A.B., Mesen-Ramirez, P., Jonscher, E., Bergmann, B., and Spielmann, T. (2017). A genetic system to study Plasmodium falciparum protein function. Nat Methods *14*, 450-456.

Botha, M., Pesce, E.R., and Blatch, G.L. (2007). The Hsp40 proteins of Plasmodium falciparum and other apicomplexa: regulating chaperone power in the parasite and the host. Int J Biochem Cell Biol *39*, 1781-1803.

Brancucci, N.M., Goldowitz, I., Buchholz, K., Werling, K., and Marti, M. (2015). An assay to probe Plasmodium falciparum growth, transmission stage formation and early gametocyte development. Nat Protoc *10*, 1131-1142.

Brancucci, N.M., Witmer, K., Schmid, C.D., Flueck, C., and Voss, T.S. (2012). Identification of a cis-acting DNA-protein interaction implicated in singular var gene choice in Plasmodium falciparum. Cell Microbiol *14*, 1836-1848.

Buchholz, K., Burke, T.A., Williamson, K.C., Wiegand, R.C., Wirth, D.F., and Marti, M. (2011). A high-throughput screen targeting malaria transmission stages opens new avenues for drug development. J Infect Dis *203*, 1445-1453.

Cevenini, L., Camarda, G., Michelini, E., Siciliano, G., Calabretta, M.M., Bona, R., Kumar, T.R., Cara, A., Branchini, B.R., Fidock, D.A.*, et al.* (2014). Multicolor bioluminescence boosts malaria research: quantitative dual-color assay and single-cell imaging in Plasmodium falciparum parasites. Anal Chem *86*, 8814-8821.

Chan, J.A., Howell, K.B., Langer, C., Maier, A.G., Hasang, W., Rogerson, S.J., Petter, M., Chesson, J., Stanisic, D.I., Duffy, M.F.*, et al.* (2016). A single point in protein trafficking by Plasmodium falciparum determines the expression of major antigens on the surface of infected erythrocytes targeted by human antibodies. Cell Mol Life Sci *73*, 4141-4158.

Chan, J.A., Howell, K.B., Reiling, L., Ataide, R., Mackintosh, C.L., Fowkes, F.J., Petter, M., Chesson, J.M., Langer, C., Warimwe, G.M.*, et al.* (2012). Targets of antibodies against Plasmodium falciparum-infected erythrocytes in malaria immunity. J Clin Invest *122*, 3227-3238.

Churcher, T.S., Bousema, T., Walker, M., Drakeley, C., Schneider, P., Ouedraogo, A.L., and Basanez, M.G. (2013). Predicting mosquito infection from Plasmodium falciparum gametocyte density and estimating the reservoir of infection. Elife *2*, e00626.

Claser, C., Malleret, B., Peng, K., Bakocevic, N., Gun, S.Y., Russell, B., Ng, L.G., and Renia, L. (2014). Rodent Plasmodium-infected red blood cells: imaging their fates and interactions within their hosts. Parasitol Int *63*, 187-194.

Cooke, B.M., Rogerson, S.J., Brown, G.V., and Coppel, R.L. (1996). Adhesion of malaria-infected red blood cells to chondroitin sulfate A under flow conditions. Blood *88*, 4040-4044.

Crabb, B.S., Cooke, B.M., Reeder, J.C., Waller, R.F., Caruana, S.R., Davern, K.M., Wickham, M.E., Brown, G.V., Coppel, R.L., and Cowman, A.F. (1997). Targeted Gene Disruption Shows That Knobs Enable Malaria-Infected Red Cells to Cytoadhere under Physiological Shear Stress. Cell *89*, 287-296.

D'Alessandro, S., Silvestrini, F., Dechering, K., Corbett, Y., Parapini, S., Timmerman, M., Galastri, L., Basilico, N., Sauerwein, R., Alano, P.*, et al.* (2013). A Plasmodium falciparum screening assay for anti-gametocyte drugs based on parasite lactate dehydrogenase detection. The Journal of antimicrobial chemotherapy *68*, 2048-2058.

Dantzler, K. (2017). Gametocyte-specific immunity provides a rationale for novel transmission blocking interventions in P. falciparum Doctoral Thesis, Harvard University.

Dantzler, K.W., Ravel, D.B., Brancucci, N.M., and Marti, M. (2015). Ensuring transmission through dynamic host environments: host-pathogen interactions in Plasmodium sexual development. Curr Opin Microbiol *26*, 17-23.

de Koning-Ward, T.F., Gilson, P.R., Boddey, J.A., Rug, M., Smith, B.J., Papenfuss, A.T., Sanders, P.R., Lundie, R.J., Maier, A.G., Cowman, A.F.*, et al.* (2009). A newly discovered protein export machine in malaria parasites. Nature *459*, 945-949.

De Niz, M., Ullrich, A.K., Heiber, A., Blancke Soares, A., Pick, C., Lyck, R., Keller, D., Kaiser, G., Prado, M., Flemming, S.*, et al.* (2016). The machinery underlying malaria parasite virulence is conserved between rodent and human malaria parasites. Nat Commun *7*, 11659.

Dearnley, M., Chu, T., Zhang, Y., Looker, O., Huang, C., Klonis, N., Yeoman, J., Kenny, S., Arora, M., Osborne, J.M.*, et al.* (2016). Reversible host cell remodeling underpins deformability changes in malaria parasite sexual blood stages. Proc Natl Acad Sci U S A *113*, 4800-4805.

Dearnley, M.K., Yeoman, J.A., Hanssen, E., Kenny, S., Turnbull, L., Whitchurch, C.B., Tilley, L., and Dixon, M.W. (2012). Origin, composition, organization and function of the inner membrane complex of Plasmodium falciparum gametocytes. J Cell Sci *125*, 2053-2063.

Deplaine, G., Safeukui, I., Jeddi, F., Lacoste, F., Brousse, V., Perrot, S., Biligui, S., Guillotte, M., Guitton, C., Dokmak, S.*, et al.* (2011). The sensing of poorly deformable red blood cells by the human spleen can be mimicked in vitro. Blood *117*, e88-95.

Desai, M., ter Kuile, F.O., Nosten, F., McGready, R., Asamoa, K., Brabin, B., and Newman, R.D. (2007). Epidemiology and burden of malaria in pregnancy. The Lancet Infectious Diseases *7*, 93-104.

Desai, S.A. (2014). Why do malaria parasites increase host erythrocyte permeability? Trends Parasitol *30*, 151-159.

Diez-Silva, M., Park, Y., Huang, S., Bow, H., Mercereau-Puijalon, O., Deplaine, G., Lavazec, C., Perrot, S., Bonnefoy, S., Feld, M.S.*, et al.* (2012). Pf155/RESA protein influences the dynamic microcirculatory behavior of ring-stage Plasmodium falciparum infected red blood cells. Sci Rep *2*, 614.

Dixon, M.W., Dearnley, M.K., Hanssen, E., Gilberger, T., and Tilley, L. (2012). Shape-shifting gametocytes: how and why does P. falciparum go banana-shaped? Trends Parasitol *28*, 471-478.

Duffy, M.F., Byrne, T.J., Carret, C., Ivens, A., and Brown, G.V. (2009). Ectopic recombination of a malaria var gene during mitosis associated with an altered var switch rate. J Mol Biol *389*, 453-469.

Duffy, M.F., Maier, A.G., Byrne, T.J., Marty, A.J., Elliott, S.R., O'Neill, M.T., Payne, P.D., Rogerson, S.J., Cowman, A.F., Crabb, B.S., *et al.* (2006). VAR2CSA is the principal ligand for chondroitin sulfate A in two allogeneic isolates of Plasmodium falciparum. Mol Biochem Parasitol *148*, 117-124.

Duffy, S., and Avery, V.M. (2013). Identification of inhibitors of Plasmodium falciparum gametocyte development. Malar J *12*, 408.

Dvorin, J.D., Martyn, D.C., Patel, S.D., Grimley, J.S., Collins, C.R., Hopp, C.S., Bright, A.T., Westenberger, S., Winzeler, E., Blackman, M.J., *et al.* (2010). A plant-like kinase in Plasmodium falciparum regulates parasite egress from erythrocytes. Science *328*, 910-912.

Elsworth, B., Matthews, K., Nie, C.Q., Kalanon, M., Charnaud, S.C., Sanders, P.R., Chisholm, S.A., Counihan, N.A., Shaw, P.J., Pino, P., *et al.* (2014). PTEX is an essential nexus for protein export in malaria parasites. Nature *511*, 587-591.

Farfour, E., Charlotte, F., Settegrana, C., Miyara, M., and Buffet, P. (2012). The extravascular compartment of the bone marrow: a niche for Plasmodium falciparum gametocyte maturation? Malar J *11*, 285.

Fivelman, Q.L., McRobert, L., Sharp, S., Taylor, C.J., Saeed, M., Swales, C.A., Sutherland, C.J., and Baker, D.A. (2007). Improved synchronous production of Plasmodium falciparum gametocytes in vitro. Mol Biochem Parasitol *154*, 119-123.

Frech, C., and Chen, N. (2013). Variant surface antigens of malaria parasites: functional and evolutionary insights from comparative gene family classification and analysis. BMC Genomics *14*, 427.

Fried, M., and Duffy, P.E. (1996). Adherence of Plasmodium falciparum to Chondroitin Sulfate A in the Human Placenta. Science *272*, 1502.

Ganesan, S.M., Morrisey, J.M., Ke, H., Painter, H.J., Laroiya, K., Phillips, M.A., Rathod, P.K., Mather, M.W., and Vaidya, A.B. (2011). Yeast dihydroorotate dehydrogenase as a new selectable marker for Plasmodium falciparum transfection. Mol Biochem Parasitol *177*, 29-34.

Ghorbal, M., Gorman, M., Macpherson, C.R., Martins, R.M., Scherf, A., and Lopez-Rubio, J.J. (2014). Genome editing in the human malaria parasite Plasmodium falciparum using the CRISPR-Cas9 system. Nat Biotechnol *32*, 819-821.

Glenister, F.K. (2002). Contribution of parasite proteins to altered mechanical properties of malaria-infected red blood cells. Blood *99*, 1060-1063.

Hawking, F., Wilson, M.E., and Gammage, K. (1971). Evidence for cyclic development and short-lived maturity in the gametocytes of Plasmodium falciparum. Trans R Soc Trop Med Hyg *65*, 549-559.

Hiller, N.L., Bhattacharjee, S., van Ooij, C., Liolios, K., Harrison, T., Lopez-Estraño, C., and Haldar, K. (2004). A Host-Targeting Signal in Virulence Proteins Reveals a Secretome in Malarial Infection. Science *306*, 1934-1937.

Hliscs, M., Millet, C., Dixon, M.W., Siden-Kiamos, I., McMillan, P., and Tilley, L. (2015). Organization and function of an actin cytoskeleton in Plasmodium falciparum gametocytes. Cell Microbiol *17*, 207-225.

Hoeijmakers, W.A.M., Bártfai, R., and Stunnenberg, H.G. (2013). Transcriptome Analysis Using RNA-Seq. In Malaria: Methods and Protocols, R. Ménard, ed. (Totowa, NJ: Humana Press), pp. 221-239.

Ikadai, H., Shaw Saliba, K., Kanzok, S.M., McLean, K.J., Tanaka, T.Q., Cao, J., Williamson, K.C., and Jacobs-Lorena, M. (2013). Transposon mutagenesis identifies genes essential for Plasmodium falciparum gametocytogenesis. Proc Natl Acad Sci U S A *110*, E1676-1684.

Jackson, K.E., Spielmann, T., Hanssen, E., Adisa, A., Separovic, F., Dixon, M.W., Trenholme, K.R., Hawthorne, P.L., Gardiner, D.L., Gilberger, T.*, et al.* (2007). Selective permeabilization of the host cell membrane of Plasmodium falciparum-infected red blood cells with streptolysin O and equinatoxin II. Biochem J *403*, 167-175.

Joice, R., Nilsson, S.K., Montgomery, J., Dankwa, S., Egan, E., Morahan, B., Seydel, K.B., Bertuccini, L., Alano, P., Williamson, K.C.*, et al.* (2014). Plasmodium falciparum transmission stages accumulate in the human bone marrow. Sci Transl Med *6*, 244re245.

Kafsack, B.F., Rovira-Graells, N., Clark, T.G., Bancells, C., Crowley, V.M., Campino, S.G., Williams, A.E., Drought, L.G., Kwiatkowski, D.P., Baker, D.A.*, et al.* (2014). A transcriptional switch underlies commitment to sexual development in malaria parasites. Nature *507*, 248-252.

Kangwanrangsan, N., Tachibana, M., Jenwithisuk, R., Tsuboi, T., Riengrojpitak, S., Torii, M., and Ishino, T. (2013). A member of the CPW-WPC protein family is expressed in and localized to the surface of developing ookinetes. Malaria Journal *12*, 129-129.

Keeling, P.J., and Rayner, J.C. (2015). The origins of malaria: there are more things in heaven and earth. Parasitology *142 Suppl 1*, S16-25.

Kilili, G.K., and LaCount, D.J. (2011). An erythrocyte cytoskeleton-binding motif in exported Plasmodium falciparum proteins. Eukaryot Cell *10*, 1439-1447.

Kim, D., Pertea, G., Trapnell, C., Pimentel, H., Kelley, R., and Salzberg, S.L. (2013). TopHat2: accurate alignment of transcriptomes in the presence of insertions, deletions and gene fusions. Genome Biol *14*, R36.

Knuepfer, E., Rug, M., Klonis, N., Tilley, L., and Cowman, A.F. (2005a). Trafficking determinants for PfEMP3 export and assembly under the Plasmodium falciparum-infected red blood cell membrane. Mol Microbiol *58*, 1039-1053.

Knuepfer, E., Rug, M., Klonis, N., Tilley, L., and Cowman, A.F. (2005b). Trafficking of the major virulence factor to the surface of transfected P. falciparum-infected erythrocytes. Blood *105*.

Kulzer, S., Charnaud, S., Dagan, T., Riedel, J., Mandal, P., Pesce, E.R., Blatch, G.L., Crabb, B.S., Gilson, P.R., and Przyborski, J.M. (2012). Plasmodium falciparum-encoded exported hsp70/hsp40 chaperone/co-chaperone complexes within the host erythrocyte. Cell Microbiol *14*, 1784-1795.

Kulzer, S., Rug, M., Brinkmann, K., Cannon, P., Cowman, A., Lingelbach, K., Blatch, G.L., Maier, A.G., and Przyborski, J.M. (2010). Parasite-encoded Hsp40 proteins define novel mobile structures in the cytosol of the P. falciparum-infected erythrocyte. Cell Microbiol *12*, 1398-1420.

Langmead, B., and Salzberg, S.L. (2012). Fast gapped-read alignment with Bowtie 2. Nat Methods *9*, 357-359.

Lasonder, E., Rijpma, S.R., van Schaijk, B.C., Hoeijmakers, W.A., Kensche, P.R., Gresnigt, M.S., Italiaander, A., Vos, M.W., Woestenenk, R., Bousema, T.*, et al.* (2016). Integrated transcriptomic and proteomic analyses of P. falciparum gametocytes: molecular insight into sex-specific processes and translational repression. Nucleic Acids Res *44*, 6087-6101.

Lavazec, C., Deplaine, G., Safeukui, I., Perrot, S., Milon, G., Mercereau-Puijalon, O., David, P.H., and Buffet, P. (2013). Microsphiltration: a microsphere matrix to explore erythrocyte deformability. Methods Mol Biol *923*, 291-297.

Lindblade, K.A., Steinhardt, L., Samuels, A., Kachur, S.P., and Slutsker, L. (2013). The silent threat: asymptomatic parasitemia and malaria transmission. Expert review of anti-infective therapy *11*, 623-639.

Lopes, S.C., Albrecht, L., Carvalho, B.O., Siqueira, A.M., Thomson-Luque, R., Nogueira, P.A., Fernandez-Becerra, C., Del Portillo, H.A., Russell, B.M., Renia, L.*, et al.* (2014). Paucity of Plasmodium vivax mature schizonts in peripheral blood is associated with their increased cytoadhesive potential. J Infect Dis *209*, 1403-1407.

López-Barragán, M.J., Lemieux, J., Quiñones, M., Williamson, K.C., Molina-Cruz, A., Cui, K., Barillas-Mury, C., Zhao, K., and Su, X.-z. (2011). Directional gene expression and antisense transcripts in sexual and asexual stages of Plasmodium falciparum. BMC Genomics *12*, 587-587.

Love, M.I., Huber, W., and Anders, S. (2014). Moderated estimation of fold change and dispersion for RNA-seq data with DESeq2. Genome Biol *15*, 550.

MacPherson, G.G., Warrell, M.J., White, N.J., Looareesuwan, S., and Warrell, D.A. (1985). Human cerebral malaria. A quantitative ultrastructural analysis of parasitized erythrocyte sequestration. The American Journal of Pathology *119*, 385-401.

Maier, A.G., Cooke, B.M., Cowman, A.F., and Tilley, L. (2009). Malaria parasite proteins that remodel the host erythrocyte. Nat Rev Microbiol *7*, 341-354.

Maier, A.G., Rug, M., O'Neill, M.T., Beeson, J.G., Marti, M., Reeder, J., and Cowman, A.F. (2007). Skeleton-binding protein 1 functions at the parasitophorous vacuole membrane to traffic PfEMP1 to the Plasmodium falciparum-infected erythrocyte surface. Blood *109*, 1289-1297.

Maier, A.G., Rug, M., O'Neill, M.T., Brown, M., Chakravorty, S., Szestak, T., Chesson, J., Wu, Y., Hughes, K., Coppel, R.L.*, et al.* (2008). Exported proteins required for virulence and rigidity of Plasmodium falciparum-infected human erythrocytes. Cell *134*, 48-61.

Marti, M., Good, R.T., Rug, M., Knuepfer, E., and Cowman, A.F. (2004). Targeting malaria virulence and remodeling proteins to the host erythrocyte. Science *306*, 1930-1933.

Mastan, B.S., Narwal, S.K., Dey, S., Kumar, K.A., and Mishra, S. (2017). Plasmodium berghei plasmepsin VIII is essential for sporozoite gliding motility. Int J Parasitol *47*, 239-245.

Mayer, C., Slater, L., Erat, M.C., Konrat, R., and Vakonakis, I. (2012). Structural analysis of the Plasmodium falciparum erythrocyte membrane protein 1 (PfEMP1) intracellular domain reveals a conserved interaction epitope. J Biol Chem *287*, 7182-7189.

McMillan, P.J., Millet, C., Batinovic, S., Maiorca, M., Hanssen, E., Kenny, S., Muhle, R.A., Melcher, M., Fidock, D.A., Smith, J.D.*, et al.* (2013). Spatial and temporal mapping of the PfEMP1 export pathway in Plasmodium falciparum. Cell Microbiol *15*, 1401-1418.

McRobert, L., Preiser, P., Sharp, S., Jarra, W., Kaviratne, M., Taylor, M.C., Renia, L., and Sutherland, C.J. (2004). Distinct Trafficking and Localization of STEVOR Proteins in Three Stages of the Plasmodium falciparum Life Cycle. Infection and Immunity *72*, 6597-6602.

Mills, J.P., Diez-Silva, M., Quinn, D.J., Dao, M., Lang, M.J., Tan, K.S.W., Lim, C.T., Milon, G., David, P.H., Mercereau-Puijalon, O.*, et al.* (2007). Effect of plasmodial RESA protein on deformability of human red blood cells harboring Plasmodium falciparum. Proceedings of the National Academy of Sciences of the United States of America *104*, 9213-9217.

Modrzynska, K., Pfander, C., Chappell, L., Yu, L., Suarez, C., Dundas, K., Gomes, A.R., Goulding, D., Rayner, J.C., Choudhary, J.*, et al.* (2017). A Knockout Screen of ApiAP2 Genes Reveals Networks of Interacting Transcriptional Regulators Controlling the Plasmodium Life Cycle. Cell Host Microbe *21*, 11-22.

Moll, K., Ljungström, I., Perlmann, H., Scherf, A., &, Wahlgren*, et al.* (2013). Methods in Malaria Research, 6th Edition.

Moon, R.W., Hall, J., Rangkuti, F., Ho, Y.S., Almond, N., Mitchell, G.H., Pain, A., Holder, A.A., and Blackman, M.J. (2013). Adaptation of the genetically tractable malaria pathogen Plasmodium knowlesi to continuous culture in human erythrocytes. Proc Natl Acad Sci U S A *110*, 531-536.

Morahan, B.J., Strobel, C., Hasan, U., Czesny, B., Mantel, P.-Y., Marti, M., Eksi, S., and Williamson, K.C. (2011). Functional Analysis of the Exported Type IV HSP40 Protein PfGECO in Plasmodium falciparum Gametocytes. Eukaryotic Cell *10*, 1492-1503.

Moreira, C.K., Naissant, B., Coppi, A., Bennett, B.L., Aime, E., Franke-Fayard, B., Janse, C.J., Coppens, I., Sinnis, P., and Templeton, T.J. (2016). The Plasmodium PHIST and RESA-Like Protein Families of Human and Rodent Malaria Parasites. PLoS One *11*, e0152510.

Naissant, B., Dupuy, F., Duffier, Y., Lorthiois, A., Duez, J., Scholz, J., Buffet, P., Merckx, A., Bachmann, A., and Lavazec, C. (2016). Plasmodium falciparum STEVOR phosphorylation regulates host erythrocyte deformability enabling malaria parasite transmission. Blood *127*, e42-53.

Nguitragool, W., Bokhari, A.A., Pillai, A.D., Rayavara, K., Sharma, P., Turpin, B., Aravind, L., and Desai, S.A. (2011). Malaria parasite clag3 genes determine channel-mediated nutrient uptake by infected red blood cells. Cell *145*, 665-677.

Nilsson, S.K., Childs, L.M., Buckee, C., and Marti, M. (2015). Targeting Human Transmission Biology for Malaria Elimination. PLoS Pathog *11*, e1004871.

Nunes-Silva, S., Dechavanne, S., Moussiliou, A., Pstrag, N., Semblat, J.P., Gangnard, S., Tuikue-Ndam, N., Deloron, P., Chene, A., and Gamain, B. (2015). Beninese children with cerebral malaria

do not develop humoral immunity against the IT4-VAR19-DC8 PfEMP1 variant linked to EPCR and brain endothelial binding. Malar J *14*, 493.

Oberli, A., Slater, L.M., Cutts, E., Brand, F., Mundwiler-Pachlatko, E., Rusch, S., Masik, M.F., Erat, M.C., Beck, H.P., and Vakonakis, I. (2014). A Plasmodium falciparum PHIST protein binds the virulence factor PfEMP1 and comigrates to knobs on the host cell surface. FASEB J *28*, 4420-4433.

Oberli, A., Zurbrugg, L., Rusch, S., Brand, F., Butler, M.E., Day, J.L., Cutts, E.E., Lavstsen, T., Vakonakis, I., and Beck, H.P. (2016). Plasmodium falciparum Plasmodium helical interspersed subtelomeric proteins contribute to cytoadherence and anchor P. falciparum erythrocyte membrane protein 1 to the host cell cytoskeleton. Cell Microbiol *18*, 1415-1428.

Parish, L.A., Mai, D.W., Jones, M.L., Kitson, E.L., and Rayner, J.C. (2013). A member of the Plasmodium falciparum PHIST family binds to the erythrocyte cytoskeleton component band 4.1. Malaria Journal *12*, 160.

Peatey, C.L., Watson, J.A., Trenholme, K.R., Brown, C.L., Nielson, L., Guenther, M., Timmins, N., Watson, G.S., and Gardiner, D.L. (2013). Enhanced gametocyte formation in erythrocyte progenitor cells: a site-specific adaptation by Plasmodium falciparum. J Infect Dis *208*, 1170-1174.

Pelle, K.G., Oh, K., Buchholz, K., Narasimhan, V., Joice, R., Milner, D.A., Brancucci, N.M., Ma, S., Voss, T.S., Ketman, K.*, et al.* (2015). Transcriptional profiling defines dynamics of parasite tissue sequestration during malaria infection. Genome Med *7*, 19.

Picelli, S., Bjorklund, A.K., Faridani, O.R., Sagasser, S., Winberg, G., and Sandberg, R. (2013). Smart-seq2 for sensitive full-length transcriptome profiling in single cells. Nat Methods *10*, 1096-1098.

Picelli, S., Faridani, O.R., Bjorklund, A.K., Winberg, G., Sagasser, S., and Sandberg, R. (2014). Full-length RNA-seq from single cells using Smart-seq2. Nat Protoc *9*, 171-181.

Pologe, L.G., Pavlovec, A., Shio, H., and Ravetch, J.V. (1987). Primary structure and subcellular localization of the knob-associated histidine-rich protein of Plasmodium falciparum. Proceedings of the National Academy of Sciences of the United States of America *84*, 7139-7143.

Ramdani, G., Naissant, B., Thompson, E., Breil, F., Lorthiois, A., Dupuy, F., Cummings, R., Duffier, Y., Corbett, Y., Mercereau-Puijalon, O.*, et al.* (2015). cAMP-Signalling Regulates Gametocyte-Infected Erythrocyte Deformability Required for Malaria Parasite Transmission. PLoS Pathog *11*, e1004815.

Rask, T.S., Hansen, D.A., Theander, T.G., Gorm Pedersen, A., and Lavstsen, T. (2010). Plasmodium falciparum erythrocyte membrane protein 1 diversity in seven genomes–divide and conquer. PLoS Comput Biol *6*.

Regev-Rudzki, N., Wilson, D.W., Carvalho, T.G., Sisquella, X., Coleman, B.M., Rug, M., Bursac, D., Angrisano, F., Gee, M., Hill, A.F.*, et al.* (2013). Cell-cell communication between malaria-infected red blood cells via exosome-like vesicles. Cell *153*, 1120-1133.

Rowe, J.A., Claessens, A., Corrigan, R.A., and Arman, M. (2009). Adhesion of Plasmodium falciparum-infected erythrocytes to human cells: molecular mechanisms and therapeutic implications. Expert reviews in molecular medicine *11*, e16.

Ruecker, A., Mathias, D.K., Straschil, U., Churcher, T.S., Dinglasan, R.R., Leroy, D., Sinden, R.E., and Delves, M.J. (2014). A male and female gametocyte functional viability assay to identify biologically relevant malaria transmission-blocking drugs. Antimicrob Agents Chemother *58*, 7292-7302.

Sanders, N.G., Sullivan, D.J., Mlambo, G., Dimopoulos, G., and Tripathi, A.K. (2014). Gametocytocidal screen identifies novel chemical classes with Plasmodium falciparum transmission blocking activity. PLoS One *9*, e105817.

Santos, J.M., Josling, G., Ross, P., Joshi, P., Orchard, L., Campbell, T., Schieler, A., Cristea, I.M., and Llinas, M. (2017). Red Blood Cell Invasion by the Malaria Parasite Is Coordinated by the PfAP2-I Transcription Factor. Cell Host Microbe *21*, 731-741 e710.

Sanyal, S., Egee, S., Bouyer, G., Perrot, S., Safeukui, I., Bischoff, E., Buffet, P., Deitsch, K.W., Mercereau-Puijalon, O., David, P.H.*, et al.* (2012). Plasmodium falciparum STEVOR proteins impact erythrocyte mechanical properties. Blood *119*, e1-8.

Sargeant, T.J., Marti, M., Caler, E., Carlton, J.M., Simpson, K., Speed, T.P., and Cowman, A.F. (2006). Lineage-specific expansion of proteins exported to erythrocytes in malaria parasites. Genome Biology *7*, R12.

Sharma, P., Wollenberg, K., Sellers, M., Zainabadi, K., Galinsky, K., Moss, E., Nguitragool, W., Neafsey, D., and Desai, S.A. (2013). An epigenetic antimalarial resistance mechanism involving parasite genes linked to nutrient uptake. J Biol Chem *288*, 19429-19440.

Silvestrini, F., Lasonder, E., Olivieri, A., Camarda, G., van Schaijk, B., Sanchez, M., Younis Younis, S., Sauerwein, R., and Alano, P. (2010). Protein Export Marks the Early Phase of Gametocytogenesis of the Human Malaria Parasite Plasmodium falciparum. Molecular & Cellular Proteomics : MCP *9*, 1437-1448.

Silvestrini, F., Tiburcio, M., Bertuccini, L., and Alano, P. (2012). Differential adhesive properties of sequestered asexual and sexual stages of Plasmodium falciparum on human endothelial cells are tissue independent. PLoS One *7*, e31567.

Sinden, R.E. (1982). Gametocytogenesis of Plasmodium falciparum in vitro: an electron microscopic study. Parasitology *84*, 1-11.

Sinden, R.E., Canning, E.U., Bray, R.S., and Smalley, M.E. (1978). Gametocyte and gamete development in Plasmodium falciparum. Proceedings of the Royal Society of London Series B, Biological sciences *201*, 375-399.

Sinha, A., Hughes, K.R., Modrzynska, K.K., Otto, T.D., Pfander, C., Dickens, N.J., Religa, A.A., Bushell, E., Graham, A.L., Cameron, R.*, et al.* (2014). A cascade of DNA-binding proteins for sexual commitment and development in Plasmodium. Nature *507*, 253-257.

Smalley, M.E., Abdalla, S., and Brown, J. (1981). The distribution of Plasmodium falciparum in the peripheral blood and bone marrow of Gambian children. Trans R Soc Trop Med Hyg *75*, 103-105.

Speake, C., and Duffy, P.E. (2009). Antigens for pre-erythrocytic malaria vaccines: building on success. Parasite Immunology *31*, 539-546.

Spielmann, T., and Gilberger, T.W. (2015). Critical Steps in Protein Export of Plasmodium falciparum Blood Stages. Trends Parasitol *31*, 514-525.

Stone, W.J., Churcher, T.S., Graumans, W., van Gemert, G.J., Vos, M.W., Lanke, K.H., van de Vegte-Bolmer, M.G., Siebelink-Stoter, R., Dechering, K.J., Vaughan, A.M.*, et al.* (2014). A scalable assessment of Plasmodium falciparum transmission in the standard membrane-feeding assay, using transgenic parasites expressing green fluorescent protein-luciferase. J Infect Dis *210*, 1456-1463.

Talman, A.M., Lacroix, C., Marques, S.R., Blagborough, A.M., Carzaniga, R., Menard, R., and Sinden, R.E. (2011). PbGEST mediates malaria transmission to both mosquito and vertebrate host. Mol Microbiol *82*, 462-474.

Tanaka, T.Q., Dehdashti, S.J., Nguyen, D.T., McKew, J.C., Zheng, W., and Williamson, K.C. (2013). A quantitative high throughput assay for identifying gametocytocidal compounds. Mol Biochem Parasitol *188*, 20-25.

Tao, D., Ubaida-Mohien, C., Mathias, D.K., King, J.G., Pastrana-Mena, R., Tripathi, A., Goldowitz, I., Graham, D.R., Moss, E., Marti, M.*, et al.* (2014). Sex-partitioning of the Plasmodium falciparum stage V gametocyte proteome provides insight into falciparum-specific cell biology. Mol Cell Proteomics *13*, 2705-2724.

Tarr, S.J., Moon, R.W., Hardege, I., and Osborne, A.R. (2014). A conserved domain targets exported PHISTb family proteins to the periphery of Plasmodium infected erythrocytes. Mol Biochem Parasitol *196*, 29-40.

Taylor, B.J., Lanke, K., Banman, S.L., Morlais, I., Morin, M.J., Bousema, T., Rijpma, S.R., and Yanow, S.K. (2017). A Direct from Blood Reverse Transcriptase Polymerase Chain Reaction Assay for Monitoring Falciparum Malaria Parasite Transmission in Elimination Settings. Am J Trop Med Hyg.

Thomson, J.G., and Robertson, A. (1935). The Structure and development of Plasmodium falciparum gametocytes in the internal organs and peripheral circulation. Trans R Soc Trop Med Hyg *14*, 31-40.

Tiburcio, M., Niang, M., Deplaine, G., Perrot, S., Bischoff, E., Ndour, P.A., Silvestrini, F., Khattab, A., Milon, G., David, P.H.*, et al.* (2012a). A switch in infected erythrocyte deformability at the maturation and blood circulation of Plasmodium falciparum transmission stages. Blood *119*, e172-180.

Tiburcio, M., Silvestrini, F., Bertuccini, L., Sander, A.F., Turner, L., Lavstsen, T., and Alano, P. (2012b). Early gametocytes of the malaria parasite Plasmodium falciparum specifically remodel the adhesive properties of infected erythrocyte surface. Cell Microbiol.

Tonkin, C.J., van Dooren, G.G., Spurck, T.P., Struck, N.S., Good, R.T., Handman, E., Cowman, A.F., and McFadden, G.I. (2004). Localization of organellar proteins in Plasmodium falciparum using a novel set of transfection vectors and a new immunofluorescence fixation method. Mol Biochem Parasitol *137*, 13-21.

Trager, W., and Jensen, J.B. (1976). Human malaria parasites in continuous culture. Science *193*.

Trelka, D.P., Schneider, T.G., Reeder, J.C., and Taraschi, T.F. (2000). Evidence for vesicle-mediated trafficking of parasite proteins to the host cell cytosol and erythrocyte surface membrane in Plasmodium falciparum infected ertythrocytes. Molecular and Biochemical Parasitology *106*, 131-145.

Tremp, A.Z., Khater, E.I., and Dessens, J.T. (2008). IMC1b is a putative membrane skeleton protein involved in cell shape, mechanical strength, motility, and infectivity of malaria ookinetes. J Biol Chem *283*, 27604-27611.

Trombetta, J.J., Gennert, D., Lu, D., Satija, R., Shalek, A.K., and Regev, A. (2014). Preparation of Single-Cell RNA-Seq Libraries for Next Generation Sequencing. Current protocols in molecular biology *107*, 4.22.21-17.

Turner, G.D., Ly, V.C., Nguyen, T.H., Tran, T.H., Nguyen, H.P., Bethell, D., Wyllie, S., Louwrier, K., Fox, S.B., Gatter, K.C.*, et al.* (1998). Systemic endothelial activation occurs in both mild and severe malaria. Correlating dermal microvascular endothelial cell phenotype and soluble cell adhesion molecules with disease severity. The American Journal of Pathology *152*, 1477-1487.

Turner, G.D.H., Morrison, H., Jones, M., Davis, T.M.E., Looareesuwan, S., Buley, I.D., Gatter, K.C., Newbold, C.I., Pukritayakamee, S., Nagachinta, B.*, et al.* (1994). An Immunohistochemical Study of the Pathology of Fatal Malaria: Evidence for Widespread Endothelial Activation and a Potential Role for Intercellular Adhesion Molecule-1 in Cerebral Sequestration. The American Journal of Pathology *145*, 1057-1069.

Turner, L., Lavstsen, T., Berger, S.S., Wang, C.W., Petersen, J.E., and Avril, M. (2013). Severe malaria is associated with parasite binding to endothelial protein C receptor. Nature *498*.

Van Schravendijk, M.R., Pasloske, B.L., Baruch, D.I., Handunnetti, S.M., and Howard, R.J. (1993). Immunochemical Characterization and Differentiation of Two ~300-KD Erythrocyte Membrane-Associated Proteins of Plasmodium Falciparum, PfEMP1 and PfEMP3. The American Journal of Tropical Medicine and Hygiene *49*, 552-565.

Wagner, J.C., Platt, R.J., Goldfless, S.J., Zhang, F., and Niles, J.C. (2014). Efficient CRISPR-Cas9-mediated genome editing in Plasmodium falciparum. Nat Methods *11*, 915-918.

Wahlgren, M., Goel, S., and Akhouri, R.R. (2017). Variant surface antigens of Plasmodium falciparum and their roles in severe malaria. Nat Rev Microbiol *15*, 479-491.

Wang, Z., Liu, M., Liang, X., Siriwat, S., Li, X., Chen, X., Parker, D.M., Miao, J., and Cui, L. (2014). A flow cytometry-based quantitative drug sensitivity assay for all Plasmodium falciparum gametocyte stages. PLoS One *9*, e93825.

Warncke, J.D., Vakonakis, I., and Beck, H.P. (2016). Plasmodium Helical Interspersed Subtelomeric (PHIST) Proteins, at the Center of Host Cell Remodeling. Microbiol Mol Biol Rev *80*, 905-927.

WHO (2016). World Malaria Report 2016.

Wickert, H., and Krohne, G. (2007). The complex morphology of Maurer's clefts: from discovery to three-dimensional reconstructions. Trends Parasitol *23*, 502-509.

Wickert, H., Wissing, F., Andrews, K.T., Stich, A., Krohne, G., and Lanzer, M. (2003). Evidence for trafficking of PfEMP1 to the surface of P. falciparum-infected erythrocytes via a complex membrane network. Eur J Cell Biol *82*, 271-284.

Wickham, M.E., Rug, M., Ralph, S.A., Klonis, N., McFadden, G.I., Tilley, L., and Cowman, A.F. (2001). Trafficking and assembly of the cytoadherence complex in Plasmodium falciparum-infected human erythrocytes. The EMBO Journal *20*, 5636-5649.

Wong, W., Skau, C.T., Marapana, D.S., Hanssen, E., Taylor, N.L., Riglar, D.T., Zuccala, E.S., Angrisano, F., Lewis, H., Catimel, B.*, et al.* (2011). Minimal requirements for actin filament disassembly revealed by structural analysis of malaria parasite actin-depolymerizing factor 1. Proc Natl Acad Sci U S A *108*, 9869-9874.

Zhang, Q., Ma, C., Oberli, A., Zinz, A., Engels, S., and Przyborski, J.M. (2017). Proteomic analysis of exported chaperone/co-chaperone complexes of P. falciparum reveals an array of complex protein-protein interactions. Sci Rep *7*, 42188.

APPENDIX

The following manuscript was published as a review article in Current Opinions in Microbiology:

*Dantzler, K. W., D. B. Ravel, N. M. Brancucci and M. Marti (2015). "Ensuring transmission through dynamic host environments: host-pathogen interactions in Plasmodium sexual development." Curr Opin Microbiol **26**: 17-23.*

Ensuring transmission through dynamic host environments: host-pathogen interactions in *Plasmodium* sexual development

Kathleen W. Dantzler*, Deepali B. Ravel*, Nicolas M. B. Brancucci and Matthias Marti

Address: Department of Immunology and Infectious Diseases, Harvard T.H. Chan School of Public Health, Boston, MA 02115, USA

*These 2 authors contributed equally to this work.

Abstract

A renewed global commitment to malaria elimination lends urgency to understanding the biology of Plasmodium transmission stages. Recent progress towards uncovering the mechanisms underlying P. falciparum sexual differentiation and maturation reveals potential targets for transmission-blocking drugs and vaccines. The identification of parasite factors that alter sexual differentiation, including extracellular vesicles and a master transcriptional regulator, suggest that parasites make epigenetically controlled developmental decisions based on environmental cues. New insights into sexual development, especially host cell remodeling and sequestration in the bone marrow, highlight open questions regarding parasite homing to the tissue, transmigration across the vascular endothelium, and maturation in the parenchyma. Novel molecular and

translational tools will provide further opportunities to define host-parasite interactions and design effective transmission-blocking therapeutics.

I. Introduction

The parasite Plasmodium falciparum causes the most severe form of malaria with around 600,000 deaths annually, mostly young children and pregnant women in sub-Saharan Africa [1]. Resistance to current drug therapies, the absence of a licensed vaccine, and a large asymptomatic reservoir [2] make the development of effective transmission-blocking therapeutics particularly important to any malaria elimination or eradication program. Given the paucity of known transmission stage-specific biomarkers or drug and vaccine targets, a deepened understanding of the biology of transmissible parasite stages, including their interaction with the host, is essential [3].

P. falciparum has a complex life cycle, in which asexual replication and sexual development take place in red blood cells (RBCs) of the human host and sexual reproduction in the mosquito vector. Though the asexual stages are responsible for all morbidity and mortality, successful transmission is dependent on generation of the sexual stages, termed gametocytes. Gametocytes sequester in deep tissues during their development and once mature, are released back into circulation where they can be taken up by the mosquito vector. Once in the mosquito midgut, gametocytes emerge from host RBCs, develop into male and female gametes, and undergo fertilization and further development. Recent discoveries of factors in the human host microenvironment contributing to sexual differentiation and development raise exciting new questions about the biological mechanisms of these processes. In this review, we will examine

recent advances in host-gametocyte interactions and discuss open questions and new tools to block malaria transmission.

II. Parasite and host factors drive commitment to gametocytogenesis

Blood stage parasites replicate asexually, with a small fraction diverting away from asexual multiplication and towards sexual development in each replication cycle. Although this process may have stochastic elements, it has long been thought that host environmental or secreted parasite factors may push cell fate decision from asexual to sexual differentiation. MicroRNAs from sickle cell erythrocytes have been associated with increased gametocyte numbers [4] while on the parasite side, genes such as P. falciparum gametocyte development gene 1 (Pfgdv1) have been implicated in control of sexual differentiation [5]. In addition, conditioned media (i.e. the supernatant of P. falciparum cultures) can stimulate sexual conversion in vitro [6,7], implying that the process is induced either by presence of parasite-secreted factors and/or by parasite depletion of nutrients present in the culture media. Several recent studies have identified parasite factors that contribute to the sexual conversion switch.

First, two groups showed that extracellular vesicles (EVs) secreted from malaria-infected red blood cells (iRBCs) can increase gametocytogenesis in vitro and hypothesized that EVs can transfer parasite and/or host factors that lead to sexual conversion (Figure 1b) [8,9]. Mantel et al observed that EVs purified from asexual parasite-conditioned media can be transferred between iRBCs and stimulate sexual conversion in a dose-dependent manner. Regev-Rudzki and colleagues demonstrated that drug pressure increased EV release and that EVs could transfer DNA between parasite lines, conferring drug resistance while also increasing sexual conversion in recipient cells. Both studies point towards EVs triggering downstream signaling that modulates the rate of

commitment to the sexual pathway; however, given that EV characteristics, including size and timing of release, differed between these studies, further work is needed to validate this central finding. Additional next steps include identifying the EV component responsible for inducing sexual conversion and exploring how this signaling feeds into epigenetic control mechanisms that underlie sexual differentiation (discussed below).

Four recent studies have uncovered a molecular framework by which parasites can integrate signals such as those provided by EVs to commit to sexual development (Figure 1a-b). A transcription factor, AP2-G, has been identified as a master transcriptional regulator for gametocytogenesis, as its deletion or disruption abolished sexual conversion in both P. falciparum and Plasmodium berghei, a murine malaria parasite. AP2-G expression during schizont stages was linked to upregulation of hundreds of genes, many of which have been implicated in gametocyte development. Positive feedback regulation may also play a role in commitment, as recombinant AP2-G in vitro binds two short recognition sequences frequently found upstream of gametocyte-specific genes including ap2-g itself [10,11]. Furthermore, two epigenetic regulators, histone deacetylase 2 (PfHda2) and heterochromatin protein 1 (PfHP1), have been shown to repress sexual development, with disruption of these proteins leading to increased gametocytogenesis and decreased asexual replication [12,13]. Conditional depletion of PfHP1 or PfHda2 in asexual parasites led to de-repression of the ap2-g locus and upregulation of gametocyte-specific genes [12,13], implying that epigenetic control of AP2-G regulates sexual commitment. Taken together, these findings support the hypothesis that epigenetic regulation allows P. falciparum to adjust developmental decisions promoting survival and transmission based on EVs, nutrients, drugs, and other host or environmental factors (illustrated in Figure 1a-b).

In the murine model, Sinha and colleagues identified an additional transcription factor from the AP2 family, AP2-G2, whose disruption completely blocks development of male gametocytes and reduces numbers of mature female gametocytes [10]. Analogous to regulation of AP2-G expression, it is hypothesized that there are environmental factors that can affect sex ratio by altering AP2-G2 expression. Indeed, mathematical and evolutionary models theorizing that plasticity in gametocyte investment enables parasites to maintain fitness in a changing host environment [14,15] highlight questions of how host factors and drugs interplay to alter male and female sexual commitment. Additional clinical and molecular studies are needed to probe mechanisms of male vs. female gametocyte formation and clearance.

III. Parasites exploit host microenvironments: sequestration in bone marrow

Mature asexual stage parasites are known to avoid splenic clearance by cytoadhering to the endothelial lining of capillaries in many tissues. The extensively characterized remodeling mechanisms that mediate asexual sequestration involve specific ligand-receptor interactions, primarily mediated by binding of the parasite antigen PfEMP1 to host endothelial receptors such as ICAM-1 and CD36 [16]. In contrast to asexual stages, only limited binding of early gametocytes to human endothelial cell lines or to CD36 and ICAM-1 has been demonstrated [17,18]. Further evidence for a gametocyte-specific sequestration mechanism includes minimal levels of PfEMP1 on the surface of early gametocyte-iRBCs and downregulation of var genes (responsible for PfEMP1 expression) [18]. Both forward and reverse genetic studies support a role for gametocyte-specific proteins, including the PfGEXPs, which are expressed during early sexual differentiation [19], in gametocyte host cell remodeling [20,21]. Previous qualitative analyses established the presence of immature P. falciparum gametocytes in the bone marrow and spleen of infected

individuals [22,23], but quantitative information about gametocyte sequestration and remodeling has only been obtained recently.

Gametocytes undergo a marked change in morphology during maturation. Beginning as a round form indistinguishable from asexual stages (termed Stage I), they then develop through several transition stages (Stages II/III) to an elongated spindle form (Stage IV) and finally, the curved sausage-like mature form seen in circulation (Stage V) [24,25]. Three groups have recently characterized the mechanical properties of these distinct morphological stages, using filtration through a bead matrix, micropipette aspiration and ektacytometry to show decreased gametocyte-iRBC deformability during Stage I-IV and restored deformability during or prior to Stage V [26-28]. Interestingly, the dissociation of polymorphic STEVOR proteins from the iRBC membrane correlates with the rigidity switch from Stage IV to V [28], suggesting a possible role for these proteins in gametocyte deformability. Fluorescence microscopy experiments probing the mechanism for gametocyte morphological and mechanical changes revealed that microtubules elongate from Stage I to IV and collapse from Stage IV to Stage V [29]. Further, an actin cytoskeleton present primarily at the gametocyte poles dissociates during the transition to Stage V [30]. Computational modeling based on iRBC deformability predicts that immature gametocytes cannot pass through sinusoidal slits during splenic filtration [26], agreeing with observations of circulating mature gametocytes vs. sequestering immature gametocytes.

Three recent studies, including a case study of a patient with subacute malaria [31], an autopsy study looking at different sequestration sites in children who died from cerebral malaria [32], and a study of bone marrow aspirates of children with nonfatal malarial anemia [33], together demonstrate by histology and transcript abundance that gametocytes are enriched in the bone marrow parenchyma. In the cerebral malaria study, the majority of bone marrow gametocytes in

most patients localized at erythroblastic islands, specialized sites of erythropoiesis, and a minority of gametocytes appeared to be developing inside erythroid precursor cells [32]. These data suggest that gametocytes can develop in the bone marrow parenchyma before returning to circulation as deformable Stage V gametocytes, but they leave open which parasites (asexually or sexually committed) migrate to the bone marrow (illustrated in Figure 1c-e). Transcriptional profiling from malaria-infected patient blood demonstrates quantitative presence of a young gametocyte population in circulation, intimating that at least a subset of these stages are homing to the bone marrow [34]. However, presence of asexual stage parasites in the bone marrow parenchyma and formation of gametocytes in erythroid precursor cells in vitro [32,35] suggests that the bone marrow may also represent a reservoir for asexual replication and gametocyte formation. Figure 1c-e illustrates a hypothesized flow of events for parasite sequestration in human bone marrow.

Further research in this exciting new area of gametocyte biology should confirm gametocyte enrichment in the bone marrow parenchyma in other patient cohorts, develop phenotypic assays to characterize the binding and transmigration properties of different gametocyte stages, and replicate the bone marrow microenvironment under in vitro or ex vivo conditions. Severe anemia, dyserythropoiesis and the presence of the parasite byproduct hemozoin have independently been associated with a higher prevalence of mature gametocytes in the bone marrow [33,36], providing a compelling foundation for future studies on the impact of host pathology on gametocyte sequestration. In addition, advances in in vivo live imaging of Plasmodium infections in rodent and non-human primate models will enable the study of gametocyte sequestration in the context of the host organism (reviewed in [37,38]).

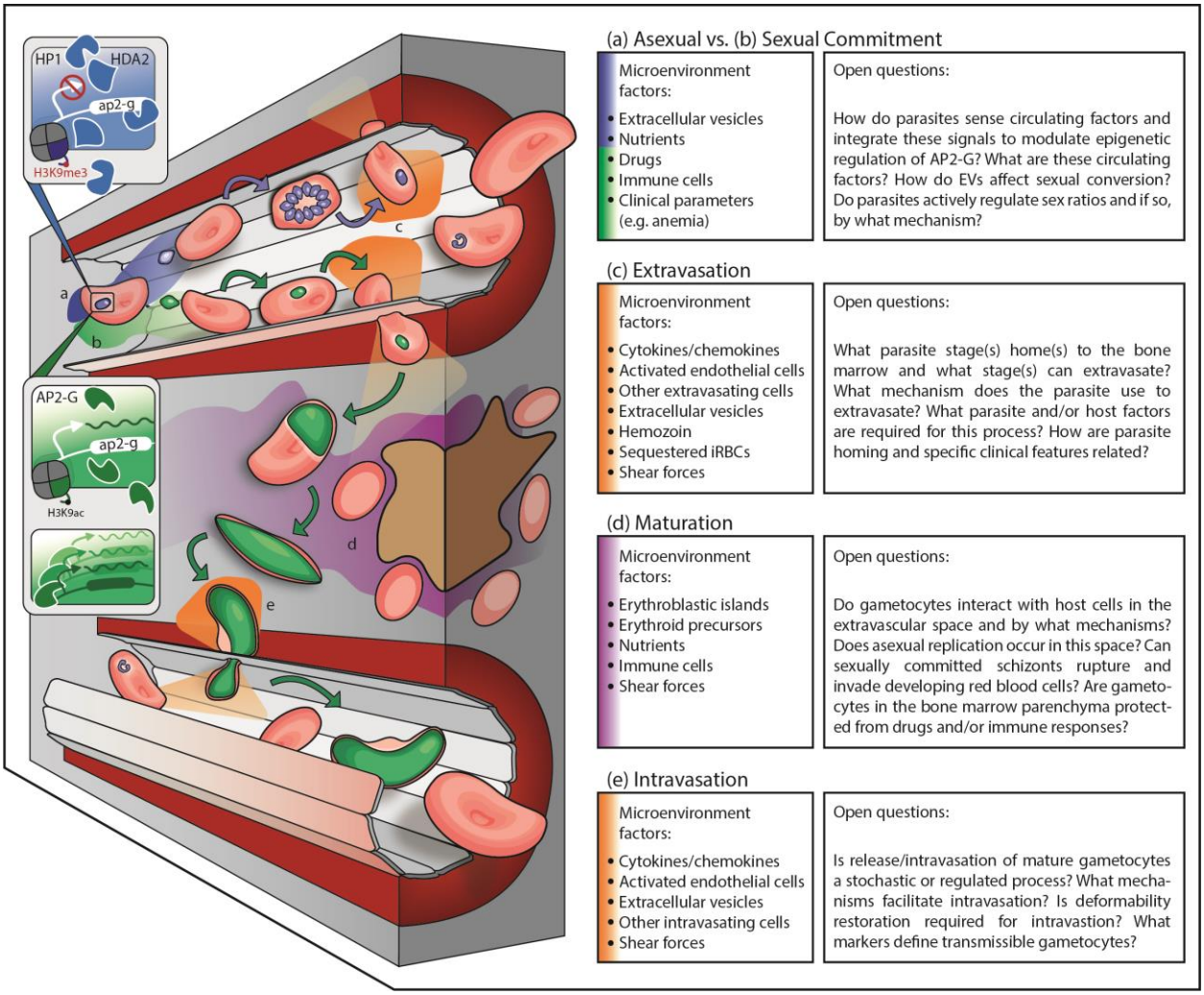

Figure 1: Model for gametocyte commitment and sequestration, including key host-parasite interactions and microenvironment characteristics for each step. In the asexual development pathway (a) (blue), HP1 and HDA2 (and potentially other proteins) inhibit ap2-g, and therefore gametocyte gene transcription. Asexual parasites develop in RBCs and may extravasate into the bone marrow parenchyma (c) (orange). In a subset of asexual parasites, ap2-g is transcribed, leading to the expression of genes essential for gametocyte development (b) (green). There are multiple parasite stages that may be involved (asexual parasite, merozoite, early gametocyte) in homing to the bone marrow and extravasation through the endothelial lining into the bone marrow parenchyma (c) (orange). Various possible parasite and host factors likely determine homing and extravasation, which may occur in a trans- or para-cellular process, and may be guided by an active endothelial cell process. Local inflammation and endothelial activation stimulated by sequestered parasites, parasite EVs, or hemozoin may contribute to extravasation (c). Upon extravasation, parasite development or ability to remain in this microenvironment may depend on local interactions with host cells, including nurse macrophages or erythroid precursors, or soluble host factors, such as nutrients, that are also present (d) (purple). Finally, gametocytes must intravasate to return to circulation, with endothelial cells again likely mediating this process (e) (orange).

IV. Discussion

Recent advances in our understanding of P. falciparum gametocyte biology and development of molecular, imaging, and drug screening tools provide exciting opportunities to better define the parasite's interaction with its host and design transmission-blocking therapeutics (summarized in Figure 2). Evidence for EV-mediated cellular communication and epigenetic/transcriptional machinery controlling commitment provides a rationale for the systematic dissection of the triggers and downstream targets involved in P. falciparum sexual differentiation. Similarly, research building on parasite sequestration in the bone marrow should define mechanisms of homing, transmigration across the vascular endothelium, and development in the parenchyma. Furthermore, it is still unknown whether other tissues of the reticulo-endothelial system, such as the spleen and liver, can also support extravascular parasite development. The application of molecular manipulation tools (most recently CRISPR-Cas-mediated genetic disruption [39,40]) to P. falciparum will enable targeted investigation of the developmental pathways involved in sexual commitment and sequestration.

Though recent findings open up numerous possible avenues for drug development, a subset of gametocyte proteins, particularly those involved in epigenetic regulation, signal transduction, metabolism, and cytoskeletal remodeling, likely represent the most realistic points of intervention (Figure 2). Identified in a transposon mutagenesis screen and transcriptional analysis during gametocyte formation and development, putative genes involved in these processes may yield novel drug or vaccine targets [5,21,34]. Several possible drug targets have also emerged from metabolomics approaches indicating increased gametocyte sensitivity to TCA-cycle inhibitors [41] and work implicating the perforin-like protein PPLP2 and sex-specific organelles in membrane permeabilization during parasite egress [42-44]. Further upstream, recent work suggest

that lipid metabolism differs between asexual stages and gametocytes [45] and that a female-specific ATP-binding cassette transporter is linked to the accumulation of lipids needed for membrane biogenesis [46]. Despite these advances, there remain many questions about parasite uptake of host nutrients and application of possible gametocyte vulnerabilities to transmission-blocking therapeutics.

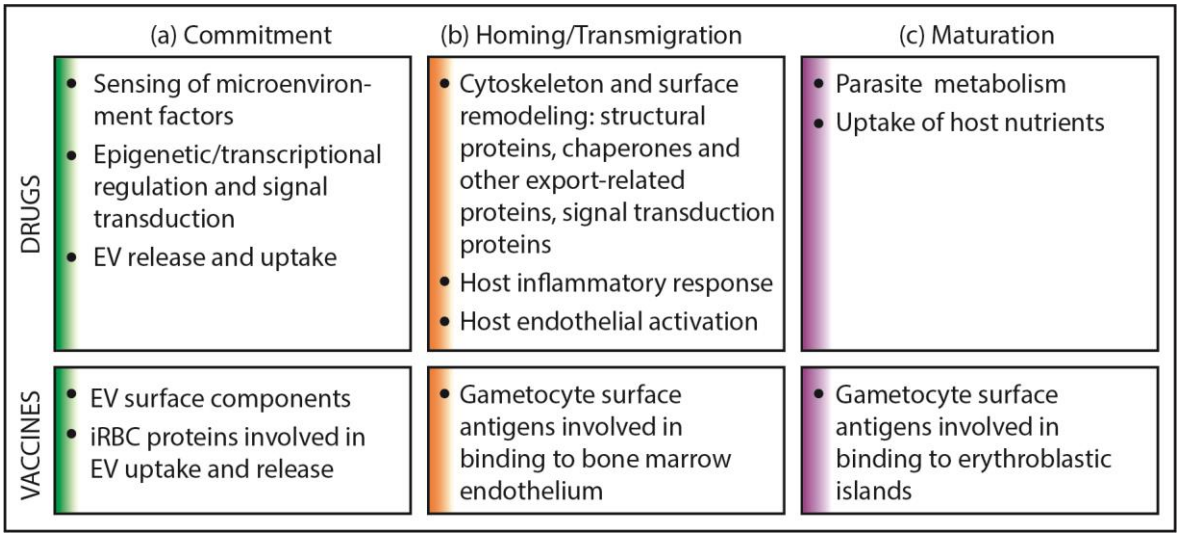

Figure 2: Points of transmission-blocking intervention. Several recently elucidated aspects of gametocyte biology outlined in this review provide potential points of intervention for new clinical tools. Drugs or vaccines could block transmission by targeting (a) commitment to sexual development, (b) homing and transmigration (including extravasation and intravasation), and (c) gametocyte maturation. (a) During commitment, epigenetic regulation and signal transduction involved in sexual conversion and sex ratio determination could be targeted by transmission blocking drugs. Additionally, drugs could target machinery involved in the release or uptake of EVs from iRBCs. Vaccines could similarly target EV surface components or iRBC proteins involved in EV uptake and release. (b) During homing and transmigration, drugs could target parasite-encoded proteins that mediate cytoskeletal or surface remodeling involved in homing or transmigration in the bone marrow. Alternatively, host-targeted drugs could be used to modulate host inflammatory responses and endothelial activation that may drive sequestration. Vaccines could target gametocyte surface proteins required for bone marrow endothelium binding or transmigration. (c) During gametocyte maturation, drugs could target gametocyte metabolic enzymes or proteins involved in host nutrient uptake. Vaccines could target gametocyte surface proteins involved in binding to erythroblastic islands. Host-targeted therapies are indicated by italics. Section colors in this figure correspond to microenvironment colors presented in Figure 1.

Several new platforms for high throughput screening of gametocytocidal drugs could be used to test drugs intervening in the processes mentioned above. Some of these assays rely on fluorescent or luminescent reporters, enabling monitoring of gametocyte-specific drug activity [47,48], while others use DNA dyes, viability dyes, or enzymatic assays to allow screening of all parasite lines including field isolates [49-52]. In addition, new readouts for transmission-blocking activity [53,54] will increase throughput of drug and vaccine testing while the sex-specific proteome of mature gametocytes [55] may help identify stage-specific biomarkers.

Finally, there is still much uncertainty about the nature and extent of transmission-blocking immunity. Numerous epidemiological studies have suggested that transmission-blocking antibodies are short-lived [56]; however, these studies have so far been in limited populations while transmission-blocking immunity likely varies by region. Furthermore, though model simulations suggest that antibodies attacking immature gametocytes would significantly lower the density of transmissible mature gametocytes [57], it is still unknown what role antibodies play compared to other immune components and if antibodies can target developing gametocytes in addition to mature gametocytes. Whatever gametocyte stage(s) is (are) ultimately targeted by a transmission-blocking drug or vaccine, promising results from a recent vaccine candidate combining the established gamete antigen Pfs48/45 with the asexual antigen GLURP [58] reinforce the value of targeting transmission stages together with asexual stages.

In conclusion, the malaria elimination agenda has driven recent discoveries with applications for novel biomarkers, drugs and vaccines. In particular, advances in illuminating the mechanisms of gametocyte commitment and sequestration uncover new parasite and host targets for transmission-blocking interventions. Further investigation of the knowledge gaps in these areas

will both deepen our understanding of host-gametocyte biology and generate new tools to block malaria transmission.

Acknowledgements

The authors wish to thank Ilana Goldowitz and Elamaran Meibalan for critical reading of the manuscript. Work in the Marti lab is funded by grants 5R01AI077558 and 1R21AI105328 from the National Institutes of Health and a career development award from the Burroughs Wellcome Fund to MM. KWD, DBR and NBMM are supported by a Herchel Smith graduate fellowship, a graduate fellowship (DGE1144152) from the U.S National Science Foundation and a postdoctoral fellowship (P2BSP3_151859) from the Swiss National Science Foundation, respectively.

References

1. WHO: **WHO Malaria Report 2014**. 2014.

2. Lindblade KA, Steinhardt L, Samuels A, Kachur SP, Slutsker L: **The silent threat: asymptomatic parasitemia and malaria transmission**. *Expert Rev Anti Infect Ther* 2013, **11**:623-639.

3. Alonso PL, Brown G, Arevalo-Herrera M, Binka F, Chitnis C, Collins F, Doumbo OK, Greenwood B, Hall BF, Levine MM, et al.: **A research agenda to underpin malaria eradication**. *PLoS medicine* 2011, **8**:e1000406.

4. LaMonte G, Philip N, Reardon J, Lacsina JR, Majoros W, Chapman L, Thornburg CD, Telen MJ, Ohler U, Nicchitta CV, et al.: **Translocation of sickle cell erythrocyte microRNAs into Plasmodium falciparum inhibits parasite translation and contributes to malaria resistance**. *Cell host & microbe* 2012, **12**:187-199.

5. Eksi S, Morahan BJ, Haile Y, Furuya T, Jiang H, Ali O, Xu H, Kiattibutr K, Suri A, Czesny B, et al.: **Plasmodium falciparum gametocyte development 1 (Pfgdv1) and gametocytogenesis early gene identification and commitment to sexual development**. *PLoS Pathog* 2012, **8**:e1002964.

6. Dyer M, Day KP: **Regulation of the rate of asexual growth and commitment to sexual development by diffusible factors from in vitro cultures of Plasmodium falciparum**. *The American journal of tropical medicine and hygiene* 2003, **68**:403-409.

7. Williams JL: **Stimulation of Plasmodium falciparum gametocytogenesis by conditioned medium from parasite cultures**. *Am J Trop Med Hyg* 1999, **60**:7-13.

8. Mantel PY, Hoang AN, Goldowitz I, Potashnikova D, Hamza B, Vorobjev I, Ghiran I, Toner M, Irimia D, Ivanov AR, et al.: **Malaria-infected erythrocyte-derived microvesicles mediate cellular communication within the parasite population and with the host immune system**. *Cell Host Microbe* 2013, **13**:521-534.

Characterizes EVs from infected RBCs, including their immunomodulatory effects on macrophages and neutrophils. Provides evidence for iRBCs internalizing EVs purified from asexual parasite-conditioned media and EVs stimulating sexual conversion in a dose-dependent manner.

9. Regev-Rudzki N, Wilson DW, Carvalho TG, Sisquella X, Coleman BM, Rug M, Bursac D, Angrisano F, Gee M, Hill AF, et al.: **Cell-cell communication between malaria-infected red blood cells via exosome-like vesicles**. *Cell* 2013, **153**:1120-1133.

In agreement with [8], shows that exosome-like vesicles from iRBCs stimulate increased sexual differentiation and release more frequently with drug pressure. Suggests that EVs can transfer DNA between parasite strains, conferring drug resistance on plasmid-recipient parasites.

10. Sinha A, Hughes KR, Modrzynska KK, Otto TD, Pfander C, Dickens NJ, Religa AA, Bushell E, Graham AL, Cameron R, et al.: **A cascade of DNA-binding proteins for sexual commitment and development in Plasmodium**. *Nature* 2014, **507**:253-257.

11. Kafsack BF, Rovira-Graells N, Clark TG, Bancells C, Crowley VM, Campino SG, Williams AE, Drought LG, Kwiatkowski DP, Baker DA, et al.: **A transcriptional switch underlies commitment to sexual development in malaria parasites**. *Nature* 2014, **507**:248-252.

References 10-11 independently identify PfAP2-G, a master transcriptional regulator for gametocytogenesis. AP2-G upregulates expression of hundreds of genes associated with gametocyte development and its disruption inhibits commitment to sexual conversion. Kafsack et al. show that loss-of-function mutations in AP2-G are absent in the genomes of 300 P. falciparum field isolates, while variation in ap2-g transcript levels correlate highly with level of gametocyte production in a reference lab strain. Sinha et al. also identify PbAP2-G2, which may be involved in determining gametocyte sex ratio.

12. Brancucci NM, Bertschi NL, Zhu L, Niederwieser I, Chin WH, Wampfler R, Freymond C, Rottmann M, Felger I, Bozdech Z, et al.: **Heterochromatin protein 1 secures survival and transmission of malaria parasites**. *Cell Host Microbe* 2014, **16**:165-176.

Highlights the importance of epigenetic control of sexual commitment by characterizing the role of heterochromatin protein 1 (HP1) in regulating PfAP2-G (see references 10-11). Conditional

depletion of HP1 in late asexual stage parasites causes 50% of progeny in the following cycle to become gametocytes and 50% to continue with asexual development and then arrest prior to schizogony. HP1-depleted gametocytes progress normally through stage V development, suggesting that the role of HP1 in gametocytogenesis is confined to commitment.

13. Coleman BI, Skillman KM, Jiang RH, Childs LM, Altenhofen LM, Ganter M, Leung Y, Goldowitz I, Kafsack BF, Marti M, et al.: **A Plasmodium falciparum histone deacetylase regulates antigenic variation and gametocyte conversion**. *Cell Host Microbe* 2014, **16**:177-186.

Parallel to [12], demonstrates an epigenetic role for histone deacetylase 2 (Hda2) in controlling PfAP2-G (see references 7-8), and therefore repressing commitment to sexual commitment. Conditional depletion of Hda2 in asexual stage parasites causes a three-fold increase in sexual commitment as well as a decrease in asexual replication.

14. Cameron A, Reece SE, Drew DR, Haydon DT, Yates AJ: **Plasticity in transmission strategies of the malaria parasite, Plasmodium chabaudi: environmental and genetic effects**. *Evol Appl* 2013, **6**:365-376.

15. Carter LM, Kafsack BF, Llinas M, Mideo N, Pollitt LC, Reece SE: **Stress and sex in malaria parasites: Why does commitment vary?** *Evol Med Public Health* 2013, **2013**:135-147.

Presents an evolutionary theory-based model that aims to understand why gametocyte densities are usually low compared to asexual densities and examines why parasites adjust investment in gametocytes according to changing host conditions. Provides mathematical support for plasticity in gametocyte investment enabling parasites to optimize fitness in a changing host environment.

16. Miller LH, Baruch DI, Marsh K, Doumbo OK: **The pathogenic basis of malaria**. *Nature* 2002, **415**:673-679.

17. Silvestrini F, Tiburcio M, Bertuccini L, Alano P: **Differential adhesive properties of sequestered asexual and sexual stages of Plasmodium falciparum on human endothelial cells are tissue independent**. *PLoS One* 2012, **7**:e31567.

18. Tiburcio M, Silvestrini F, Bertuccini L, Sander AF, Turner L, Lavstsen T, Alano P: **Early gametocytes of the malaria parasite Plasmodium falciparum specifically remodel the adhesive properties of infected erythrocyte surface**. *Cell Microbiol* 2012.

19. Silvestrini F, Lasonder E, Olivieri A, Camarda G, van Schaijk B, Sanchez M, Younis Younis S, Sauerwein R, Alano P: **Protein export marks the early phase of gametocytogenesis of the human malaria parasite Plasmodium falciparum**. *Mol Cell Proteomics* 2010, **9**:1437-1448.

20. Morahan BJ, Strobel C, Hasan U, Czesny B, Mantel PY, Marti M, Eksi S, Williamson KC: **Functional analysis of the exported type IV HSP40 protein PfGECO in Plasmodium falciparum gametocytes**. *Eukaryotic cell* 2011, **10**:1492-1503.

21. Ikadai H, Shaw Saliba K, Kanzok SM, McLean KJ, Tanaka TQ, Cao J, Williamson KC, Jacobs-Lorena M: **Transposon mutagenesis identifies genes essential for Plasmodium falciparum gametocytogenesis**. *Proc Natl Acad Sci U S A* 2013, **110**:E1676-1684.

Uses piggyBac transposon-mediated insertional mutagenesis to identify parasite clones that no longer form mature gametocytes. Ultimately identified 16 genes putatively responsible for the loss of gametocytogenesis; some appear to arrest gametocyte maturation while others may be involved in commitment.

22. Smalley ME, Abdalla S, Brown J: **The distribution of Plasmodium falciparum in the peripheral blood and bone marrow of Gambian children**. *Trans R Soc Trop Med Hyg* 1981, **75**:103-105.

23. Thomson JG, Robertson A: **The Structure and development of Plasmodium falciparum gametocytes in the internal organs and peripheral circulation**. *Trans R Soc Trop Med Hyg* 1935, **14**:31-40.

24. Hawking F, Wilson ME, Gammage K: **Evidence for cyclic development and short-lived maturity in the gametocytes of Plasmodium falciparum**. *Trans R Soc Trop Med Hyg* 1971, **65**:549-559.

25. Sinden RE, Canning EU, Bray RS, Smalley ME: **Gametocyte and gamete development in Plasmodium falciparum**. *Proc R Soc Lond B Biol Sci* 1978, **201**:375-399.

26. Aingaran M, Zhang R, Law SK, Peng Z, Undisz A, Meyer E, Diez-Silva M, Burke TA, Spielmann T, Lim CT, et al.: **Host cell deformability is linked to transmission in the human malaria parasite Plasmodium falciparum**. *Cell Microbiol* 2012, **14**:983-993.

27. Dearnley MK, Yeoman JA, Hanssen E, Kenny S, Turnbull L, Whitchurch CB, Tilley L, Dixon MW: **Origin, composition, organization and function of the inner membrane complex of Plasmodium falciparum gametocytes**. *Journal of cell science* 2012.

28. Tiburcio M, Niang M, Deplaine G, Perrot S, Bischoff E, Ndour PA, Silvestrini F, Khattab A, Milon G, David PH, et al.: **A switch in infected erythrocyte deformability at the maturation and blood circulation of Plasmodium falciparum transmission stages**. *Blood* 2012, **119**:e172-180.

29. Dixon MW, Dearnley MK, Hanssen E, Gilberger T, Tilley L: **Shape-shifting gametocytes: how and why does P. falciparum go banana-shaped?** *Trends Parasitol* 2012, **28**:471-478.

30. Hliscs M, Millet C, Dixon MW, Siden-Kiamos I, McMillan P, Tilley L: **Organization and function of an actin cytoskeleton in Plasmodium falciparum gametocytes**. *Cell Microbiol* 2015, **17**:207-225.

Demonstrates that an F-actin cytoskeleton is present at the ends of maturing gametocytes under the inner membrane complex, and that this actin cytoskeleton is dismantled in stage V gametocytes

at the same time as microtubule cytoskeleton disassembly. Also shows the presence of Formin-1 at gametocyte ends.

31. Farfour E, Charlotte F, Settegrana C, Miyara M, Buffet P: **The extravascular compartment of the bone marrow: a niche for Plasmodium falciparum gametocyte maturation?** *Malar J* 2012, **11**:285.

32. Joice R, Nilsson SK, Montgomery J, Dankwa S, Egan E, Morahan B, Seydel KB, Bertuccini L, Alano P, Williamson KC, et al.: **Plasmodium falciparum transmission stages accumulate in the human bone marrow**. *Sci Transl Med* 2014, **6**:244re245.

Using autopsy tissue samples from children who died from cerebral malaria, reveals gametocyte enrichment in the bone marrow, particularly in the bone marrow parenchyma. Specific localization of gametocytes at the erythroblastic island, the site of RBC development, raises new questions about which parasite stage homes to the bone marrow and how gametocytes develop in the bone marrow microenvironment.

33. Aguilar R, Magallon-Tejada A, Achtman AH, Moraleda C, Joice R, Cistero P, Li Wai Suen CS, Nhabomba A, Macete E, Mueller I, et al.: **Molecular evidence for the localization of Plasmodium falciparum immature gametocytes in bone marrow**. *Blood* 2014, **123**:959-966.

Using bone marrow aspirates from children with nonfatal malarial anemia, shows higher prevalence and transcript levels of immature gametocytes in the bone marrow than in the peripheral blood. Severe anemia and dyserythropoiesis were associated with a higher prevalence of mature gametocytes in bone marrow.

34. Pelle K, Oh K, Buchholz K, Narasimhan V, Milner D, Ketman K, Seydel K, Taylor T, Barteneva N, Huttenhower C, et al.: **Transcriptional profiling defines dynamics of parasite tissue sequestration during malaria infection**. *Genome Med, In press*.

35. Peatey CL, Watson JA, Trenholme KR, Brown CL, Nielson L, Guenther M, Timmins N, Watson GS, Gardiner DL: **Enhanced gametocyte formation in erythrocyte progenitor cells: a site-specific adaptation by Plasmodium falciparum**. *J Infect Dis* 2013, **208**:1170-1174.

36. Aguilar R, Moraleda C, Achtman AH, Mayor A, Quinto L, Cistero P, Nhabomba A, Macete E, Schofield L, Alonso PL, et al.: **Severity of anaemia is associated with bone marrow haemozoin in children exposed to Plasmodium falciparum**. *Br J Haematol* 2014, **164**:877-887.

Analyzes the presence of malaria parasites and hemozoin in bone marrow aspirates from anemic children. An association of hemozoin presence with decreased hemoglobin and increased dyserythropoiesis implies that hemozoin is involved in the pathogenesis of malarial anemia.

37. Beignon AS, Le Grand R, Chapon C: **In vivo imaging in NHP models of malaria: challenges, progress and outlooks**. *Parasitol Int* 2014, **63**:206-215.

38. Claser C, Malleret B, Peng K, Bakocevic N, Gun SY, Russell B, Ng LG, Renia L: **Rodent Plasmodium-infected red blood cells: imaging their fates and interactions within their hosts**. *Parasitol Int* 2014, **63**:187-194.

39. Ghorbal M, Gorman M, Macpherson CR, Martins RM, Scherf A, Lopez-Rubio JJ: **Genome editing in the human malaria parasite Plasmodium falciparum using the CRISPR-Cas9 system**. *Nat Biotechnol* 2014, **32**:819-821.

40. Wagner JC, Platt RJ, Goldfless SJ, Zhang F, Niles JC: **Efficient CRISPR-Cas9-mediated genome editing in Plasmodium falciparum**. *Nat Methods* 2014, **11**:915-918.

41. MacRae JI, Dixon MW, Dearnley MK, Chua HH, Chambers JM, Kenny S, Bottova I, Tilley L, McConville MJ: **Mitochondrial metabolism of sexual and asexual blood stages of the malaria parasite Plasmodium falciparum**. *BMC Biol* 2013, **11**:67.

42. Deligianni E, Morgan RN, Bertuccini L, Wirth CC, Silmon de Monerri NC, Spanos L, Blackman MJ, Louis C, Pradel G, Siden-Kiamos I: **A perforin-like protein mediates disruption of the erythrocyte membrane during egress of Plasmodium berghei male gametocytes**. *Cell Microbiol* 2013, **15**:1438-1455.

43. Olivieri A, Bertuccini L, Deligianni E, Franke-Fayard B, Curra C, Siden-Kiamos I, Hanssen E, Grasso F, Superti F, Pace T, et al.: **Distinct properties of the egress-related osmiophilic bodies in male and female gametocytes of the rodent malaria parasite Plasmodium berghei**. *Cell Microbiol* 2014.

44. Wirth CC, Glushakova S, Scheuermayer M, Repnik U, Garg S, Schaack D, Kachman MM, Weissbach T, Zimmerberg J, Dandekar T, et al.: **Perforin-like protein PPLP2 permeabilizes the red blood cell membrane during egress of Plasmodium falciparum gametocytes**. *Cell Microbiol* 2014, **16**:709-733.

45. Lamour SD, Straschil U, Saric J, Delves MJ: **Changes in metabolic phenotypes of Plasmodium falciparum in vitro cultures during gametocyte development**. *Malar J* 2014, **13**:468.

Based on analysis of parasite uptake and release of nutrients in culture medium, proposes that energy metabolism and lipid utilization are different in gametocytes than in asexual stages. Provides support for future investigations of acetate and fatty acid metabolism in gametocytes.

46. Tran PN, Brown SH, Mitchell TW, Matuschewski K, McMillan PJ, Kirk K, Dixon MW, Maier AG: **A female gametocyte-specific ABC transporter plays a role in lipid metabolism in the malaria parasite**. *Nat Commun* 2014, **5**:4773.

Identifies a role for a female gametocyte-specific ATP-binding cassette (ABC) transporter in the regulation of gametocyte numbers and in the aggregation of lipids needed for membrane biogenesis. The structure containing these lipids may function to prepare the parasite for the transition from the human host to the mosquito host and may also play a role in gametocyte commitment.

47. Cevenini L, Camarda G, Michelini E, Siciliano G, Calabretta MM, Bona R, Kumar TR, Cara A, Branchini BR, Fidock DA, et al.: **Multicolor bioluminescence boosts malaria research: quantitative dual-color assay and single-cell imaging in Plasmodium falciparum parasites**. *Anal Chem* 2014, **86**:8814-8821.

48. Wang Z, Liu M, Liang X, Siriwat S, Li X, Chen X, Parker DM, Miao J, Cui L: **A flow cytometry-based quantitative drug sensitivity assay for all Plasmodium falciparum gametocyte stages**. *PLoS One* 2014, **9**:e93825.

49. D'Alessandro S, Silvestrini F, Dechering K, Corbett Y, Parapini S, Timmerman M, Galastri L, Basilico N, Sauerwein R, Alano P, et al.: **A Plasmodium falciparum screening assay for anti-gametocyte drugs based on parasite lactate dehydrogenase detection**. *J Antimicrob Chemother* 2013, **68**:2048-2058.

50. Duffy S, Avery VM: **Identification of inhibitors of Plasmodium falciparum gametocyte development**. *Malar J* 2013, **12**:408.

51. Sanders NG, Sullivan DJ, Mlambo G, Dimopoulos G, Tripathi AK: **Gametocytocidal screen identifies novel chemical classes with Plasmodium falciparum transmission blocking activity**. *PLoS One* 2014, **9**:e105817.

52. Tanaka TQ, Dehdashti SJ, Nguyen DT, McKew JC, Zheng W, Williamson KC: **A quantitative high throughput assay for identifying gametocytocidal compounds**. *Mol Biochem Parasitol* 2013, **188**:20-25.

53. Ruecker A, Mathias DK, Straschil U, Churcher TS, Dinglasan RR, Leroy D, Sinden RE, Delves MJ: **A male and female gametocyte functional viability assay to identify biologically relevant malaria transmission-blocking drugs**. *Antimicrob Agents Chemother* 2014, **58**:7292-7302.

54. Stone WJ, Churcher TS, Graumans W, van Gemert GJ, Vos MW, Lanke KH, van de Vegte-Bolmer MG, Siebelink-Stoter R, Dechering KJ, Vaughan AM, et al.: **A scalable assessment of Plasmodium falciparum transmission in the standard membrane-feeding assay, using transgenic parasites expressing green fluorescent protein-luciferase**. *J Infect Dis* 2014, **210**:1456-1463.

55. Tao D, Ubaida-Mohien C, Mathias DK, King JG, Pastrana-Mena R, Tripathi A, Goldowitz I, Graham DR, Moss E, Marti M, et al.: **Sex-partitioning of the Plasmodium falciparum stage V gametocyte proteome provides insight into falciparum-specific cell biology**. *Mol Cell Proteomics* 2014, **13**:2705-2724.

56. Bousema T, Sutherland CJ, Churcher TS, Mulder B, Gouagna LC, Riley EM, Targett GA, Drakeley CJ: **Human immune responses that reduce the transmission of Plasmodium falciparum in African populations**. *Int J Parasitol* 2011, **41**:293-300.

57. McQueen PG, Williamson KC, McKenzie FE: **Host immune constraints on malaria transmission: insights from population biology of within-host parasites**. *Malar J* 2013, **12**:206.

58. Theisen M, Roeffen W, Singh SK, Andersen G, Amoah L, van de Vegte-Bolmer M, Arens T, Tiendrebeogo RW, Jones S, Bousema T, et al.: **A multi-stage malaria vaccine candidate targeting both transmission and asexual parasite life-cycle stages**. *Vaccine* 2014, **32**:2623-2630.